

**IMPROVED SUCCESSIVE INTERFERENCE CANCELLATION SCHEMES  
USING SELECTIVE PRE-CANCELLATION AND CROSS-CORRELATION**

**HO KIN SOON DOUGLAS**

*(B.Eng (Hons.), University of Sheffield, UK)*

A THESIS SUBMITTED  
FOR THE DEGREE OF MASTER OF ENGINEERING  
DEPARTMENT OF ELECTRICAL AND COMPUTER ENGINEERING  
NATIONAL UNIVERSITY OF SINGAPORE

2003

## ACKNOWLEDGEMENTS

First of all, I am thankful to my Lord, Jesus Christ, for His grace and mercy. He has provided me with the wisdom and the strength to pull me through this chapter of my life. Without Him, I would not have achieved what I have today.

I also would like to express my sincerest gratitude to Dr. Yen Kai, my supervisor, for providing so much guidance and kind advice during my course of my studies. His light-hearted manner and his confidence in me has always been a motivation to me. I am also grateful to Dr. Chew, another supervisor, for his constructive suggestions during my research work that has refined my work. His advice has made this thesis possible.

I am also very grateful to my third supervisor, Ang Kay Wee, for the many discussions and ideas he has given that had led to the three patents that are currently pending for filing. His good humor has always been enlightenment whenever a tough situation arises.

I am thankful to the reviewing committee for the invention disclosures for their kind and constructive comments.

I would like to say a big thank you to all my friends and colleagues in I<sup>2</sup>R (Institute of Infocomm Research) who have made my two years of studies a memorable one. Special thanks to Huahui, who has never hesitated in giving help and advice, Gao Qing, for being such a nice and friendly person, Suwandi, for his jokes and laughter, Keng Hoe, for his unending motivation and help, and Stephen, for the timely encouragements.

Finally, I am grateful for my parents. Though they are in Taiwan, their love, concern and encouragement has always helped me to persevere on.

# TABLE OF CONTENTS

Acknowledgments	i
Summary	v
Nomenclature	vii
List of Symbols	ix
List of Figures	xi
List of Tables	xiv
1 Introduction	1
1.1. Spread Spectrum Signal	2
1.2. CDMA System Model	4
1.2.1. Transmission	4
1.2.2. Channel	5
1.2.3. Reception	6
1.3. Conventional Detection: The Matched Filter (MF)	10
1.3.1. Matched Filter in a Synchronous CDMA system	10
1.3.2. Matched Filter in an Asynchronous CDMA system	13
1.4. Motivation and Contribution	15
1.3. Thesis Outline	11
2 Multiuser Detection Schemes – Literature Review	18
2.1. Optimum Multiuser Detector	18
2.2. Decorrelating Detector	20
2.3. Linear Minimum Mean Square Error (MMSE) Detector	22
2.4. Interference Cancellation Schemes	24
2.4.1. Interference Cancellation Basic Building Block	24
2.4.2. Serial Interference Cancellation (SIC)	26

2.4.3.	Parallel Interference Cancellation (PIC)	32
2.4.4.	SIC with re-matched filtering (SICRM)	34
2.5.	Chapter Summary	36
3	Analysis of Interference Cancellation	38
3.1.	BER Performance Comparison Between Different ICs	38
3.2.	Computation Complexity	42
3.3.	Processing time	47
3.4.	Summary	50
4	Cross-correlation Implementation (CCI)	52
4.1.	Basic IC Building Block using Cross-correlation	53
4.2.	Complexity Reduction in CCI-SICRM	58
4.3.	Asynchronous application of CCI	62
4.4.	Processing time Reduction in SIC with Re-matched Filtering	66
4.5.	Another Application: Pipelined SIC	67
4.6.	Conclusion	75
5	Improved Successive Interference Cancellation	77
5.1.	Issues of Successive Interference Cancellation Schemes	78
5.1.1.	Mapping functions for decision bit	78
5.1.2.	Block cancellations	79
5.1.3.	Varying channel conditions	80
5.1.4.	Ranking System	81
5.2.	Adaptive Bit-Select Cancellation (ABC) Device	82
5.3.	Improved Successive Interference Cancellation Scheme (ISIC)	85
5.3.1.	ISIC Structure	86
5.3.2.	BER Performance of the ISIC	91

5.3.3. Computation Complexity and Processing time of ISIC	96
5.4. ISIC using the Cross-correlation Implementation	98
5.4. Chapter Summary	102
6 Conclusion and Suggestion for Future Works	103
6.1. Conclusion	103
6.2. Suggestion for Future Works	104
References	106
List of Submitted IP	111
Appendices	
Appendix A: Minimizing The Likelihood Function in Decorrelating Detector	112
Appendix B: Minimizing The Mean Square Error Function in MMSE Detector	113
Appendix C: Process Time Block Comparison Between Different IC	116

## SUMMARY

In direct-sequence code division multiple access system (DS-CDMA), the limiting factor on capacity is not just the bit-error-rate (BER), but the receiver computation complexity and its signal processing time are two important aspects that need to be considered as well. Taking these two aspects into consideration, the interference cancellation (IC) scheme is one of the most commonly used detectors amongst multiuser detectors because of its superior BER performance as compared to the simple matched filter and also its low computation complexity as compared to the optimum detector and linear detectors. Advanced IC schemes, built from the basic IC schemes, require higher computation complexity or processing time than the basic IC schemes for better BER performance.

In this thesis, we aim to improve the IC schemes in terms of their BER, processing time and computation complexity. Since there are no standard procedure to measure receiver computation complexity and processing time, we proposed a simple method for the analysis of IC schemes in these two aspects. We show that advanced IC schemes require high amount of additional computation complexity to achieve BER improvement while successive interference cancellation (SIC) schemes suffer from severely long processing time.

We identified two independent approaches to the existing IC schemes. In the first approach, we aim to reduce the processing time and computation complexity of IC schemes without sacrificing the BER performance. To achieve this, we proposed the cross-correlation implementation (CCI). The CCI is an alternative implementation of the IC scheme by using the cross-correlations between different users to perform the cancellation as opposed to the conventional method that uses the received signal and the channel conditions to regenerate the signals. We show that the CCI approach

reduces the implementation gate count without affecting the BER. The CCI can be applied to any IC scheme to reduce the processing time and to advanced IC schemes to reduce the computation complexity.

The second approach is to improve the BER performance of the SIC scheme with minimal increase in computation complexity and processing time. We propose the improved successive interference cancellation (ISIC) scheme that is comprised of a selective parallel interference cancellation (PIC) integrated into a successive interference cancellation (SIC). The selective PIC section ‘cleans’ the received signal before it is used in the SIC part. This increases the reliability of bit detection in the SIC and hence, improves the BER performance. We also introduce the adaptive bit-select cancellation (ABC) device for the ISIC - a simple device that identifies and selects reliable decision bits to be used in the PIC part. This device adapts to different channel conditions and updates its control parameters for optimum performance of the ISIC. We show that the ISIC has superior BER performance as compared to the SIC and the PIC at the cost of minimal increment in computation complexity and processing time.

In summary, IC schemes using CCI and ISIC with the ABC device are better and more efficient schemes as compared to other conventional IC schemes in a DS-CDMA system.

## ABBREVIATIONS

LAN	Local Area Network
UMTS	Universal Mobile Telecommunications System
IMT2000	International Mobile Telecommunications 2000
CDMA	Code Division Multiple Access
TDMA	Time Division Multiple Access
FDMA	Frequency Division Multiple Access
SIC	Serial (or successive) Interference Cancellation
PIC	Parallel Interference Cancellation
BER	Bit-Error Rate
AWGN	Additive White Gaussian Noise
SSS	Spread Spectrum Signals
SIR	Signal-to-Interference Ratio
BPSK	Binary Pulse Shift Keying
PN	Pseudo-noise
MAI	Multiple Access Interference
MF	Matched Filter
MMSE	Minimum Mean Square Error
SNR	Signal-to-Noise Ratio
IC	Interference Cancellation
SICRM	Successive Interference Cancellation with Re-Matched Filtering
MS	Master Selector
SS	Sub Selector
NMB	Number of Multiplications per Bit
NAB	Number of Addition/Subtraction per Bit



PTB	Processing Time Block
ABC	Adaptive Bit-select Cancellation
ISIC	Improved Successive Interference Cancellation
DSP	Digital Signal Processing

## LIST OF SYMBOLS

$\varepsilon$	Transmitted power
$b$	Data bit
$N$	Processing gain
$T_c$	Chip duration
$T_b$	Bit duration
$s(t)$	Spreading signal
$r(t)$	Received signal
$K$	Number of users in CDMA system
$\beta$	Complex channel coefficient
$\alpha$	Received signal's complex amplitude
$A$	Received signal's real amplitude
$\theta$	Received signal's phase
$\tau$	Received signal's time delay
$M$	Number of bits in one block of received data
$n(t)$	Additive white Gaussian noise
$N_0$	Noise power spectral density
$E_b$	Energy per bit
$y$	Matched filter output or correlation value
$\rho$	Cross-correlation value
$\mathbf{r}$	Received signal vector
$\mathbf{b}$	Data bit vector
$\mathbf{A}$	Received amplitude matrix
$\mathbf{R}$	Cross-correlation matrix

$\hat{\mathbf{b}}$	Estimated data or decision bit matrix
$\Gamma$	Continuous-time partial cross-correlation
$\hat{b}$	Estimated data or decision bit
$\hat{\alpha}$	Estimated received complex amplitude
$S$	Number of stages in IC schemes
$\psi$	MAI coefficient
$P$	Number of pipelines in PSIC
$\Pi$	MAI cancellation in PSIC
$\Omega$	Number of MAI coefficient generation in CCI-PSIC
$p$	Control parameter in the ABC device
$p'$	Scaling factor in the ABC device
$\gamma$	Number of cancellations in selective PIC section of ISIC
$\zeta$	Additional MAI generations in CCI-ISIC

## LIST OF FIGURES

- 1.1 Asynchronous CDMA model
- 1.2 Matched Filter of user  $k$
- 1.3 Bank of matched filter
- 2.1 Decorrelating detector for synchronous channel
- 2.2 MMSE detector for synchronous channel
- 2.3 Basic building blocks of interference cancellation scheme
- 2.4 SIC schematics – stage 0 and 1 and its ICU unit
- 2.5 Stage 2 to  $S$ -th stage of  $S$ -stage SIC and its ICU unit
- 2.6  $S$ -stage Parallel Interference Cancellation (PIC) scheme
- 2.7 Stage 0 and stage 1 of serial interference cancellation with re-matched filtering
- 2.8 Stage 1's Interference Cancellation Unit (ICU) of SICRM
- 3.1 Performance of matched filter and 1-stage interference cancellers in Rayleigh channel
- 3.2 Performance of matched filter and 2-stage interference cancellers in Rayleigh channel
- 3.3 Performance of matched filter and 1-stage interference cancellers in AWGN channel
- 3.4 Performance of matched filter and 2-stage interference cancellers in AWGN channel
- 3.5 A matched filter of user  $k$
- 3.6  $NMB$  and  $NAB$  comparison between SIC, SICRM and PIC
- 3.7 Operations of the matched filter, signal regeneration and signal cancellation in terms of processing time blocks
- 3.8 Processing time block comparison between SIC, SICRM and PIC

- 4.1 Basic building blocks of interference cancellation using CCI
- 4.2 *Block A*: Signal regeneration versus *Block E*: MAI generation
- 4.3 *Block B*: Signal cancellation versus *Block F*: MAI cancellation
- 4.4 MAI co-efficient calculation in terms of *NMB*, *NAB* and *PTB*
- 4.5 Stage 0 and Stage 1 of SICRM using cross-correlation method
- 4.6  $s^{\text{th}}$  stage of the SIC equivalent structure using cross-correlation
- 4.7 *NMB* and *NAB* comparison between the conventional SIC and SICRM against the CCI-SICRM
- 4.8 Partial cross-correlation between 3 users, with  $\tau_{j2} > \tau_k > \tau_{j1}$
- 4.9 MAI co-efficient calculation for asynchronous channel ( $\tau_j > \tau_k$ ) in terms of *NMB*, *NAB* and *PTB*
- 4.10 *NMB* and *NAB* comparison between synchronous SICRM, conventional and cross-correlation, and asynchronous SICRM using CCI
- 4.11 Processing time block comparison between SIC, conventional SICRM, PIC and cross correlation SICRM
- 4.12 Pipelined Successive Interference Cancellation (PSIC) with 3 “pipelines”
- 4.13 *NMB* and *NAB* comparison between SIC and PSIC
- 4.14 PSIC equivalent scheme using cross correlation for  $K$  users and 4 “pipelines”
- 4.15 The MAI cancellation unit (MC)
- 4.16 *NMB* and *NAB* comparison between conventional PSIC and CCI-PSIC
- 4.17 Processing time block comparison between conventional PSIC and CCI-PSIC
- 5.1 Decision devices
- 5.2 Adaptive Bit-wise Cancellation Device
- 5.3 Calculation of the control parameter using correlation values

- 5.4 Bit-wise Cancellation Within a Block Processing System
- 5.5 Improved Successive Interference Cancellation Scheme
- 5.6 Performance of ISIC with various scaling factor in AWGN channel
- 5.7 Performance of ISIC with various scaling factor in Rayleigh fading channel
- 5.8 Scaling factor  $p'$  versus empirical variance of  $\bar{y}_k$  graph
- 5.9 Obtaining the scaling factor function
- 5.10 Capacity of SIC, PIC and ISIC in a AWGN channel using perfect power control
- 5.11 Performance of SIC and ISIC in a AWGN channel using perfect power control
- 5.12 Capacity of SIC, PIC and ISIC in a Rayleigh fading channel
- 5.13 Capacity of SIC, PIC and ISIC in a AWGN channel using perfect power control with erroneous amplitude estimation
- 5.14 Capacity of SIC and ISIC in a Rayleigh fading channel with erroneous amplitude estimation
- 5.15  $NMB$  and  $NAB$  comparison between conventional SIC, SICRM and ISIC in AWGN channel with perfect power control
- 5.16 PTB comparison between the conventional SIC, SICRM and ISIC
- 5.17 CCI-ISIC with adaptive bit-select cancellation (ABC) device in a synchronous channel
- 5.18 Comparison of computation complexity and processing time between conventional ISIC and CCI-ISIC

## LIST OF TABLES

- 1.1 Summarized description of received signal notations
- 3.1 Assessment of matched filter and various IC schemes
- 5.1 Range of  $p'$  for optimum performance in ISIC
- 5.2 Variance of  $\bar{y}_k$  in an AWGN channel and fading channel
- 5.3 Number of parallel cancellations in ISIC for different channels
- 5.4 Number of additional MAI generation and cancellations required in the selective PIC part of ISIC for different channels,  $E_b/N_0$  and number of users

## **CHAPTER 1**

### **INTRODUCTION**

The past twenty years has seen the tremendous development of wireless communication for reliable yet affordable voice and low-rate data communications. At the same time, there has been tremendous growth of the Internet and emergence of internet-based techniques to provide multimedia services. Therefore, the need for high-rate data transmission over the radio channel has drawn the industry to the “third generation” (3G) of mobile communication. Integrating 3G into the current “second generation” (2G) system will extend its capabilities to support multimedia services with high bit rates [1].

The Universal Mobile Telecommunications System (UMTS)/International Mobile Telecommunications 2000 (IMT2000), the standard used for the 3G system, is based on direct sequence code division multiple access (DS-CDMA) [2]. DS-CDMA is one of several CDMA technologies. It is a method of multiplexing users, enabling them to share the same radio frequency to transmit data simultaneously. It has many attractive features such as soft capacity, soft handover and diversity combining (RAKE reception), which distinguish it from other multiplexing methods. However, the performance and capacity of DS-CDMA is severely limited by multiple access interference (MAI). Exhaustive research work has been carried out to mitigate the effect of MAI. Multiuser detection is one of the areas that has shown great potential and forms the theme of this study.



In this chapter, we discuss the DS-CDMA system. In Section 1.1, we discuss the direct-sequence spread spectrum signals, a wireless communication technique from which CDMA is based on. In the same section, we explain some concepts such as spreading code, processing gain and chip rate. In Section 1.2, we define the mathematical system model for a single-path DS-CDMA system. Included is a matrix-vector notation that is very useful for discussing multiuser detection in Chapter 2. We review the conventional detector for DS-CDMA and the problem of MAI in subsection 1.3. Section 1.4 explains the motivation behind this thesis and the contributions achieved. Section 1.5 presents an outline of this thesis.

## 1.1 Spread Spectrum Signal

Spread spectrum signal is used to mitigate the effects of two problems – pulse noise jamming and multipath propagation. Large redundancy where a wideband signal is used to transmit a narrowband signal (this is inherent in spread spectrum signals) is used to overcome these problems that is encountered in digital information transmissions over satellite and radio channels.

A spread spectrum signal has a bandwidth  $W$  that is much larger than the information bit rate  $R$  (in bits/s). It is generated from a data modulated carrier that is further modulated with a very wideband spreading signal. The spreading modulation may be a rapid changing of the carrier frequency or phase modulation. Spreading modulation by rapid changing of the carrier is called a frequency-hop (FH) spreading. When spectrum spreading is achieved through phase modulation of the data signal with the spreading signal, the resultant signal is direct-sequence (DS) spread spectrum signal. Since CDMA is an application of direct-sequence spread spectrum signal, we limit our discussion in this section to this type of spreading modulation.

The simplest form of DS spread spectrum uses binary phase shift keying (BPSK) as the spreading modulation. Consider a constant envelope data-modulated carrier having power  $\varepsilon$ , radian frequency  $\omega_c$  and data bit  $b(t)$  given by

$$x_{data}(t) = \sqrt{\varepsilon} b(t) \cos(\omega_c t) \quad (1.1)$$

BPSK spreading is accomplished by multiplying  $x(t)$  with the spreading signal  $s(t)$ .

Therefore, the transmitted signal is

$$x_{tx}(t) = \sqrt{\varepsilon} b(t) s(t) \cos(\omega_c t) \quad (1.2)$$

The spreading signal  $s(t)$  is characterized by a spreading code of length  $N$ ,  $\{c(1), c(2), \dots, c(N)\}$ , and chip waveform,  $p_{T_c}$ , with chip duration  $T_c$  such that

$$\int_{-\infty}^{\infty} p_{T_c}(t) p_{T_c}(t - nT_c) dt = 0 \quad (1.3)$$

There are a few functions that can be used for  $p_{T_c}$  which fulfills (1.3). In this thesis, we use a unit pulse shape for  $p_{T_c}$ :

$$p_{T_c}(t) = \begin{cases} 1 & \text{for } 0 \leq t \leq T_c \\ 0 & \text{otherwise} \end{cases} \quad (1.4)$$

There are  $N$  chips per data bit and hence,  $T_b = NT_c$ .  $N$  is also known as the processing gain. The spreading code is used to modulate the chip waveform antipodally, and we obtain the direct-sequence spreading signal with duration  $NT_c$ :

$$s(t) = \frac{1}{\sqrt{N}} \sum_{n=1}^N c(n) p_{T_c}(t - (n-1)T_c) \quad 0 \leq t \leq T_b \quad (1.5)$$

In (1.5), without loss of generality, we have normalized  $s(t)$  such that it has unit energy:

$$\int_0^{T_b} s^2(t) dt = 1 \quad (1.6)$$

The spreading code does not carry information and it is assumed known at the intended receiver. It is essentially a pseudonoise (PN) sequence and there are many methods to generate these PN sequences, such Gold and Kasami [4].

At the receiver, demodulation of the spread spectrum signal is accomplished in part by re-modulating the received signal with the spreading signal appropriately delayed. This re-modulation or correlation of the delayed spreading signal with the received signal is called despreading and is a critical function in all spread spectrum systems.

## 1.2 CDMA system model

As mentioned earlier, CDMA is an application of the direct-sequence spread spectrum signal. The basic idea of CDMA is to multiplex users by distinct spreading codes, instead of by orthogonal frequency or time slots in frequency division multiple access (FDMA) or time division multiple access (TDMA). In CDMA, all users transmit at the same time. In this section, we define the CDMA system model that is used throughout this thesis.

### 1.2.1 Transmission

In CDMA, each user is assigned a spreading signal described in (1.5). In this thesis, the CDMA model used is discussed in terms of baseband signals. This drops the carrier frequency term in (1.1) and (1.2). Therefore, from (1.2), the transmitted spread spectrum signal of user  $k$  is:

$$x_{tx,k}(t) = \sqrt{\varepsilon_k} b_k(t) s_k(t) \quad (1.7)$$

where  $\varepsilon_k$  is user  $k$ 's transmitted power,  $b_k(t) = \{1, -1\}$  is user  $k$ 's data bit sequence and  $s_k(t)$  is user  $k$ 's spreading signal with properties described in (1.5) and (1.6).

### 1.2.2 Channel

The mobile communications channel is time variant because of the constantly changing properties of the media. For the analysis of these variations in the radio channel, several channel models have been proposed [5]. In this section, three components of the channel models are briefly discussed.

The first component is the path loss between the transmitter and receiver. Path loss accounts for the very slow decreasing received signal level as the receiver moves away from the transmitter. The second component is shadow fading. Shadow fading or shadowing relates to the slow variations in signal attenuation as various physical obstructions are encountered in the propagation path.

The third component of the channel model is multipath propagation. There are two different categories of multipath propagation. The first category is non-selective fading where a group of propagation paths with path length differences so small that the intended receiver cannot resolve the different time of arrival. In this case, the receiver perceives the summation of these multiple unresolvable paths (direct, refracted and reflected) as a single-path signal. The second category is frequency-selective fading where different paths (or group of paths) can be resolved by the receiver. In CDMA, signals from these resolvable paths can be strengthened by coherently combining these paths using the RAKE receiver.

In this thesis, we only consider non-selective Rayleigh fading while path loss and shadowing are assumed to be compensated. Rayleigh fading occurs when there is no line-of-sight (LOS) or dominant path between the transmitter and the receiver. The

real and imaginary part of the complex channel coefficient,  $\beta$ , are independent zero-mean Gaussian random variables and its phase is uniformly distributed on  $[0, 2\pi]$ . The envelope of  $\beta$ , defined as  $|\beta|$ , follows a Rayleigh distribution given by:

$$f_{|\beta|}(r) = re^{-r^2/2} \quad (1.8)$$

Now, to apply non-selective Rayleigh fading into the our CDMA system model, we insert the complex channel coefficient into (1.7) to produce user  $k$ 's signal at the receiver:

$$\begin{aligned} x_{rx,k}(t) &= \sqrt{\varepsilon_k} \beta_k(t) b_k(t) s_k(t) \\ &= \alpha_k(t) b_k(t) s_k(t) \end{aligned} \quad (1.9)$$

where  $\alpha_k(t) = \sqrt{\varepsilon_k} \beta_k(t)$  is the complex received amplitude of  $x_{c,k}(t)$ .

### 1.2.3 Reception

In CDMA, all the users share the same frequency bandwidth and are only distinguishable by their spreading codes. Therefore, in a system with  $K$  users, the signals arriving at the receiver are combined into one received signal  $r(t)$ . In an asynchronous CDMA system, users' signal arrive at different delays  $\tau_k$ . Also, the signals are received in blocks of  $M$  bits. Therefore, modified from (1.9), the received signal in an asynchronous CDMA system is:

$$r(t) = \sum_{k=1}^K \sum_{m=1}^M \alpha_k(m) b_k(m) s_k(t - mT_b - \tau_k) \quad (1.10)$$

where  $T_b$  is the bit duration,  $b_k(m)$  is  $m$ -th data bit of user  $k$ 's block of  $M$  bits and  $\alpha_k(m)$  is the  $m$ -th complex received amplitude of user  $k$ . Note that we have assumed slow fading within one bit by replacing  $\alpha_k(t)$  in (1.9) with  $\alpha_k(m)$  in (1.10). Since  $\alpha_k(m)$  is a complex number, it has two components:

$$\alpha_k(m) = A_k(m)e^{j\theta_k(m)} \quad (1.11)$$

where  $A_k(m) = |\alpha_k(m)|$  is the real-value received amplitude of user  $k$  and  $e^{j\theta_k(m)}$  refers to the phase change imposed by the channel on the signal.

There is also noise at the receiver, which is attributed by thermal noise, background electromagnetic noise and man-made interference. It is modeled as a zero-mean Gaussian random variable with probability density function given by:

$$f_N(n) = \frac{\exp\left(-\frac{n^2}{2(N_0/2)}\right)}{2\pi(N_0/2)} \quad (1.12)$$

where  $N_0/2$  is the noise variance. This background noise is generally known as additive white Gaussian noise (AWGN) and it is independent of the transmitted signal. Adding AWGN into the received signal in (1.10), the received signal is given by:

$$r(t) = \sum_{k=1}^K \sum_{m=1}^M \alpha_k(m)b_k(m)s_k(t - mT_b - \tau_k) + n(t) \quad (1.13)$$

where  $n(t)$  is AWGN with zero mean and double-sided power spectral density of  $N_0/2$ .

Figure 1.1 illustrates the asynchronous CDMA system model in (1.13).

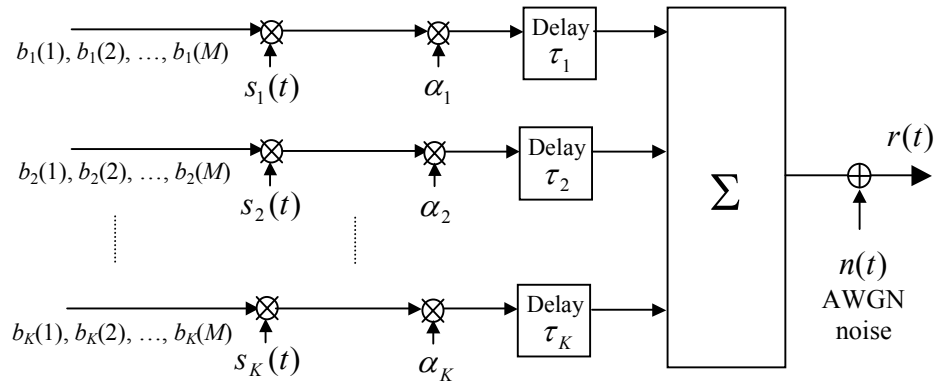


**Figure 1.1:** Asynchronous CDMA model

One of the features of CDMA is power control. It enables mobiles to adjust the powers at which they transmit. This ensures that the base station receives each signal at the appropriate power levels. When perfect power control is assumed, all the users received powers are at the same level, therefore  $\alpha_k = \alpha_j$  for  $j \neq k$ . The main contribution of interference is AWGN. When this condition is assumed, the channel is called an AWGN channel. For simplification, we assume that  $\alpha_k = 1$  for all  $k$  in this condition. Therefore, the received signal for the AWGN channel (in an asynchronous CDMA system) is given by:

$$r(t) = \sum_{k=1}^K \sum_{m=1}^M b_k(m) s_k(t - mT_b - \tau_k) + n(t) \quad (1.14)$$

In a synchronous CDMA system, all the signals arrive at the receiver at the same time, i.e.  $\tau_k = \tau_j$  for  $j \neq k$ . Again, for simplification, we assume that  $\tau_k = 0$  for synchronous CDMA. Therefore, the received signal for a synchronous CDMA system is:

$$r(t) = \sum_{k=1}^K \sum_{m=1}^M \alpha_k(m) b_k(m) s_k(t - mT_b) + n(t) \quad (1.15)$$

Now, we define the matrix-vector notation for the synchronous CDMA system. This notation is used later to explain some of the multiuser detection schemes in Chapter 2. For the matrix-vector notation, we simplify (1.15) by assuming that  $M = 1$ . Therefore, the received signal for bit-wise reception of synchronous CDMA system in fading channel is:

$$r(t) = \sum_{k=1}^K \alpha_k b_k s_k(t) + n(t) \quad (1.16)$$

In the matrix-vector notation, for simplicity, we assume  $\alpha_k$  is real, and thus  $\theta_k = 0$ . Sampling at chip rate, (1.16) is rewritten in matrix-vector notation, where the baseband received signal vector is:

$$\mathbf{r} = \mathbf{S}\mathbf{A}\mathbf{b} + \mathbf{n} \quad (1.17)$$

where:

- $\mathbf{r} = [r(1) \ r(2) \ \dots \ r(N)]^T$  where  $N$  is the processing gain (in this case the number of chips in  $s(t)$  as well).

- $\mathbf{S} = \begin{bmatrix} c_1(1) & c_2(1) & \dots & c_K(1) \\ c_1(2) & c_2(2) & \dots & c_K(2) \\ \vdots & \vdots & \ddots & \vdots \\ c_1(N) & c_2(N) & \dots & c_K(N) \end{bmatrix}$  is the spreading signal matrix of the  $K$  users.

- $\mathbf{A} = \begin{bmatrix} \alpha_1 & 0 & \dots & 0 \\ 0 & \alpha_2 & \dots & 0 \\ \vdots & \vdots & \ddots & \vdots \\ 0 & 0 & \dots & \alpha_K \end{bmatrix}$  is a diagonal matrix with the users' received amplitude.

- $\mathbf{b} = [b_1 \ b_2 \ \dots \ b_K]^T$  is the users' data bit vector.

- $\mathbf{n} = [n(1) \ n(2) \ \dots \ n(N)]^T$  is the AWGN vector.

In this section, we have defined several received signal notations for the CDMA system for different conditions. For convenience of reference, we summarize these notations in the table below:

Equation	Description
1.13	Rayleigh slow fading channel, asynchronous, block-wise reception
1.14	AWGN channel (perfect power control), asynchronous, block-wise reception
1.15	Rayleigh slow fading channel, synchronous, block-wise reception
1.16	Rayleigh slow fading channel, synchronous, bit-wise reception
1.17	Simplified fading channel, synchronous, bit-wise reception, matrix-vector notation

**Table 1.1:** Summarized description of received signal notations



Having established the CDMA system models, we can now review the conventional method of detection for CDMA signal in the next section.

### 1.3 Conventional Detection: The Matched Filter (MF)

As mentioned earlier, the conventional method of demodulating spread spectrum signals is the matched filter. Since CDMA signals are spread spectrum signals, we discuss the detection of CDMA signals using the matched filter in this section. Also, using the matched filter outputs, we identify the relationship between multiple access interference (MAI) and the cross-correlations between different users' spreading signals.

#### 1.3.1 Matched Filter in a Synchronous CDMA system

The matched filter is actually optimal for an AWGN channel without MAI but it is actually sub-optimal in a CDMA system. This is because MAI is approximated as random noise in this detection scheme but this approximation is not accurate [4]. However, this scheme is widely used in CDMA systems due to its simplicity. It is also commonly used as the initial or zeroth stage of more complicated multiuser detection schemes.

For the detection of the  $k$ -th user signal in a synchronous CDMA system, we assume knowledge of its spreading signal,  $s_k(t)$ , and phase,  $\theta_k$ . Using (1.16), the received signal  $r(t)$  is coherently detected using the matched filter of user  $k$ ,  $\text{MF}_k$ , which correlator outputs for user  $k$  is:

$$\begin{aligned} y_k &= \text{Re} \left\{ \int_0^{T_b} r(t) e^{-j\theta_k} s_k(t) dt \right\} \\ &= A_k b_k + \text{Re} \left\{ \sum_{j=1, j \neq k}^K \alpha_j b_j \rho_{j,k} e^{-j\theta_k} \right\} + n_k \end{aligned} \quad (1.18)$$

where  $y_k$  is defined as user  $k$ 's correlation value,  $r(t)$  is defined in (1.16),  $\alpha_k$  is the received complex amplitude,  $T_b$  is the bit period,  $\rho_{j,k}$  is the cross-correlation of  $s_j(t)$  on  $s_k(t)$ :

$$\rho_{j,k} = \int_0^{T_b} s_j(t)s_k(t) dt \quad (1.19)$$

and

$$n_k = \text{Re} \left\{ \int_0^{T_b} n(t)e^{-j\theta_k} s_k(t) dt \right\} \quad (1.20)$$

is a Gaussian random variable with zero mean and variance equals to  $N_0/2$ . To estimate the transmitted data, the decision bit of  $k$ th user,  $\hat{b}_k$ , is

$$\hat{b}_k = \text{sgn}\{y_k\} \quad (1.21)$$

where

$$\text{sgn}\{x\} = \begin{cases} 1 & \text{for } x \geq 0 \\ -1 & \text{otherwise} \end{cases} \quad (1.22)$$

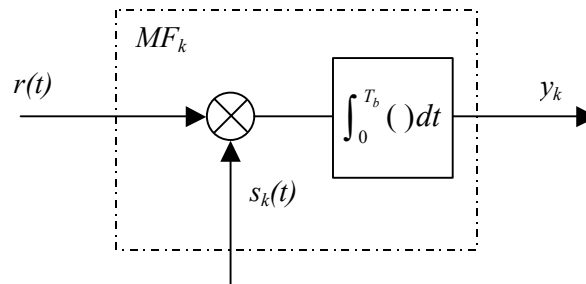


**Figure 1.2:** Matched filter of user  $k$

The correlation value in (1.18) consists of three terms. The first term contains the desired user  $k$ 's information while the third term is the noise correlation. The second term in (1.18) is the MAI term produced when the spreading signals are non-orthogonal. This non-orthogonality produces the cross-correlation  $\rho_{j,k}$ . If spreading signals are orthogonal, the cross-correlation term is zero and the MAI term is

eliminated.

In matrix-vector form, from (1.17), the correlators output in vector form is:

$$\begin{aligned}
 \mathbf{y} &= [y_1 \quad y_2 \quad \cdots \quad y_K]^T \\
 &= \mathbf{S}^T \mathbf{r} \\
 &= \mathbf{S}^T \mathbf{S} \mathbf{A} \mathbf{b} + \mathbf{S}^T \mathbf{n} \\
 &= \mathbf{R} \mathbf{A} \mathbf{b} + \mathbf{n}'
 \end{aligned} \tag{1.23}$$

where  $\mathbf{R}$  is the normalized cross-correlation matrix:

$$\mathbf{R} = \begin{bmatrix} 1 & \rho_{2,1} & \cdots & \rho_{K,1} \\ \rho_{1,2} & 1 & \cdots & \rho_{K,2} \\ \vdots & \vdots & \ddots & \vdots \\ \rho_{1,K} & \rho_{2,K} & \cdots & 1 \end{bmatrix}. \tag{1.24}$$

and  $\mathbf{S}$  is the spreading signal matrix,  $\mathbf{A}$  is received amplitude matrix,  $\mathbf{b}$  is the users' data bit vector,  $\mathbf{n}'$  is zero-mean Gaussian random vector with covariance

$$E[\mathbf{n}' \mathbf{n}'^T] = \frac{N_0}{2} \mathbf{R} \tag{1.25}$$

where  $N_0/2$  is the variance of  $\mathbf{n}'$  and  $\mathbf{R} = \mathbf{S}^T \mathbf{S}$ . In a synchronous CDMA system,  $\rho_{1,2} = \rho_{2,1}$ . The decision bit vector is

$$\hat{\mathbf{b}} = [\hat{b}_1 \quad \hat{b}_2 \quad \cdots \quad \hat{b}_K]^T = \text{sgn}\{\mathbf{y}\}. \tag{1.26}$$

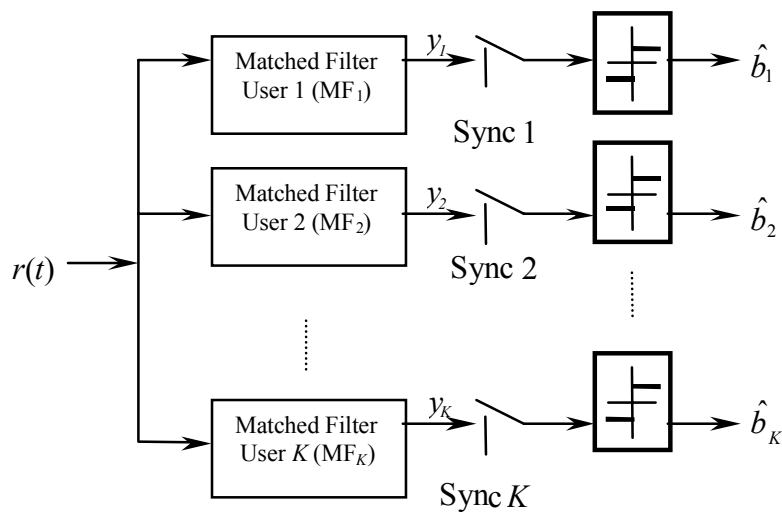


**Figure 1.3:** Bank of matched filters

### 1.3.2 Matched filter in an Asynchronous CDMA system

For an asynchronous CDMA system, from (1.13), the  $m$ -th correlation value of the  $k$ -th user is:

$$y_k(m) = A_k(m)b_k(m) + \sum_{j=1, j \neq k}^K MAI_{j,k}(m) + n_k \quad (1.27)$$

where  $MAI_{j,k}(m)$  is the MAI of the  $j$ -th user on the  $k$ -th user's  $m$ -th bit given by:

$$MAI_{j,k}(m) = \begin{cases} \text{Re}\{\alpha_j(m-1)e^{-j\theta_k(m)}\}b_j(m-1)\Gamma_{j,k}(m) \\ \quad + \text{Re}\{\alpha_j(m)e^{-j\theta_k(m)}\}b_j(m)\bar{\Gamma}_{j,k}(m) & ; \tau_j > \tau_k \\ \text{Re}\{\alpha_j(m)e^{-j\theta_k(m)}\}b_j(m)\Gamma_{j,k}(m) \\ \quad + \text{Re}\{\alpha_j(m+1)e^{-j\theta_k(m)}\}b_j(m+1)\bar{\Gamma}_{j,k}(m) & ; \tau_j < \tau_k \end{cases} \quad (1.28)$$

where  $\Gamma_{j,k}(m)$  and  $\bar{\Gamma}_{j,k}(m)$  are the continuous-time partial cross-correlation functions for bit  $m$  (modified from [22]):

$$\Gamma_{j,k}(m) = \begin{cases} \int_{(m-1)T+\tau_j}^{(m-1)T+\tau_k} s_k(t-\tau_k)s_j(t-\tau_j)dt & ; \tau_j > \tau_k \\ \int_{mT+\tau_j}^{mT+\tau_k} s_k(t-\tau_k)s_j(t-\tau_j)dt & ; \tau_j < \tau_k \end{cases} \quad (1.29)$$

$$\bar{\Gamma}_{j,k}(m) = \begin{cases} \int_{(m-1)T+\tau_j}^{mT+\tau_k} s_k(t-\tau_k)s_j(t-\tau_j)dt & ; \tau_j > \tau_k \\ \int_{mT+\tau_k}^{(m-1)T+\tau_j} s_k(t-\tau_k)s_j(t-\tau_j)dt & ; \tau_j < \tau_k \end{cases} \quad (1.30)$$

### 1.3.3 Multiple Access Interference in CDMA systems

From (1.18), (1.27) and (1.28), it is observed that the MAI term is dependent on the number of users  $K$ , the cross-correlation term  $\rho_{j,k}$  and the received amplitude (or power) of the interfering users  $\alpha_k$ . As the number of users increases, the MAI

increases. This degrades the signal-to-interference ratio and thus reduces the reliability of using the correlation values  $y_k$  for data estimation.

As mentioned earlier, the cross-correlation term can be eliminated using orthogonal codes. However, in practical implementation, multipath propagation and asynchronous transmission make this almost impossible. Therefore, the alternative is using sets of spreading codes that have very good cross-correlation properties.

Another method of mitigating the effect of the MAI term is through power control. By controlling the users' transmitted powers  $\varepsilon_k$ , we reduce the risk of having a high-power user (due to channel conditions) causing excessive interference to other users. However, in fast fading channels, it is difficult to have good power control because of the rapid changes in the received powers.

To allow CDMA to display its full potential, multiuser detection schemes have been exhaustively researched on for the last few years. Interference cancellation (IC) schemes are a group of multiuser detectors that operate on the concept of signal regeneration and cancellation based on data estimates. It has shown tremendous potential due to its more linear complexity as compared to other multiuser detectors.

Successive (or serial) interference cancellation (SIC) and parallel interference cancellation (PIC) are the two basic IC schemes. These two schemes have their own sets of strengths and weaknesses. Advanced IC schemes are built on these two schemes to utilize the strengths of these two schemes. However, like other multiuser detectors, IC schemes need to overcome many issues such as computation complexity and processing time. A review of these multiuser detection schemes is presented in Chapter 2.

## 1.4 Motivation and Contribution

Apart from the BER performance, computation complexity and processing time are the next two most important considerations for multiuser detection. The maximum likelihood detector, also known as the optimum detector, has the best BER performance amongst all multiuser detectors. However, it has very high computation complexity and therefore, not practical for implementation [4]. Linear detectors such as the decorrelating detector and the MMSE detector have a lower computation complexity but suffer from difficulty in calculating the inverse cross-correlation matrix  $\mathbf{R}^{-1}$ . IC schemes, on the other hand, have computation complexity linear with the number of users. However, there are many types of IC schemes, and each of them has its own level of computation complexity, processing time and BER performance. Therefore, the objective of this thesis is to improve the IC schemes in one or more of these areas.

Although there are comparisons of the BER performance between different IC schemes, there are no standard ways to measure computation complexity and processing delay. Therefore, to analyze the IC schemes with respect to these two considerations, we introduced three parameters in this thesis. These parameters are number of multiplications per bit (NMB), number of additions per bit (NAB) and processing time block (PTB). NMB and NAB are used to measure the relative computation complexity of different IC schemes while PTB is used to measure their relative processing time. Using these parameters, we establish basic operation constants to analyze any IC schemes with respect to their computation complexity and processing time.

From our analysis, we establish that advanced IC schemes such as the SIC with re-matched filtering (SICRM) have very high computation complexity compared to

basic IC schemes such the SIC and the PIC. However, advanced IC schemes can achieve much better BER performance than basic IC schemes. Also, SIC schemes have an overall better BER performance than PIC schemes especially in a fading channel or AWGN channel with high MAI. But SIC schemes have long processing time because the users are processed in series. Therefore, we consider the methods to implement IC schemes, particularly SIC types, at lower computation complexity and shorter processing time without sacrificing the BER performance.

For this purpose, we propose the cross-correlation implementation (CCI) for IC schemes. Using the users' spreading signals, the cross-correlations between different pairs of users are calculated. The MAI of different users are estimated using the cross-correlation values and interference cancellation is performed using the estimated MAI. This is a different approach because interference cancellation is usually carried out using the users' regenerated signals in the literature. The CCI reduces the arithmetic operations, and thus, reduces the computation complexity. Since the CCI is an alternate implementation, there is no degradation in the performances of CCI-IC schemes. When applied to advance IC schemes, the reduction in the computation complexity is up to 85%. The CCI also reduces the processing time of SIC schemes up to a third of their original values.

In another approach, we look for better IC schemes by improving the BER performance. Using the SIC as our basic scheme, we aim to improve it without introducing too much computation complexity and processing time as other advanced schemes have.

With these considerations, we propose an improved successive interference cancellation scheme (ISIC). The ISIC uses selective pre-cancellation techniques to make the signals more reliable for detection. The selective pre-cancellation technique

incorporates an adaptive bit-select cancellation (ABC) device for optimum performance in different channel conditions. The ISIC has a capacity that is 40% better than PIC in the AWGN channel and 26% better than the SIC in the Rayleigh fading channel. The improved scheme is also very resistant against amplitude estimation errors. Compared to the SIC, this scheme requires up to 50% additional computation complexity and about 15% increase in processing delay. This is considered very low as compared to the pipelined SIC, another advanced IC considered in this thesis, which could increase the computation complexity of the SIC up to ten times and the processing delay up to 30%.

## 1.5 Thesis Outline

In this chapter, we presented the CDMA system model and identified the MAI problem in the conventional detection in CDMA. Chapter 2 presents our literature review on existing multiuser detection schemes. We also discuss in greater details some of the existing interference cancellation schemes. In Chapter 3, we simulate and compare the BER performance of some of the interference cancellation schemes discussed in Chapter 2. In the same chapter, we analyze and compare the computation complexity and processing time of various known interference cancellation schemes. Chapter 4 introduces the CCI for IC schemes to reduce the computation complexity and processing time of some of the advanced interference cancellation schemes. In Chapter 5, we propose the ISIC scheme that has low computation complexity and very good BER performance in both AWGN and fading channel. Chapter 6 concludes the thesis and provides some suggestions for future research.



## CHAPTER 2

### MULTIUSER DETECTION – LITERATURE REVIEW

The performance of the matched filter discussed in the previous section is severely limited by the MAI term. However, interference can be completely or partially eliminated if better receivers are designed. These receivers can be divided into two categories – improved single-user detectors and multiuser detectors. This chapter focuses only on the latter.

Multiuser detection, also referred as ‘joint detection’, uses the spreading signals and timing information of multiple users to improve the detection of each individual user. This chapter discusses some of the main techniques available for multiuser detection. The strengths and weaknesses of these techniques are discussed as well.

#### 2.1 Optimum Multiuser Detector

In 1986, Verdu proposed the maximum likelihood sequence estimator, also known as the optimum detector [6]. For synchronous CDMA, the optimum detector chooses the most probable combination of the transmitted bits corresponding to the  $K$  users,  $\hat{\mathbf{b}} = [\hat{b}_1 \ \hat{b}_2 \ \dots \ \hat{b}_K]^T$ , given the received signal observed over the time interval  $0 \leq t \leq T_b$  [4]. This combination is jointly optimum. Optimum detection assumes knowledge of the timing of every user as well as knowledge (or estimate) of the complex amplitudes and spreading signals (or cross-correlations) of all users.

Consider a jointly optimum detection for a synchronous CDMA system described in (1.16). For simplification of this discussion, we assume that  $\theta_k = 0$  for all users. Therefore, given knowledge of the received amplitude,  $\alpha_k$ , and the signature of each user,  $s_k(t)$ , the optimum detector computes the estimated data sequence  $\hat{\mathbf{b}}$  from the received signal  $r(t)$  that gives the minimum value of the log-likelihood function [5]:

$$\begin{aligned}\Lambda(\hat{\mathbf{b}}) &= \int_0^{T_b} [r(t) - \sum_{k=1}^K \alpha_k \hat{b}_k s(t)]^2 dt \\ &= \int_0^{T_b} r^2(t) dt - 2 \int_0^{T_b} r(t) \sum_{k=1}^K \alpha_k \hat{b}_k s(t) dt + \int_0^{T_b} [\sum_{k=1}^K \alpha_k \hat{b}_k s(t)]^2 dt \\ &= \int_0^{T_b} r^2(t) dt - 2 \sum_{k=1}^K \alpha_k \hat{b}_k y_k + \sum_{k=1}^K \sum_{j=1}^K \alpha_k \alpha_j \hat{b}_k \hat{b}_j \rho_{j,k}\end{aligned}\quad (2.1)$$

The first integral can be discarded because it is common for all possible combinations of  $\hat{\mathbf{b}}$ . Therefore, (2.1) can be rewritten to maximize:

$$\begin{aligned}\Lambda(\hat{\mathbf{b}}) &= 2 \sum_{k=1}^K \alpha_k \hat{b}_k y_k - \sum_{k=1}^K \sum_{j=1}^K \alpha_k \alpha_j \hat{b}_k \hat{b}_j \rho_{j,k} \\ &= 2\hat{\mathbf{b}}^T \mathbf{A} \mathbf{y} - \hat{\mathbf{b}}^T \mathbf{H} \hat{\mathbf{b}}\end{aligned}\quad (2.2)$$

where  $\mathbf{A}$  is the received amplitude matrix defined in (1.17),  $\mathbf{y}$  is the correlation value vector defined in (1.23) and

$$\mathbf{H} = \mathbf{A} \mathbf{R} \mathbf{A} \quad (2.3)$$

is the unnormalized cross correlation matrix with  $\mathbf{R}$  defined in (1.24).

Although the optimum detector provides the best performance amongst all the detectors [4], it must compute  $2^K$  combinations of  $\Lambda(\hat{\mathbf{b}})$  and selects the sequence  $\hat{\mathbf{b}}$  of length  $K$  that corresponds to the largest  $\Lambda(\hat{\mathbf{b}})$  value. This is not practical as the computation complexity increases exponentially with the number of simultaneous transmitting users. This limits the usage of optimum detectors to an extremely small

number of users, to about  $K < 10$  [5]. Therefore, sub-optimal detectors are needed with a complexity that grows linearly with  $K$ .

## 2.2 Decorrelating Detector

This detector is a sub-optimal linear multiuser detector first proposed in [7,8]. Linear detectors are detectors that have linear decision regions. The decorrelating detector, also known as the decorrelator, is extensively analysed by Lupas and Verdu in [9,10]. It is a simple and natural scheme that is optimal according to three criteria: least-squares, near-far resistance and maximum likelihood when the received users' amplitudes are unknown [4].

From (1.23), as noise vector  $\mathbf{n}'$  is Gaussian,  $\mathbf{y}$  can be modelled by a  $K$ -dimensional Gaussian probability density function (pdf) with mean  $\mathbf{R}\mathbf{A}\mathbf{b}$  and covariance  $\mathbf{R}$  (assuming that  $\mathbf{R}$  has an inverse matrix  $\mathbf{R}^{-1}$ ) i.e.

$$p(\mathbf{y} | \mathbf{b}) = \frac{1}{\sqrt{(2\pi)^K \det \mathbf{R}}} \exp\left[-\frac{1}{2}(\mathbf{y} - \mathbf{R}\mathbf{A}\mathbf{b})^T \mathbf{R}^{-1}(\mathbf{y} - \mathbf{R}\mathbf{A}\mathbf{b})\right] \quad (2.4)$$

The decorrelating detector minimizes the likelihood function,

$$\Lambda(\hat{\mathbf{b}}) = (\mathbf{y} - \mathbf{R}\mathbf{A}\hat{\mathbf{b}})^T \mathbf{R}^{-1}(\mathbf{y} - \mathbf{R}\mathbf{A}\hat{\mathbf{b}}), \quad (2.5)$$

where  $\hat{\mathbf{b}}$  is the bit estimate vector. To minimize (2.5), the best linear estimate of  $\mathbf{b}$ , defined as  $\mathbf{b}^0$ , is:

$$\begin{aligned} \mathbf{b}^0 &= \mathbf{R}^{-1}\mathbf{y} \\ &= \mathbf{A}\mathbf{b} + \mathbf{R}^{-1}\mathbf{n}'. \end{aligned} \quad (2.6)$$

A detailed derivation of (2.6) is shown in Appendix A. This is the maximum likelihood estimate of  $\mathbf{b}$  obtained by performing a linear transformation of the outputs from the matched filters. Therefore, the decision bit vector is:

$$\begin{aligned}\hat{\mathbf{b}} &= \text{sgn}\{\mathbf{b}^0\} \\ &= \text{sgn}\{\mathbf{R}^{-1}\mathbf{y}\}\end{aligned}\quad (2.7)$$

Implementation of the decorrelating detector on the synchronous model is shown in Figure 2.1.

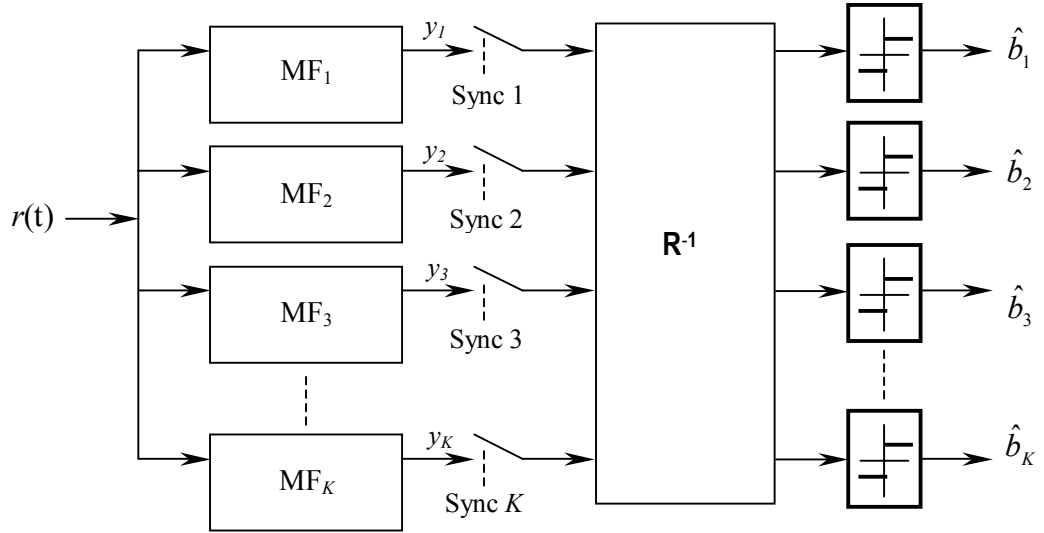


**Figure 2.1:** Decorrelating detector for synchronous channel

The two important features that the decorrelator are that it does not need the knowledge of the received users' amplitudes and it can be readily decentralized, i.e. the demodulation of each user can be implemented independently [4]. Also, the computation complexity does not grow exponentially with the increase in users as it would in the optimum detector. In addition to that, there are computational efficient methods to obtain solutions to (2.6) and one of them is the square-root factorization [5].

One problem with using the decorrelator is that it might enhance the background noise (shown in (2.6)). The norm of  $\mathbf{R}$  is not always less than or equal to unity. This could give the new noise vector,  $\mathbf{R}^{-1}\mathbf{n}'$ , a greater variance. Also, the spreading code assignments needs to be looked into carefully to ensure that the inverse of  $\mathbf{R}$  exists.

### 2.3 Linear Minimum Mean Square Error (MMSE) Detector

Another approach to linear multi-user detection is the minimum mean square error (MMSE) detector which takes background noise into consideration [11]. The decorrelator detector described previously solves (2.5) by using the maximum likelihood estimate of  $\mathbf{b}$ . The MMSE detector uses a different approach to that equation.

Consider an estimate of users' data bit matrix  $\mathbf{b}$  defined as:

$$\mathbf{b}^0 = \mathbf{M}\mathbf{y} \quad (2.8)$$

where the matrix  $\mathbf{M}$  minimizes the mean square error (MSE) function:

$$\begin{aligned} J(\mathbf{b}) &= E[(\mathbf{A}\mathbf{b} - \mathbf{b}^0)^T (\mathbf{A}\mathbf{b} - \mathbf{b}^0)] \\ &= E[(\mathbf{A}\mathbf{b} - \mathbf{M}\mathbf{y})^T (\mathbf{A}\mathbf{b} - \mathbf{M}\mathbf{y})]. \end{aligned} \quad (2.9)$$

Solving (2.9) (details can be found in Appendix B), we obtain  $\mathbf{M}$  that minimizes (2.9):

$$\mathbf{M} = [\mathbf{R} + \frac{N_0}{2} \mathbf{B}^{-1}]^{-1}. \quad (2.10)$$

where  $\mathbf{B}$  is a diagonal matrix with diagonal elements  $\{\alpha_k^2, 1 \leq k \leq K\}$ . Therefore, the decision bit vector for MMSE detector is:

$$\begin{aligned} \hat{\mathbf{b}} &= \text{sgn}\{\mathbf{b}^0\} \\ &= \text{sgn}\{\mathbf{M}\mathbf{y}\} \\ &= \text{sgn}\{[\mathbf{R} + \frac{N_0}{2} \mathbf{B}^{-1}]^{-1} \mathbf{y}\}. \end{aligned} \quad (2.11)$$

For the MMSE, the linear transformation  $\mathbf{R}^{-1}$  of the decorrelator in Figure 2.1 is replaced by  $[\mathbf{R} + \frac{N_0}{2} \mathbf{B}^{-1}]^{-1}$  in Figure 2.2.

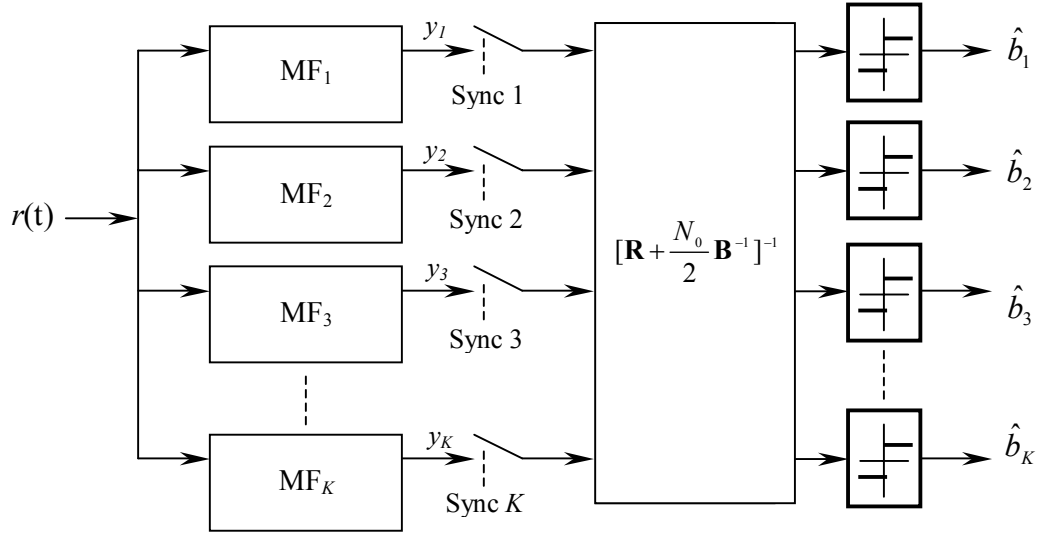


**Figure 2.2:** MMSE detector for synchronous channel

One interesting property of the linear MMSE detector is that it becomes a matched filter or a decorrelator at certain limits. For example, for synchronous CDMA, if  $\alpha_1$  is held fixed and  $\alpha_2, \dots, \alpha_K \rightarrow 0$ , the first row of  $[\mathbf{R} + \frac{N_0}{2} \mathbf{B}^{-1}]^{-1}$  tends to

$$\left[ \frac{\alpha_1^2}{\alpha_1^2 + N_0/2} \quad 0 \quad \dots \quad 0 \right] \quad (2.12)$$

which corresponds to the matched filter for user 1. As noise power increase  $[\mathbf{R} + \frac{N_0}{2} \mathbf{B}^{-1}]^{-1}$  becomes a strongly diagonal matrix, the MMSE detector approaches the conventional matched filter. Also, as the signal-to-noise ratio (SNR) goes to infinity, then  $[\mathbf{R} + \frac{N_0}{2} \mathbf{B}^{-1}]^{-1} \rightarrow \mathbf{R}^{-1}$ , i.e. the MMSE approaches a decorrelator.

To compute the value of  $\mathbf{b}^0$ , the set of linear equation

$$[\mathbf{R} + \frac{N_0}{2} \mathbf{B}^{-1}] \mathbf{b}^0 = \mathbf{y}, \quad (2.13)$$

is solved efficiently by computing using a square-root factorisation of the matrix  $[\mathbf{R} + \sigma^2 \mathbf{A}^{-2}]^{-1}$  [5].

## 2.4 Interference Cancellation Schemes

So far, we have discussed the matched filter, the optimum receiver and two linear detectors – the decorrelating detector and the MMSE detector. Now, we look at one type of the non-linear detectors – interference cancellation (IC) schemes. These schemes have non-linear decision regions. IC schemes has a more linear increase in computation complexity as the number of users increases as compared to the linear detectors because they do not require the calculation of the inverse cross-correlation matrix  $\mathbf{R}^{-1}$ .

### 2.4.1 Interference Cancellation Basic Building Block

Unlike the detectors discussed in the previous chapters, interference cancellation scheme (IC) attempts to mitigate the MAI by regenerating the interfering users' signals using known or estimated channel parameters (phase, delay, amplitude) and canceling the regenerated signals from the received signal before data detection of the desired user.

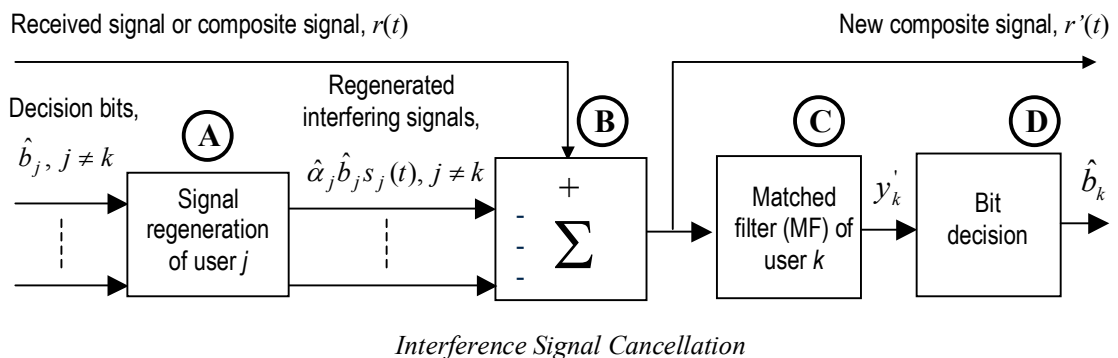


**Figure 2.3:** Basic building blocks of interference cancellation scheme (for data detection of user  $k$ )

If a cancellation is done correctly, there will be less one interfering user in the received signal. However, an erroneous cancellation results in doubling that user's

MAI contribution (four times in terms of power) [12]. In this subsection, we discuss the basic building block on which all IC schemes are based on. Figure 2.3 shows this basic building block for data detection of user  $k$ .

In *Block A*, decision bits of interfering users are used to regenerate their signals. These regenerated signals are used in *Block B* to remove the interference to user  $k$  in the received signal (or composite signal from previous cancellations). This produces a new composite signal,  $r'(t)$ , that can be used in future cancellations. *Block C* is user  $k$ 's matched filter that produces the corresponding correlation value from  $r'(t)$  while *Block D* performs bit detection based on the correlation value.

There are many methods to implement Figure 2.3. One of them is the serial interference cancellation (SIC) [4]. In this system, users are cancelled from the received signal in decreasing order of their signal “strength”. This method is based on the assumption that a user with higher received signal strength can be detected more reliably. After detection, the correlation value or decision bit of the desired user is used to regenerate its signal and this signal is cancelled from the received signal,  $r(t)$ .

The SIC ranks all the users according to their received signal strength and cancels them in the decreasing order. Note that for user  $k$ , the interfering users' signals that are regenerated in *Block A* for the SIC are those that has already been detected before user  $k$ .

Another IC scheme is based on parallel interference cancellation (PIC) [13]. In this scheme, all interfering users' signals are detected, regenerated and cancelled simultaneously from the received signal before coherent detection of the desired user. For detection of user  $k$  in PIC, the interfering users' signals that are regenerated in *Block A* are all users except user  $k$ .

Therefore, SIC is a scheme that cancels MAI one by one in series, while PIC, on



the other hand, cancels all the MAI at once. To improve the performance of IC schemes, these two basic schemes are used to form enhanced techniques in advanced IC schemes. However, this is at the cost of additional complexity and processing time. Examples of such advanced IC schemes are the SIC with re-matched filtering [16] and pipelined SIC [17]. There are also hybrid interference cancellation schemes such as those in [20-23] that use a combination of both serial and parallel cancellation. Hybrid schemes are aimed more towards reducing the processing time of SIC (by integrating parallel cancellations into the scheme) while attempting to retain the performance (if not improving) and stability of SIC.

Another important feature of IC is that it can be implemented in multiple stages [24] to achieve better performance. Tentative decision bits are formed at the output of one stage. These decision bits, more reliable in the tentative stages, are used to generate the users' signals and perform interference cancellations in the following stages.

#### **2.4.2 Serial Interference Cancellation (SIC)**

The SIC detector was first proposed for DS-CDMA in [14] and [25]. The basic mechanism of the SIC is to rank all the users according to a certain criteria and perform interference cancellation in that order. The zeroth and first stage schematic of a conventional  $S$ -stage SIC is shown in Figure 2.4.

The received signal  $r(t)$  is used to coherently detect all the users through a bank of  $K$  matched filters. This bank of matched filter is also known as the initial or zeroth stage. The zeroth stage outputs  $K$  correlation values  $y_k$  defined in (1.18).

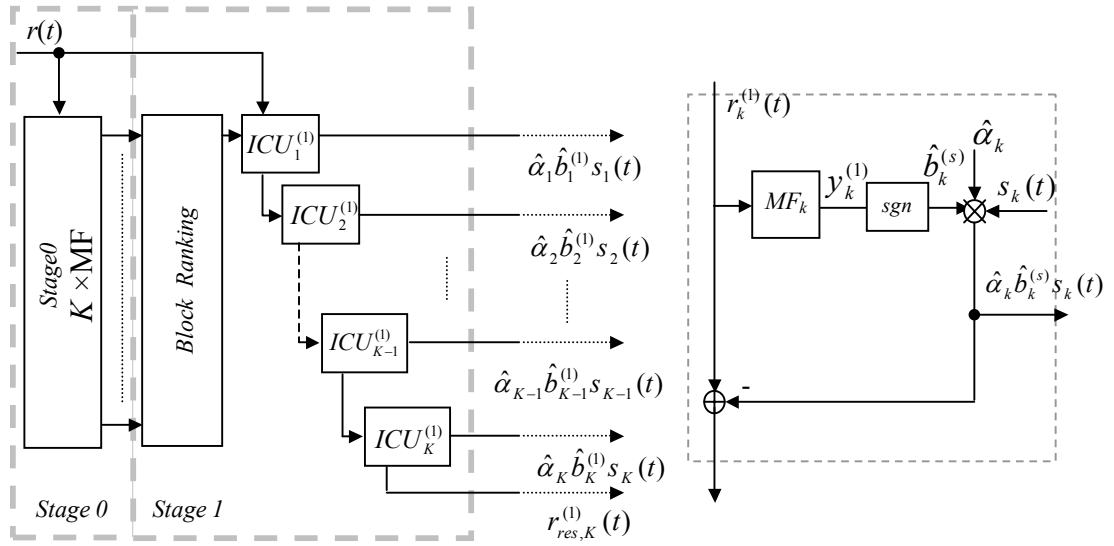


**Figure 2.4:** SIC schematics – stage 0 and 1 (left) and its ICU unit (right)

After the zeroth stage, ranking is performed based on the users' signal strength. There are basically two methods of measuring the users' signal strength - the absolute value of the correlation value  $y_k$  (known as correlation ranking) or the received power as an estimate of the signal strength (known as power ranking). (Note: Ranking the users according to their estimated received amplitude is equivalent to power ranking). A performance comparison between these two ranking methods is shown in [27].

If the bits are processed in terms of blocks of  $M$  bits (usually in asynchronous systems), the averaged value is used. Therefore, for correlation ranking, the average absolute correlation value of user  $k$ , defined as:

$$\bar{y}_k = \frac{1}{M} \sum_{m=1}^M |y_k(m)| \quad (2.14)$$

is used while for power ranking, the averaged received amplitude defined as:

$$\bar{\alpha}_k = \frac{1}{M} \sum_{m=1}^M |\hat{\alpha}_k(m)| \quad (2.15)$$

is used. Note that the absolute function used in (2.14) and (2.15) is defined as:

$$|x| = \begin{cases} x & \text{for } x \geq 0 \\ -x & \text{for } x < 0 \end{cases} \quad (2.16)$$

The users are ranked in descending order. User 1 is assigned as the user with the highest signal strength; user 2 is the second strongest user and so on. User  $K$  is the weakest user and last to be detected.

User 1 is coherently detected and from its correlation value,  $y_k$ , its stage 1's decision bit is obtained ( $\hat{b}_1^{(1)} = \text{sgn}\{y_1\}$  where the subscript denotes the user and the superscript denotes the current stage). Then,  $\hat{b}_1^{(1)}$  is multiplied with the estimated channel coefficient,  $\hat{\alpha}_1$ , and the spreading signal  $s_1(t)$  to regenerate the user  $k$ 's received signal. This signal is then cancelled from the received signal.

These few steps are performed in an interference cancellation unit (ICU) shown in Figure 2.4. This removes user 1's signal from the received signal if bit detection of user 1 was correct. An incorrect  $\hat{b}_1^{(1)}$  results in adding another user 1 into the received signal.

With these few steps, we have effectively performed *Block A* (regeneration of user 1 as an interfering user to user 2) and *Block B* (cancellation of that interfering user's signal) of Figure 2.3 on user 2. *Block C* and *D* correspond to the matched filtering and bit detection of user 2 respectively.

The same cycle of signal regeneration, removal from the composite signal and detection is continued until every user has been detected and cancelled from the composite received signal.

For the selected  $k$ -th user, the stage 1 composite signal,  $r_k^{(1)}$ , and the resulting correlation value,  $y_k^{(1)}$ , after  $k-1$  users are cancelled are:

$$r_k^{(1)}(t) = r(t) - \sum_{j=1}^{k-1} \hat{\alpha}_j \hat{b}_j^{(1)} s_j(t), \quad (2.17)$$

$$y_k^{(1)} = y_k - \operatorname{Re}\left\{\sum_{j=1}^{k-1} \hat{\alpha}_j e^{-j\theta_k}\right\} \hat{b}_j^{(1)} \rho_{j,k} \quad (2.18)$$

respectively where  $\hat{b}_k^{(1)} = \operatorname{sgn}\{y_k^{(1)}\}$ . At the end of stage 1, the residual composite received signal,  $r_{res,K}^{(1)}(t)$ , that is passed on to the next stage is:

$$r_{res,K}^{(1)}(t) = r(t) - \sum_{j=1}^K \hat{\alpha}_j \hat{b}_j^{(1)} s_j(t). \quad (2.19)$$

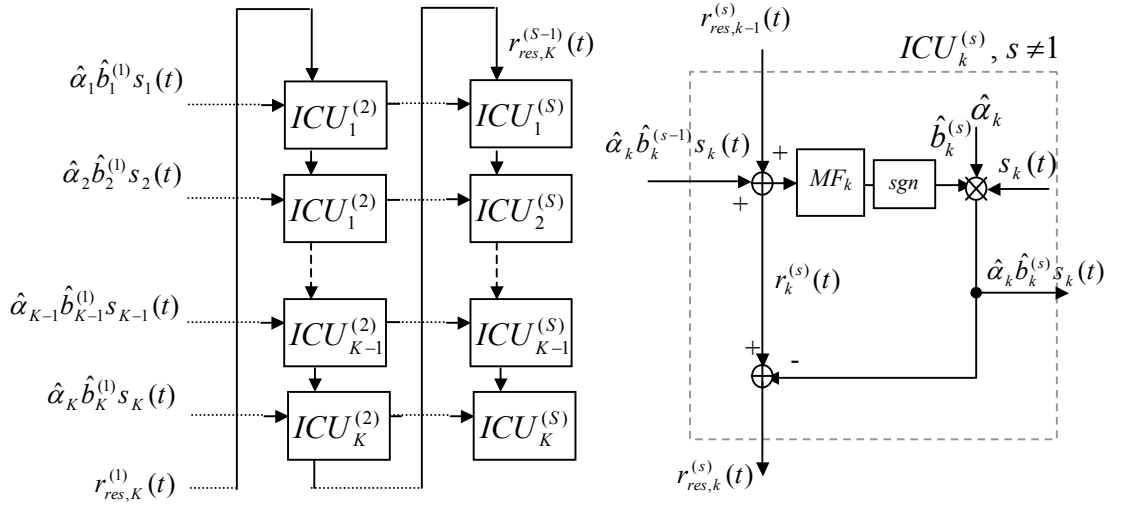


**Figure 2.5:** Stage 2 to  $S$ -th stage of  $S$ -stage SIC and its ICU unit

For the remaining stages (Figure 2.5), for the  $k$ -th interference cancellation unit of the  $s$ -th stage,  $ICU_k^{(s)}$ , these following steps are performed:

*Step 1:* After  $(k - 1)$  users has been cancelled, the residual signal,  $r_{res,k-1}^{(s)}(t)$ , is:

$$r_{res,k-1}^{(s)}(t) = r(t) - \sum_{j=k}^K \hat{\alpha}_j \hat{b}_j^{(s-1)} s_j(t) - \sum_{j=1}^{k-1} \hat{\alpha}_j \hat{b}_j^{(s)} s_j(t) \quad (2.20)$$

The second term in (2.20) is contributed by the interference cancellation performed in the previous stage while the third term is contributed by the interference cancellation performed in the current stage (before user  $k$ ). This residual signal is added to the user  $k$ 's regenerated signal from the

previous stage to produce  $k$ -th user's composite signal:

$$r_k^{(s)}(t) = r(t) - \sum_{j=k+1}^K \hat{\alpha}_j \hat{b}_j^{(s-1)} s_j(t) - \sum_{j=1}^{k-1} \hat{\alpha}_j \hat{b}_j^{(s)} s_j(t) \quad (2.21)$$

*Step 2:* The resulting signal is coherently detected, giving the  $k$ -th user's

correlation value,  $y_k^{(s)}$ , and decision bit,  $\hat{b}_k^{(s)}$ :

$$y_k^{(s)} = \text{Re} \left\{ y_k - \sum_{j=k+1}^K \hat{\alpha}_j e^{-j\theta_k} \hat{b}_j^{(s-1)} \rho_{j,k} - \sum_{j=1}^{k-1} \hat{\alpha}_j e^{-j\theta_k} \hat{b}_j^{(s)} \rho_{j,k} \right\}, \quad (2.22)$$

$$\hat{b}_k^{(s)} = \text{sgn} \{ y_k^{(s)} \}. \quad (2.23)$$

*Step 3:* Using  $\hat{b}_k^{(s)}$ , the  $k$ -th user's signal is regenerated and cancelled from  $r_k^{(s)}(t)$

and produces an updated residual signal

*Step 4:* *Step 1* is repeated for the next user,  $k+1$ , defined earlier through ranking in stage 1. The regenerated signal is also passed on to the  $(s+1)$ th stage.

Note that in *Step 1*, (2.21) performs *Block A* and *Block B* of Figure 2.3 while in *Step 2*, (2.22) and (2.23) represent *Block C* and *D* respectively.

These steps are repeated until all users have been detected in one stage, then the regenerated signals and residual received signal is passed on to the next stage. The final decision bit,  $\hat{b}_k^{(S)}$ , is from the  $S$ -th stage.

For an asynchronous channel, the time delay of the  $k$ -th user,  $\tau_k$ , is introduced. Also, we process the users block-wise with  $M$  bits in one block. Therefore, (2.17) is rewritten as:

$$r_k^{(1)}(t) = r(t) - \sum_{m=1}^M \sum_{j=1}^{k-1} \hat{\alpha}_j(m) \hat{b}_j^{(1)}(m) s_j(t - mT_b - \tau_j) \quad (2.24)$$

where  $T_b$  is the bit duration. Since the  $m$ -th bit of any user is now also either overlapped by the  $(m+1)$ th bit or the  $(m-1)$ th bit, the  $m$ -th correlation value of the  $k$ -th user after cancellations in stage 1 is:

$$y_k^{(1)}(m) = y_k(m) - \sum_{j=1}^{k-1} \hat{MAI}_{j,k}^{(1)}(m) \quad (2.25)$$

where

$$\hat{MAI}_{j,k}^{(s)}(m) = \begin{cases} \text{Re}\{\hat{\alpha}_j(m-1)e^{-j\theta_k(m)}\}\hat{b}_k^{(s)}(m-1)\Gamma_{jk}(m) \\ \quad + \text{Re}\{\hat{\alpha}_j(m)e^{-j\theta_k(m)}\}\hat{b}_k^{(s)}(m)\bar{\Gamma}_{jk}(m) & ; \tau_j > \tau_k \\ \text{Re}\{\hat{\alpha}_j(m)e^{-j\theta_k(m)}\}\hat{b}_k^{(s)}(m)\Gamma_{jk}(m) \\ \quad + \text{Re}\{\hat{\alpha}_j(m+1)e^{-j\theta_k(m)}\}\hat{b}_k^{(s)}(m+1)\bar{\Gamma}_{jk}(m) & ; \tau_j < \tau_k \end{cases} \quad (2.26)$$

is the  $s$ -th stage estimated MAI of the  $j$ -th user on the  $k$ -th user's  $m$ -th bit (equivalent to  $\text{Re}\{\hat{\alpha}_j e^{-j\theta_k}\}\hat{b}_k^{(s)}\rho_{j,k}$  in a synchronous channel) where  $\Gamma_{jk}(m)$  and  $\bar{\Gamma}_{jk}(m)$  are the continuous-time partial cross-correlation functions defined in (1.29) and (1.30) respectively. Also, for detection in subsequent stages ( $s > 1$ ), (2.21) and (2.22) are rewritten as:

$$r_k^{(s)}(t) = r(t) - \sum_{m=1}^M \sum_{j=k+1}^K \hat{\alpha}_j(m)\hat{b}_j^{(s-1)}(m)s_j(t-mT_b - \tau_j) - \sum_{j=1}^{k-1} \hat{\alpha}_j(m)\hat{b}_j^{(s)}(m)s_j(t-mT_b - \tau_j) \quad (2.27)$$

$$y_k^{(s)} = y_k(m) - \sum_{j=k+1}^K \hat{MAI}_{j,k}^{(s-1)}(m) - \sum_{j=1}^{k-1} \hat{MAI}_{j,k}^{(s)}(m) \quad (2.28)$$

respectively.

A few observations are made regarding the SIC. Firstly, the SIC requires the estimation of the received signal powers (or complex received amplitude) of the users for interference cancellation. Estimation errors produce residual multiuser interference, which degrades the performance of the scheme [5]. Secondly, the computation complexity in the demodulation of a user's data bit is linear in the number of users. Finally, the processing time of the SIC increases linearly with the number of users.

### 2.4.3 Parallel Interference Cancellation (PIC)

The PIC is proposed by Kohno [13,14] for one stage implementation and Varanasi [24] for multistage implementation. However, earlier structures have very high computation complexity. A simplified structure is shown in [15] and Figure 2.6.

In the single stage PIC receiver (shown in stage 1 of Figure 2.6), initial decision bits (provided by the zeroth stage bank of matched filters) are multiplied by their relative signal amplitudes and re-spread by their corresponding spreading signals to reproduce a delayed estimate of the received signal of each user.

All the regenerated signals are subtracted from the received signal. The desired user's regenerated signal is then added back to the resultant signal to produce a composite signal for detection of that particular user. This process is similar to cancelling all interfering users of the desired user from the received signal before matched filtering. The following matched filters produce  $K$  correlation values of the first stage,  $y_k^{(1)}$ . Signal regeneration, cancellation and detection are performed simultaneously (in parallel) for all the  $K$  users.

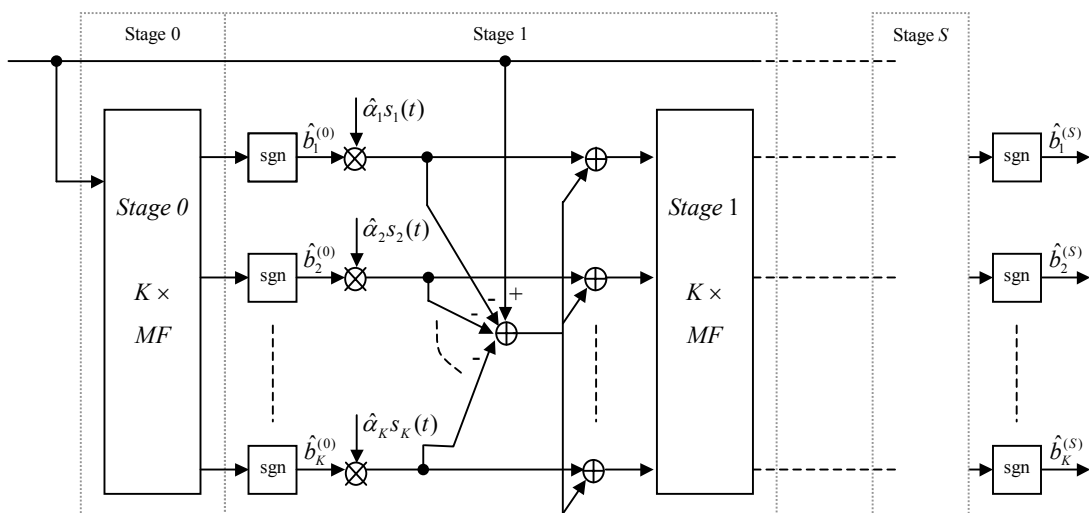


**Figure 2.6:**  $S$ -stage Parallel Interference Cancellation (PIC) scheme

The following stages have the same structure as the first stage. Using the correlation values from the previous stage, the signal regeneration, cancellation and addition process is repeated to produce the composite signal of the  $k$ -th user in the  $s$ -th stage:

$$r_k^{(s)}(t) = r(t) - \sum_{j=1, j \neq k}^K \hat{\alpha}_j \hat{b}_j^{(s-1)} s_j(t). \quad (2.29)$$

The corresponding matched filter output is:

$$y_k^{(s)} = y_k - \text{Re} \left\{ \sum_{j=1, j \neq k}^K \hat{\alpha}_j e^{-j\theta_k} \hat{b}_j^{(s-1)} \rho_{j,k} \right\}. \quad (2.30)$$

where  $\hat{b}_k^{(s)} = \text{sgn}\{y_k^{(s)}\}$  is the decision bit and  $\hat{\alpha}_j = \hat{A}_j e^{-j\theta_j}$  is the complex amplitude estimate.

Similar to the SIC, the PIC requires the estimation of the users' received powers for interference cancellation. Computation complexity of the PIC is also linear with the number of users. However, the processing time of the PIC is much shorter as compared to the SIC and independent of the number of the users because all the users are detected at the same time.



### 2.4.4 Serial Interference Cancellation with re-matched filtering (SICRM)

The SICRM is an advanced IC scheme that uses re-matched filtering to enhance the performance of the SIC. The SIC used in most research works [16,18] actually refers to this scheme.

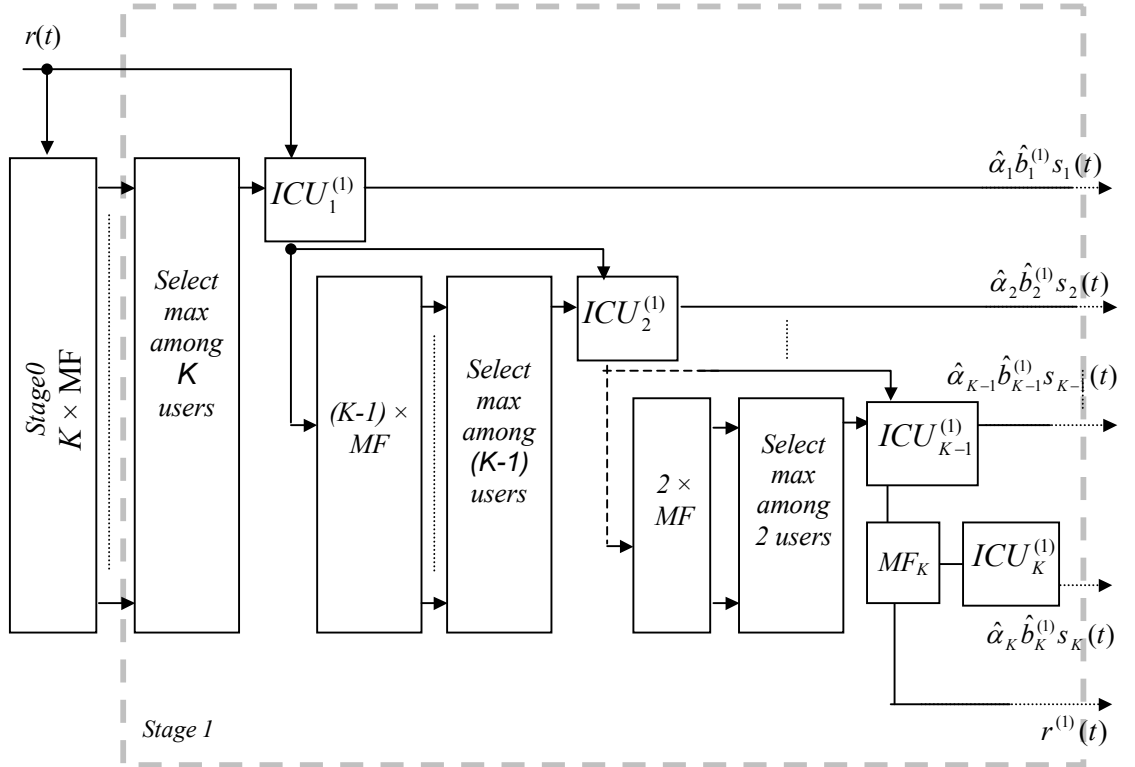


**Figure 2.7:** Stage 0 and stage 1 of serial interference cancellation with re-matched filtering

The zeroth and first stage of the SICRM is shown in Figure 2.7. Instead of fixing the rank of all users at the beginning of stage 1, the user with the highest correlation value (user 1), is coherently detected first. Then user 1's signal is regenerated and cancelled from the received signal. The composite signal is then passed through a bank of  $(K - 1)$  matched filters to coherently re-detect the remaining users. This produces  $(K - 1)$  correlation values of user 2 to user  $K$ .

The highest correlation value is then selected from these updated correlation values and the cycle of detection, signal regeneration and cancellation, and re-matched filtering is continued until all users have been detected.

After regeneration and cancellation of the  $k$ th user, the remaining  $(K - k)$  users' re-matched filtered correlation values, used to select user  $k+1$ , is given by:

$$y_{l,k}^{(1)} = y_l - \operatorname{Re}\left\{\sum_{j=1}^k \hat{\alpha}_j e^{-j\theta_l} \hat{b}_j^{(1)} \rho_{j,l}\right\} \quad l = k+1, \dots, K \quad (2.31)$$

Compared to the SIC, from (2.31), the SICRM requires an additional  $\frac{K(K-1)}{2}$  matched filters. However, (2.31) also removes the matched filters in stage 1's ICUs as shown in Figure 2.8. Thus, there is a reduction of  $K$  matched filters as well. Re-matched filtering is only applied to the first stage of the SIC due to the exponential increase in computation complexity (contributed by the additional matched filters).

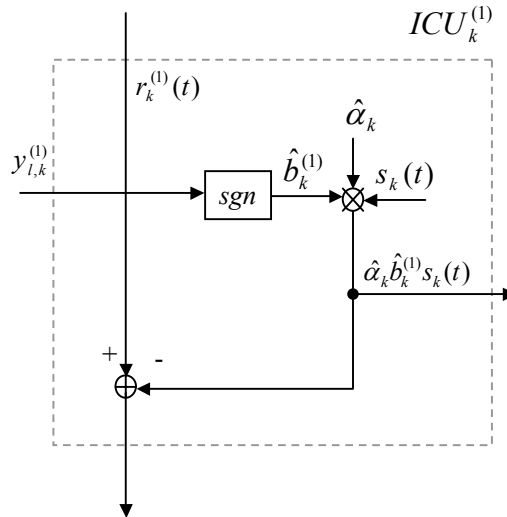


**Figure 2.8:** Stage 1's Interference Cancellation Unit (ICU) of SICRM

From Figure 2.7, it is observed that the SICRM uses correlation ranking. Unlike the SIC, the SICRM uses correlation values that is updated after each user is

cancelled. This increases the reliability of the correlation values and hence, improves the ranking of the users.

The SICRM follows the basic IC block in Figure 2.3. As each user is detected in their respective ICUs (Figure 2.8), its signal is interference to the next user in line to be detected. Therefore, for the detection of user  $k$ ,  $\hat{b}_{k-1}^{(1)}$  is used to regenerate user  $(k-1)$ 's signal (*Block A*), and then cancelled from the composite received signal (*Block B*) (Note: User 1 to user  $(k-2)$  has been cancelled from the composite received signal). Then, re-matched filtering is applied to the composite signal and this is equivalent to *Block C*. Finally, bit detection of user  $k$ , which is the user with the highest correlation value among the remaining  $(K-k+1)$  users, is performed as *Block D*.

## 2.5 Chapter Summary

In this chapter we have discussed some of the existing multiuser detection schemes - the matched filter, the optimum receiver, the decorrelating detector, the MMSE detector and the interference cancellation schemes. The matched filter, although very simple, suffers easily from near-far problems. The optimum receiver is too complex to be practically implemented, while the calculation of the inverse matrix in the decorrelating detector and the MMSE detector is still too large for practical implementation.

Interference cancellers, with computation complexity that grows linearly with the number of users, are discussed with some examples – the PIC, SIC and SICRM. We had established that all the IC schemes follow the IC basic building block in Section 2.3.1. This allows the introduction of an alternative basic building block in Chapter 4 that reduces the processing time and computation complexity.

In the next chapter, we analyze and compare the BER performance, computation complexity and processing time of the three interference cancellation schemes discussed earlier.

## **CHAPTER 3**

### **ANALYSIS OF INTERFERENCE CANCELLATION**

In this chapter, several comparative studies are performed among the few interference cancellation (IC) schemes described in Section 2.4. One of the benchmarks used is the BER performance – a measure of how reliable is the detector in data recovery. Computation complexity is another issue that is analyzed and discussed in Section 3.2. The processing time of IC schemes is discussed and analyzed in Section 3.3. A good IC scheme should have very good BER performance, low computation complexity and short processing time.

#### **3.1 BER Performance Comparison Between Different IC Schemes**

Simulations are carried out to compare the performance of the SIC, the SICRM and the PIC, although a comparative study between the SICRM and the PIC has been carried out in [27]. This is to establish the strengths and weaknesses of these three schemes. Also, this provides us a simulation platform to compare the performance of the new interference cancellation scheme introduced in Chapter 5.

The asynchronous CDMA system described in (1.13) is used. The amplitude, phase and time delays are assumed known (or perfectly estimated) at the receiver. The rationale behind this assumption is to see the optimum performance of these schemes (without channel estimation errors). The processing gain,  $N$ , is 31.

Two channel conditions have been considered – the AWGN channel (perfect power control) and a Rayleigh flat-fading channel with high SNR. In the AWGN

channel, it is assumed that all the users' received powers are equal. For the fading channel, the channel frequency used is 2GHz, the chip rate is 3.84 Mchips/s and the vehicular speed is 120km/h corresponding to a Doppler frequency of 222Hz. The model used for simulating the Rayleigh fading is Jakes' Model shown in [26]. In practice, frequency selective fading channel is more likely to happen. Fortunately, the use of RAKE receiver and under the assumptions that perfect estimation of path gains and delays are possible to remove the intersymbol interference, we can limit our simulation to only flat fading channel. The users' spreading codes used are long Gold codes as specified in the 3GPP standard specifications described in [35]. In this thesis, we have used the scrambling codes in [35] as the spreading codes and assignment of code numbers to different users is random.

The schemes that are compared here are the matched filter, 1-stage and 2-stage interference cancellation schemes – SIC using correlation ranking, SIC using power ranking, PIC and SICRM.

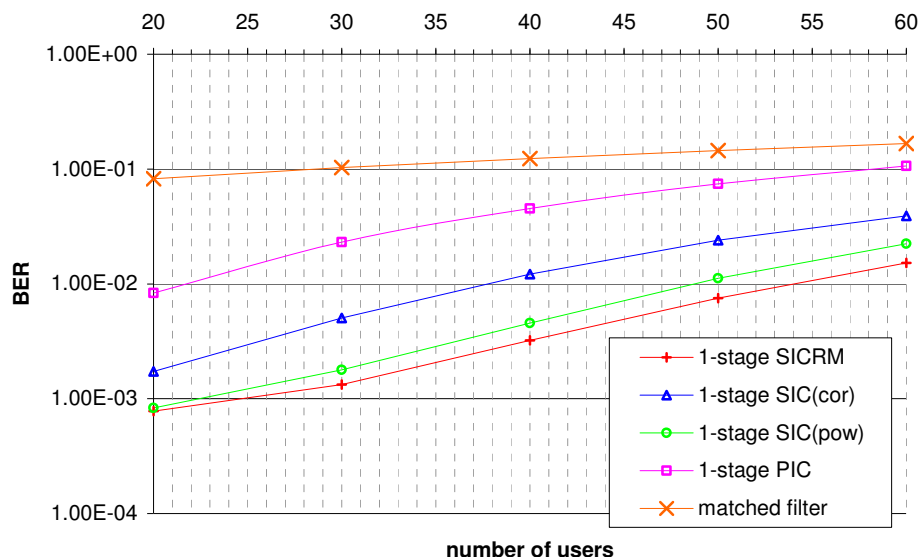


**Figure 3.1:** Performance of matched filter and 1-stage interference cancellers in Rayleigh channel, processing gain = 31,  $E_b/N_0 = 40$  dB, Doppler frequency = 222Hz

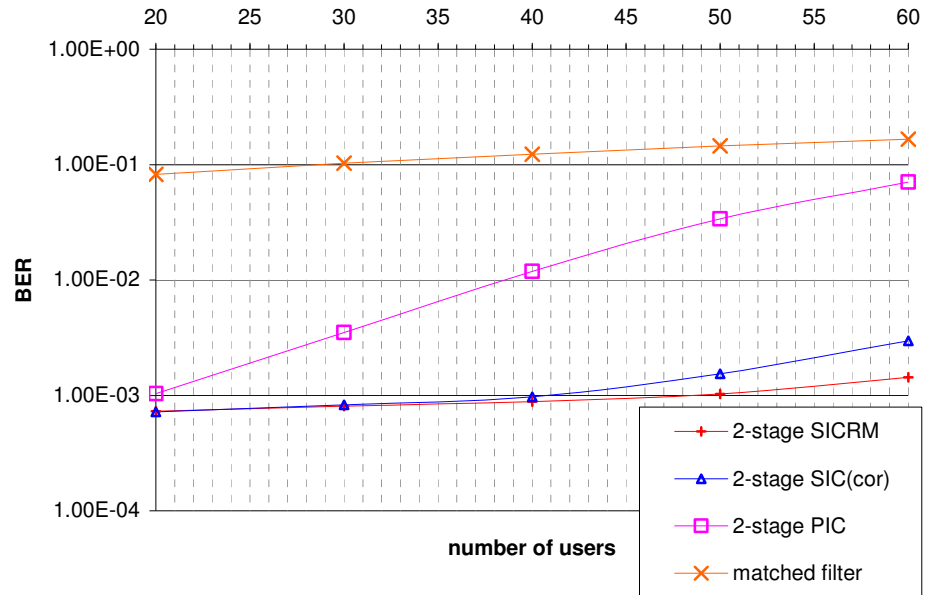


**Figure 3.2:** Performance of matched filter and 2-stage interference cancellers in Rayleigh channel, processing gain = 31,  $E_b/N_0 = 40\text{dB}$ , Doppler frequency = 222Hz

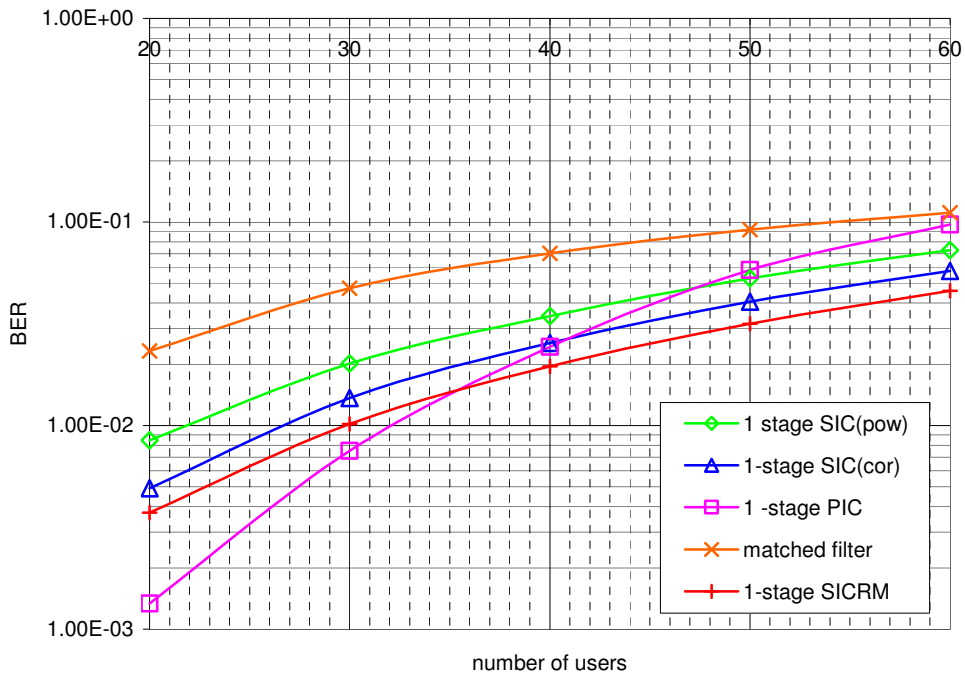


**Figure 3.3:** Performance of matched filter and 1-stage interference cancellers in AWGN channel, processing gain = 31,  $E_b/N_0 = 10\text{dB}$

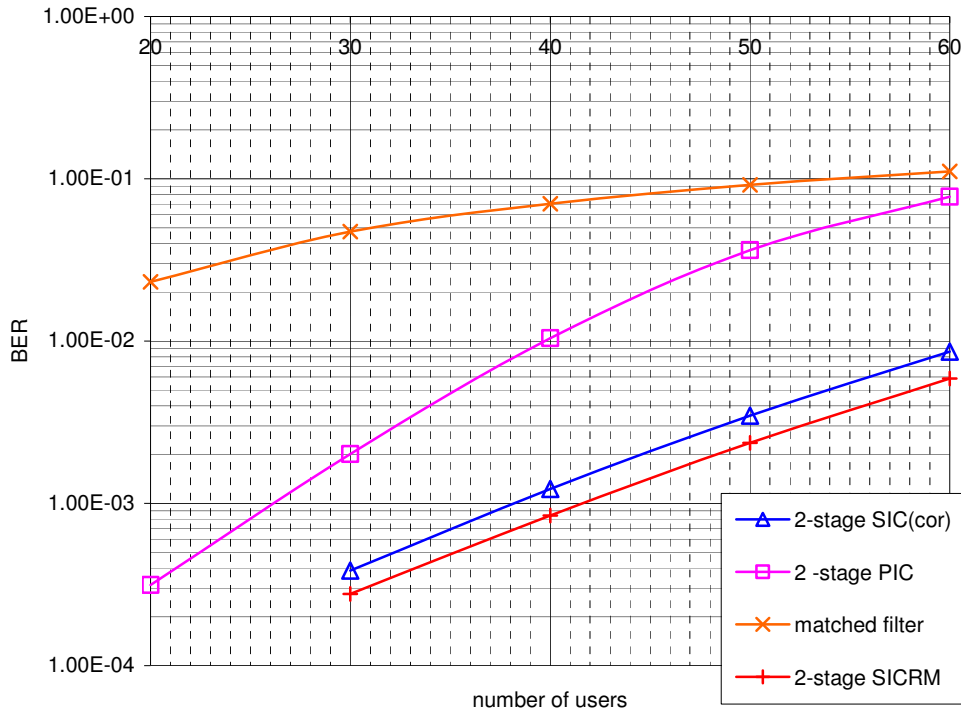


**Figure 3.4:** Performance of matched filter and 2-stage interference cancellers in AWGN channel, processing gain = 31,  $E_b/N_0 = 10\text{dB}$

From Figure 3.1, in a Rayleigh fading channel and at 1% BER, the 1-stage SICRM can support up to 54 users, which is 145% higher than the 1-stage PIC's capacity of 22 users. Also, its capacity is 42% better than the 1-stage SIC using correlation ranking and about 10% better than the 1-stage SIC using power ranking. In Figure 3.2, at 0.1% BER, when the number of stages increased to two, the SICRM have a capacity that is about 2½ times the capacity of the PIC.

From Figure 3.3, in an AWGN channel, the 1-stage PIC is shown to be better than the SIC at about 1% BER with a capacity that is 6% higher than the 1-stage SICRM, 18.5% better than the 1-stage SIC using correlation ranking and 45% better than the 1-stage SIC using power ranking. However, from Figure 3.4, the 2-stage SICRM has a capacity 57% higher than the capacity of the 2-stage PIC for a BER of 1%.

Although the PIC is better than the SICRM for a 1-stage implementation, when



$K > N$ , (i.e. high MAI) the SIC schemes start to outperform the PIC. Through these simulations, we have demonstrated that SIC schemes are superior to the PIC in Rayleigh fading but not in an ideal power control environment. Also, it is shown that the SIC have a higher BER performance improvement as the number of stages increases as compared to the PIC.

### 3.2 Computation Complexity

In the previous chapter, we have shown that the SIC scheme is superior to the PIC in a fading channel. Since practical environments are more likely to be a fading channel or imperfect power control is present, the SIC is a better choice if BER performance is the main consideration.

However, the SIC has a much higher processing time as compared to the PIC. Also, the SICRM, although having a higher capacity than the SIC, has a much higher computation complexity compared to the SIC or the PIC.

The computation complexity of an interference system depends mainly on a few factors:

- Number of matched filters;
- Number of signal regenerations (which translates to multiplication nodes);
- Number of cancellations (which translates to addition/subtraction nodes);
- User cancellation order (applicable to IC schemes using ranking system).

These factors also influence the processing time as well. However, it is not easy to quantify computation complexity. An attempt is made in this thesis for the first time in the literature. Two parameters are used to measure the computation complexity of interference cancellation schemes. These two parameters are the number of multiplications per bit ( $NMB$ ) and the number of additions per bit ( $NAB$ ), which are

defined as the total number of multiplications that is involved in processing one bit of every user (meaning  $K$  bits for  $K$  users) and the total number of additions or subtractions (negative addition) that is performed over one bit period respectively. To compare the different processing time, we introduce another parameter called the processing time block (PTB) in Section 3.3. In this section we discuss the computational complexity of various IC schemes. This will help us to set a platform for the introduction of an alternate implementation method in Chapter 4 to reduce the processing time and computation complexity of IC schemes.

To simplify the analysis later, synchronous CDMA described in (1.16) is used. Operations that contribute to  $NMB$  are matched filters (coherent detection of the signature waveform) and signal regenerations.  $NAB$  is contributed by the correlation involved in matched filters and the subtraction in signal cancellations. (Note: When a complex number is multiplied by another complex number, and the real value is taken, the number of multiplications involved is 2 and the number of addition is 1).

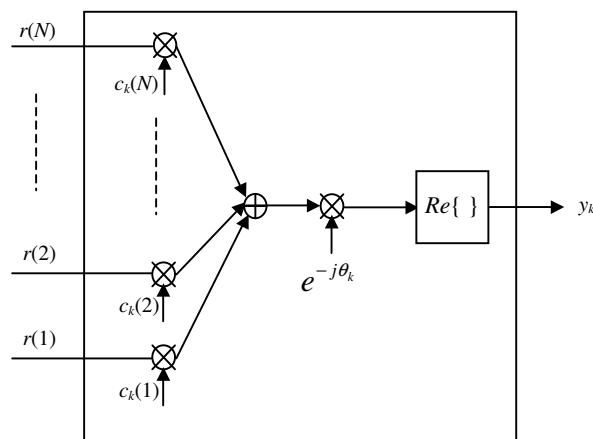


**Figure 3.5:** A matched filter of user  $k$

Within a matched filter (Figure 3.5), the  $N$  chip samples of the signal is first correlated with the corresponding spreading sequence of  $N$  chips ( $c_k(1), \dots, c_k(N)$ ), and this requires  $NMB$  of  $2N$  and  $NAB$  of  $2(N - 1)$ . Then, the correlation value is

multiplied with the phase conjugate,  $e^{-j\theta_k}$ , and the real value is taken (assuming BPSK), which gives  $NMB$  of 2 and  $NAB$  of 1. It is assumed that the phase of one bit is almost constant within one bit period. Thus, the number of multiplications per bit for each matched filter,  $NMB_{MF}$ , and the number of additions per bit for each matched filter,  $NAB_{MF}$ , are respectively given by:

$$NMB_{MF} = 2N + 2, \quad (3.1)$$

$$NAB_{MF} = 2N - 1. \quad (3.2)$$

where  $N$  is the processing gain.

For every signal regenerated, which is the generation of  $\hat{A}_k e^{j\theta_k} \hat{b}_k s_k(t)$ , the number of multiplications is  $4 + 2N$ . However, since  $\hat{A}_k$  and  $e^{-j\theta_k}$  are reused in subsequent stages after the first stage,  $\hat{A}_k e^{-j\theta_k} \hat{b}_k s_k(t)$  becomes  $\hat{\alpha}_k \hat{b}_k s_k(t)$ . Hence, the actual number of multiplications per bit for every signal regeneration is:

$$NMB_{RG} = 2 + 2N. \quad (3.3)$$

For every signal cancellation, the number of additions (or subtractions) per bit for every signal cancellation or summation,  $NAB_{CANC}$ , is

$$NAB_{CANC} = 2N. \quad (3.4)$$

Now, we have established the four basic computation complexity constants in (3.1) to (3.4). Using these four equations, we analyze the computation complexity of the SIC, the SICRM and the PIC.

For the conventional SIC described in Section 2.4.2, the number of matched filters includes the  $K$  matched filters in stage 0 and the subsequent  $S \times K$  matched filters inside the ICUs from stage 1 to stage  $S$  (Figure 2.4 and Figure 2.5). Therefore, the total number of matched filters is  $K(S + 1)$ .

Signal regeneration is performed after every decision bits starting from stage 1 to stage  $S$ . Therefore, the number of signal regenerations is  $S \times K$ . The number of cancellations is also  $S \times K$  as each signal regeneration is followed by a signal cancellation. The number of signal additions, performed in every ICU after stage 1, is  $(S-1) \times K$  because there are  $K$  ICUs in every stage. Thus, the number of multiplications per bit for the conventional SIC,  $NMB_{SIC}$ , and the number of additions (or subtractions) per bit,  $NAB_{SIC}$ , are respectively given by:

$$\begin{aligned}
 NMB_{SIC} &= K(S+1) \cdot NMB_{MF} + SK \cdot NMB_{RG} \\
 &= K(S+1)(2N+2) + SK(2N+2) = K(2S+1)(2N+2) \\
 NAB_{SIC} &= K(S+1) \cdot NAB_{MF} + (SK + (S-1)K) \cdot NAB_{CANC} \\
 &= K(S+1)(2N-1) + 2NK(2S-1)
 \end{aligned} \tag{3.5}$$

For the SICRM, as mentioned in Section 2.4.4, there are an additional  $\frac{K(K-1)}{2}$  number of matched filters used for re-matched filtering but there is also a reduction of  $K$  matched filters from stage 1's ICUs (Figure 2.8). Thus, the number of multiplications per bit for SICRM,  $NMB_{SICRM}$ , and the number of additions per bit,  $NAB_{SICRM}$  are respectively given by:

$$\begin{aligned}
 NMB_{SICRM} &= NMB_{SIC} + \frac{K(K-1)}{2} NMB_{MF} - K \cdot NMB_{MF} \\
 &= K(2N+2)(2S + \frac{(K-1)}{2}) \\
 NAB_{SICRM} &= NAB_{SIC} + \frac{K(K-1)}{2} NAB_{MF} - K \cdot NAB_{MF} \\
 &= K(S + \frac{K-1}{2})(2N-1) + 2NK(2S-1)
 \end{aligned} \tag{3.6}$$

In the conventional PIC, discussed in Section 2.4.3, the number of matched filters in every stage is  $K$ . Therefore, for  $S$  stage PIC, the number of stages with  $K$  matched filters is  $S+1$  because stage 0 also contains  $K$  matched filters. So, the total number of matched filters is  $(S+1)K$ .

There are  $K$  signal regenerations in every stage after stage 0. Therefore, there is  $S \cdot K$  number of signal regenerations.

There are  $K$  signal cancellations from the received signal in every stage after stage 0. Also, there are  $K$  signal additions to the composite signal before every stage's bank of matched filters. Therefore, the number of additions per bit in every stage (not including stage 0) is  $2K$ . Thus, the total number of signal cancellations and additions is  $2K \cdot S$ . The total number of multiplications per bit for the PIC,  $NMB_{PIC}$ , and number of additions per bit,  $NAB_{PIC}$ , are respectively given by:

$$\begin{aligned}
 NMB_{PIC} &= K(S+1) \cdot NMB_{MF} + SK \cdot NMB_{RG} \\
 &= K(S+1)(2N+2) + SK(2N+2) = K(2S+1)(2N+2) \\
 NAB_{PIC} &= K(S+1) \cdot NAB_{MF} + 2K \cdot S \cdot NAB_{CANC} \\
 &= K(S+1)(2N-1) + 4SNK
 \end{aligned} \tag{3.7}$$

Using (3.5) to (3.7), the computation complexity graphs are plotted out in Figure 3.6. It is observed that the PIC and the SIC has the same  $NMB$ . The computation complexity of the SICRM is much higher than the computation complexity of the SIC. In fact the computation complexity of the SICRM is growing exponentially with

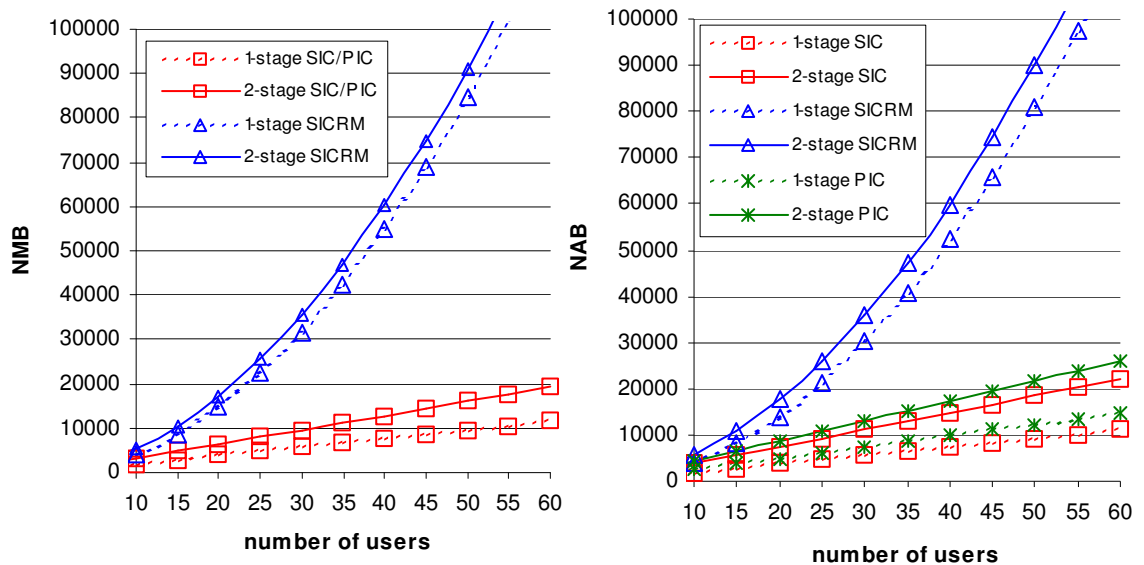


**Figure 3.6:**  $NMB$  and  $NAB$  comparison between SIC, SICRM and PIC, processing gain = 31

However, the SICRM outperforms the SIC in terms of BER. Therefore, it is desirable to find an alternative implementation of the SICRM at a lower computation complexity while retaining the same BER performance or capacity.

### 3.3 Processing time

A processing time block (PTB) is defined as the time taken for one operation (addition, cancellation, multiplication) performed in serial. If similar operations are done in parallel, the time required is the same as that for one operation.

From (3.1) and (3.2), for a matched filter, the required operations are the correlation between the input signal with the corresponding signature, multiplying with the corresponding phase conjugate and taking the real value of the resultant complex value. The correlation part requires  $2N$  multiplications (which can be performed in parallel) and  $2N-2$  additions (again, can be performed in parallel). This requires 2 PTB. The remaining operations involve 2 multiplications (in parallel) and 1 addition. Again, this requires 2 PTB. So, every time a matched filter is used, the total PTB required is 4 (Figure 3.7).

From Figure 3.7, signal regeneration in (3.3) and signal cancellation in (3.4) require 1 PTB respectively. Therefore, in summary, the processing time block for different operations is given by:

$$PTB \begin{cases} \text{matched filter}(MF) = 4 \\ \text{signal regeneration}(RG) = 1 \\ \text{signal cancellation}(CANC) = 1 \end{cases} \quad (3.8)$$

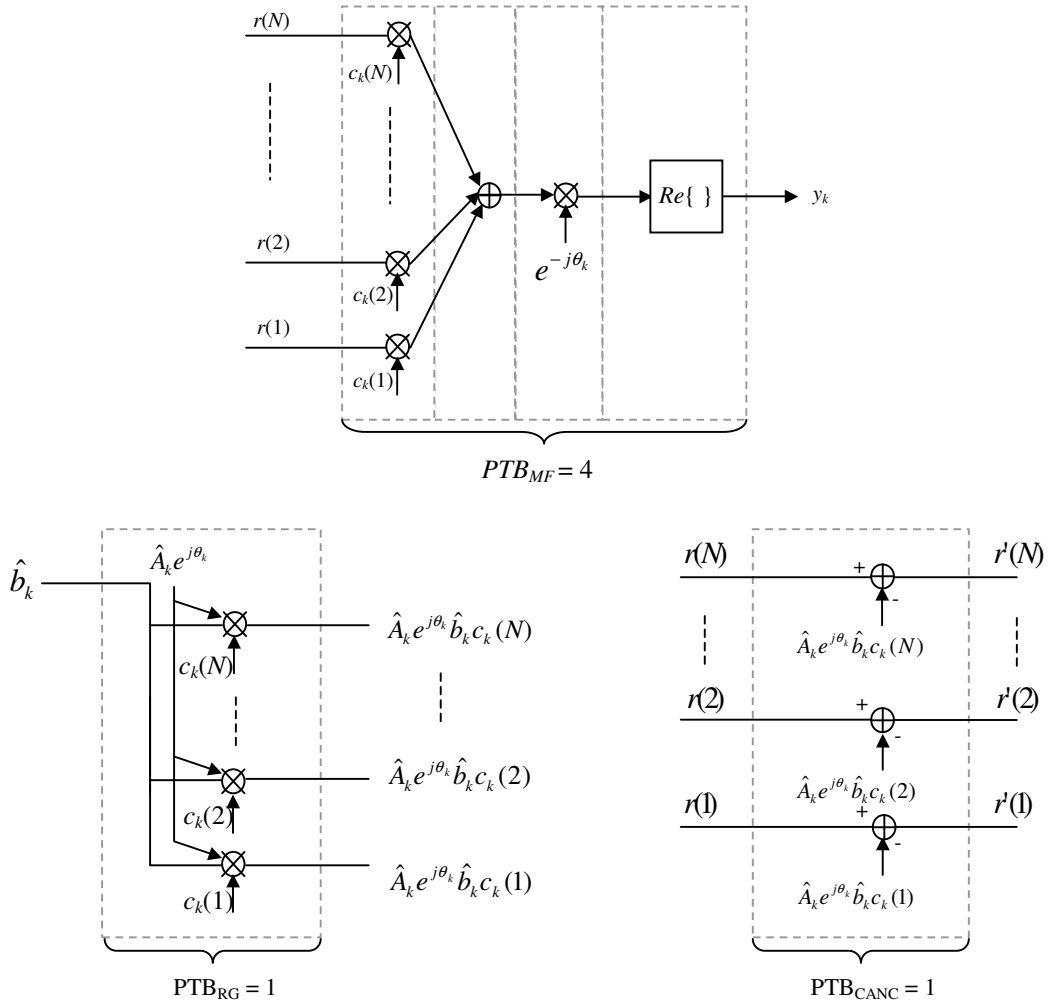


**Figure 3.7:** Operations of the matched filter (top), signal regeneration (bottom left) and signal cancellation (bottom right) in terms of processing time blocks

For the  $S$ -stage SIC ( $S$ -SIC), there is 1 column of  $K$  matched filters in parallel at stage 0 and another  $(K \cdot S - 1)$  matched filters in series from stage 1 to stage  $S$  (user 1 at stage 1 does not need re-detection). This contributes to a total of  $(K \cdot S)$   $PTB_{MF}$ . There are also  $K \cdot S - 1$  signal regenerations in series (after every decision bit but user  $K$  at stage  $S$  does not need to be regenerated since all users have been detected),  $K \cdot S - 1$  signal cancellations in series (after the signal has been regenerated but user  $K$  at stage  $S$  does not need to be cancelled) and  $(S - 1)K$  serial additions of

regenerated signals to composite signal (performed before matched filters in the ICUs after stage one). Therefore, a  $S$ -stage SIC requires a total of:

$$\begin{aligned} PTB_{SIC} &= KS \cdot PTB_{MF} + (KS - 1)PTB_{RG} + (KS - 1)PTB_{CANC} + K(S - 1)PTB_{CANC} \\ &= 7KS - K - 2 \end{aligned} \quad (3.9)$$

For the  $S$ -stage SICRM ( $S$ -SICRM), the processing time is increased because of the  $K - 1$  columns of parallel matched filters used to update the correlation value after every cancellation (Figure 2.7). But, the PTB is also reduced by the same amount because the  $K - 1$  serial matched filters in the stage 1's ICUs is not required (Figure 2.8). Therefore, the  $S$ -stage SICRM requires the same PTB as the  $S$ -stage SIC:

$$PTB_{SICRM} = PTB_{SIC} = 7KS - K - 2. \quad (3.10)$$

The  $S$ -stage PIC ( $S$ -PIC), from Figure 2.6, has 1 column of  $K$  matched filters in parallel (stage 0) and  $S$  columns of parallel matched filters (stage 1 to stage  $S$ ). Also, there are  $S$  columns of  $K$  signal regenerations in parallel,  $S$  columns of  $K$  signal cancellations in parallel from received signal and  $S$  columns of  $K$  additions of corresponding users' regenerated signal to the resultant signal (performed in parallel). Thus, the PTB of the  $S$ -stage PIC is:

$$\begin{aligned} PTB_{PIC} &= (1 + S)PTB_{MF} + S \cdot PTB_{RG} + S \cdot PTB_{CANC} + S \cdot PTB_{CANC} \\ &= 4 + 7S \end{aligned} \quad (3.11)$$

As seen from Figure 3.8, the processing time of the SIC is very high as compared to the PIC. Also, as the number of stages increases, the increase in processing time for the SIC and the SICRM is very high. Although it has very good performance as compared to the PIC in a fading channel, the capacity of the SIC is very restricted because of the limit to the processing time.



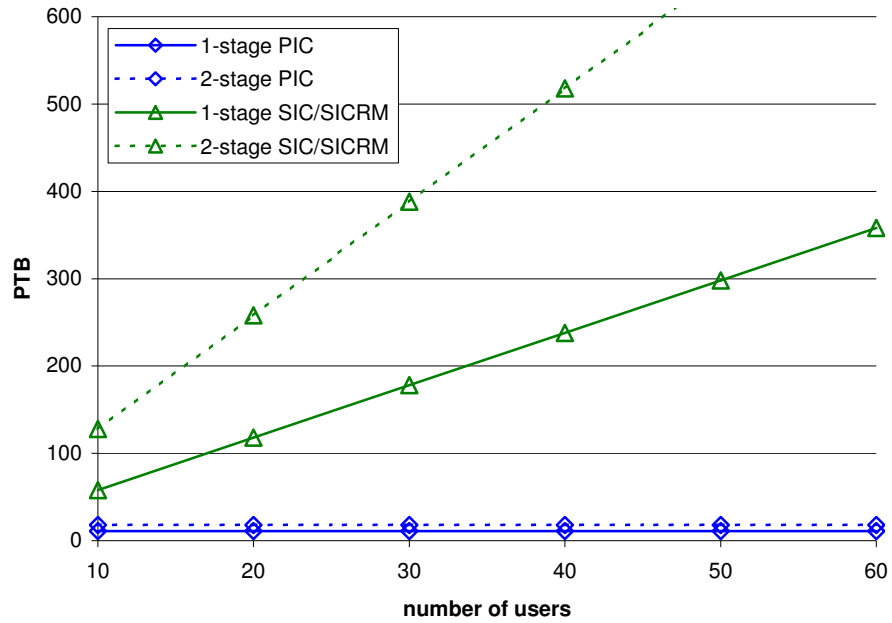


**Figure 3.8:** Processing time block comparison between the SIC, the SICRM and the PIC

### 3.4 Summary

In this chapter we have analyzed the performance of SIC, PIC and SICRM in various categories – BER performance, complexity and delay. We have introduced the principle to quantify computation complexity and processing time to be used in the next two chapters. Our comparisons are summarized in the following table:

Multiuser Detector	BER (AWGN)	BER (Rayleigh)	NMB	NAB	PTB
MF	Bad	Very Bad	Very Low	Very Low	Very Low
PIC	Very Good	Bad	Low	Low	Low
SIC (power)	Moderate	Very Good	Low	Low	High
SIC (correlation)	Good	Good	Low	Low	High
SICRM	Good	Very Good	High	High	High

**Table 3.1:** Assessment of matched filter and various IC schemes

Table 3.1 rates the schemes relative to one another. Overall, SIC schemes have better BER performance than the PIC but their processing time is much higher than PIC's. The SICRM, an advanced SIC scheme, requires very high computation complexity to achieve its BER superiority over the conventional SIC.

From these observations, we formed two approaches to improve the SIC while taking into consideration the BER performance, computation complexity and processing time. The first approach is to reduce the computation complexity and processing time of advanced SIC schemes that have very good BER performance to make them more feasible for implementation. This is through the cross-correlation implementation (CCI) in Chapter 4. Another approach is shown in Chapter 5 where we consider an advanced SIC scheme that improves the SIC scheme without adding in too much computation complexity and processing time.

## CHAPTER 4

### CROSS-CORRELATION IMPLEMENTATION (CCI)

In the previous chapter, we have established that for improvement in the capacity of interference schemes, additional computation complexity is required. This is clearly shown in the SICRM, which is an enhanced SIC. Although the SICRM has a better BER performance, the computational complexity of the SICRM is much higher than the SIC's. Also, processing time is a major disadvantage suffered by serial (or successive) cancellation schemes when compared to parallel cancellation schemes.

However, it is possible to reduce the computation complexity and processing time while maintaining the same capacity. This can be achieved by using cross-correlations when implementing IC schemes. We call this method the cross-correlation implementation or CCI.

Conventional schemes are usually based on the time domain equations, such as (2.17) and (2.21). However, it is possible to implement the system in the “correlation domain”. This realization is based on equations like (2.18) and (2.22). This method requires the calculation of cross-correlation value,  $\rho_{j,k}$ , through the users' signature waveforms,  $s_k(t)$  and the time delay,  $\tau_k$ , to produce a bank of cross-correlation values that can be reused in all different stages. Since this method is an equivalent version of the conventional method, there is no trade-off at all in terms of performance and capacity.

In Section 4.1, we show how the CCI is used to replace the basic IC block (described in Section 2.3.1). In the same section, we establish the alternate operation

constants for the CCI and compare them to the basic operation constants formed in the earlier chapter. Section 4.2 discusses on the application of this new IC building block in the SICRM and how it achieves computation complexity reduction. In Section 4.3 we discuss how the cross-correlation method is applied to an asynchronous channel. In Section 4.4, we show that how the cross-correlation method reduces processing time. To show the flexibility of the cross-correlation method, it is applied to another advanced SIC scheme - the pipelined SIC (PSIC) in Section 4.5.

#### 4.1 Basic IC Building Block using CCI

For simplicity we consider a synchronous CDMA system first. To minimize computation complexity and processing time, we use the cross-correlations between different users,  $\rho_{j,k}$ , to generate the MAI contribution of the  $j$ -th user on the  $k$ -th user,

$$MAI_{j,k} = \psi_{j,k} \hat{b}_j^{(1)} \quad (4.1)$$

where the MAI coefficient,

$$\psi_{j,k} = \text{Re}\{\hat{\alpha}_j e^{-j\theta_k}\} \rho_{j,k}. \quad (4.2)$$

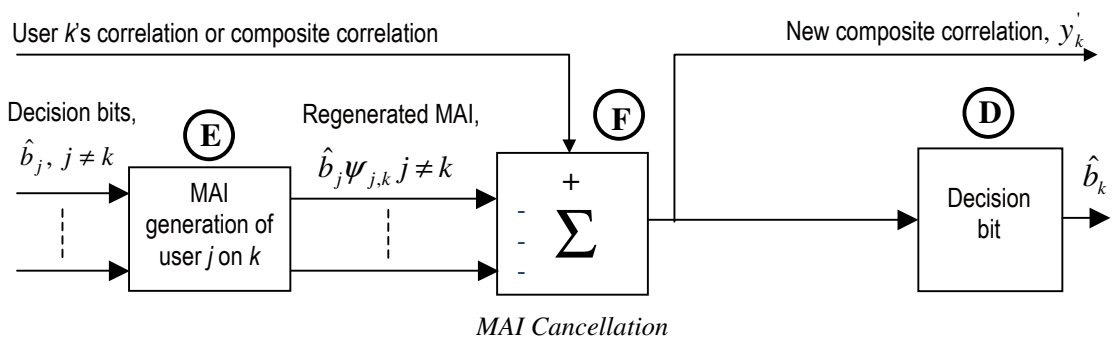


**Figure 4.1:** Basic building blocks of interference cancellation scheme (for data detection of user  $k$ ) using CCI

Notice that from Figure 4.1, instead of using the received signal or composite signal as an input, we use the correlation value (stage 0's matched filter output) or the

composite correlation value (correlation value that has been processed by previous blocks). Now, we analyze the changes block by block

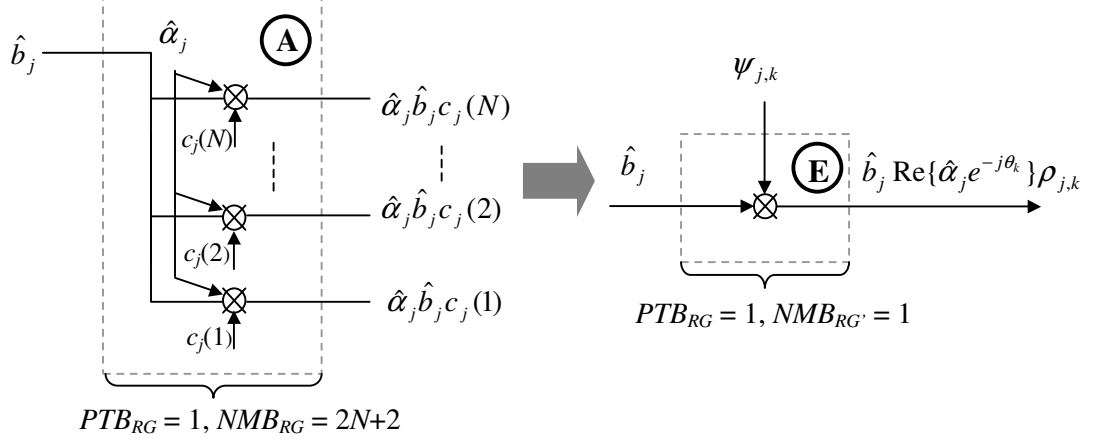


**Figure 4.2:** Block A: Signal regeneration, versus Block E: MAI generation

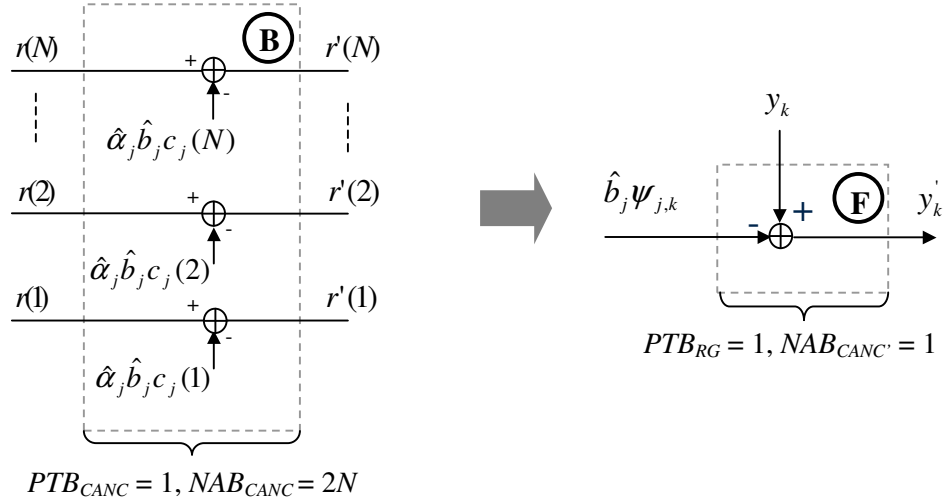


**Figure 4.3:** Block B: Signal cancellation versus Block F: MAI cancellation

Instead of using *Block A* that regenerates the interfering signals, we now use *Block E* in Figure 4.2 to regenerate the MAI. Although the processing time block (PTB) required for MAI regeneration is the same as the PTB required for signal regenerations, the number of multiplications,  $NMB_{RG'}$ , required is only 1 (compared to  $2N + 2$  required by the conventional method):

$$NMB_{RG'} = 1 \quad (4.3)$$

*Block B*, which performs signal interference cancellations, is replaced with *Block F* in Figure 4.3. Again, we see the reduction in terms of  $NAB$ , where the CCI requires only one subtraction compared to  $2N$  required by the conventional method.

$$NMB_{CANC'} = 1 \quad (4.4)$$

Since we are performing cancellations based on the correlation values, the resultant composite correlation can be bit detected immediately without the need of a matched filter. This means the removal of the matched filters as shown in Figure 4.1. As discussed in Section 3.2, each matched filter contributes  $NMB$  of  $2N + 2$ ,  $NAB$  of  $2N - 1$  and  $PTB$  of 4.

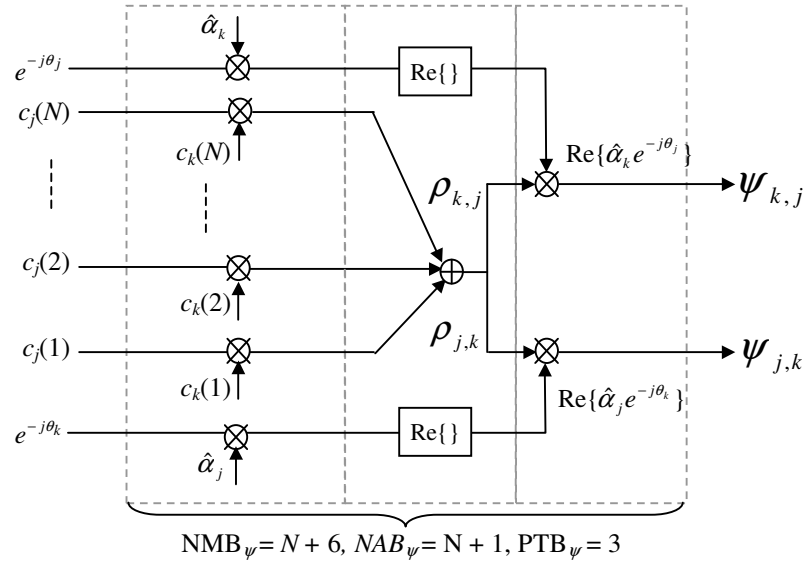


**Figure 4.4:** MAI co-efficient calculation in terms of  $NMB$ ,  $NAB$  and  $PTB$

For this new IC block to work, we need to generate  $\psi_{j,k}$  in (4.1) which is required for MAI generation in *Block E*. This, in turn, requires the generation of  $\rho_{jk}$ . Therefore, a  $\psi_{j,k}$  generation block is required. For Figure 4.4 to be realized, additional  $NMB$  and  $NAB$  are required. In the case of a synchronous system, the number of multiplications for the calculation of each  $\rho_{jk}$ ,  $NMB_\rho$ , and the number of

additions for the calculation for each  $\rho_{jk}$ ,  $NAB_\rho$  are given by:

$$NMB_\rho = N \quad (4.5)$$

$$NAB_\rho = N - 1 \quad (4.6)$$

respectively.

In a synchronous system  $\rho_{j,k} = \rho_{k,j}$ . Therefore, there are  $K(K-1)/2$  pairs of  $\rho_{k,j}$  and  $\rho_{j,k}$ . Similar to a matched filter, each calculation of  $\text{Re}\{\hat{\alpha}_k e^{-j\theta_j}\}$  and  $\text{Re}\{\hat{\alpha}_j e^{-j\theta_k}\}$  pairs requires a total  $NMB$  of 4 and  $NAB$  of 2 (number of multiplications between two complex numbers is 2 since we take only the real value). These pairs are multiplied by  $\rho_{k,j}$  and  $\rho_{j,k}$  respectively (adding another  $NMB$  of 2). Therefore, for each calculation of  $\psi_{j,k}$  and  $\psi_{k,j}$ , the total number of multiplications per bit required,  $NMB_\psi$  and the number of additions per bit required,  $NAB_\psi$  are respectively given by:

$$NMB_\psi = N + 6 \quad (4.7)$$

$$NAB_\psi = N + 1 \quad (4.8)$$

The  $\psi_{j,k}$  pairs are calculated after the zeroth stage bank of matched filters. The calculations are performed once and can be reused in subsequent stages without recalculation. In a synchronous channel with  $K$  users, there are  $\frac{1}{2}K(K-1)$  pairs of  $\psi_{j,k}$  and  $\psi_{k,j}$ . Therefore, the maximum  $NMB$  required for  $\psi_{j,k}$  calculation is  $\frac{1}{2}K(K-1)(N+6)$  and maximum  $NAB$  required is  $\frac{1}{2}K(K-1)(N+1)$ . All the pairs can be calculated in parallel. Therefore, the total required PTB for  $\psi_{j,k}$  calculation is only 3:

$$PTB_\psi = 3. \quad (4.9)$$

With the removal of the matched filters after stage 0, the immediate benefit is the reduction in processing time. The bulk of computation complexity for the cross correlation method is on the MAI coefficient calculation. Also, since the number of operations required for generation and cancellation in the cross-correlation method is much lower than that of the conventional method, the effectiveness of the cross correlation method increases as the number of *Block A*'s (signal regeneration), *Block B*'s (signal cancellation) and *Block C*'s (matched filters) used in the conventional method increases.

Similar to what was done in Section 3.2, we have established the alternate operation constants for computation complexity of the cross-correlation implementation with (4.3), (4.4), (4.7) and (4.8). In the following sections, these constants are used to compute the computation complexity of interference cancellation schemes that uses the cross-correlation implementation.

In the following section, we apply the CCI into the SICRM. The SICRM is a very good example because of its high amount of matched filters (compared to the conventional SIC), which contribute to a lot of computation complexity. It is also from the SIC family of IC schemes and thus, have high processing time.



## 4.2 Complexity Reduction in CCI-SICRM

Consider a synchronous CDMA system described by (1.16). The CCI-SICRM structure is shown in Figure 4.5. Notice that this is an equivalent structure of Figure 2.7. Similar to the SICRM, the first bank of matched filter (at stage 0) consists of  $K$  matched filters, which involve coherent detection of the corresponding users. This involves  $(2N+2)K$  number of multiplications and  $(2N-1)K$  number of additions per bit (from (3.1) and (3.2)).

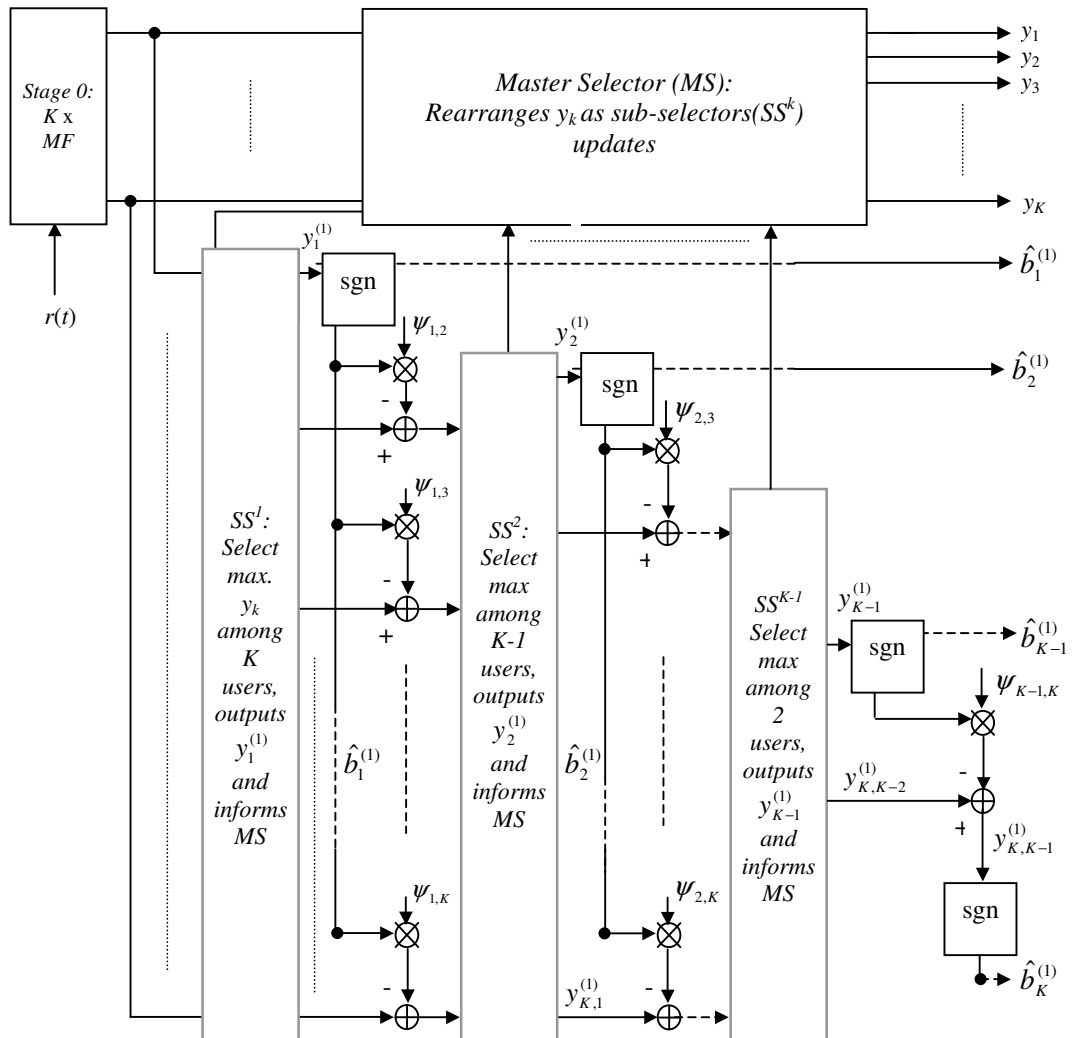


Figure 4.5: Stage 0 and Stage 1 of SICRM using CCI

For stage 1, the following operations are performed:

- The strongest correlation value from the first bank of matched filters is selected in the first sub-selector,  $SS^1$ , where the strongest user is defined as user 1 and  $SS^1$  informs the master selector, MS, to assign the corresponding user's correlation value as user 1 in subsequent stages.
- User 1 is then bit detected and its corresponding MAI to the other  $(K - 1)$  users is regenerated and cancelled. To regenerate the MAI contribution of the  $j$ -th user on the  $k$ -th user,  $\hat{MAI}_{j,k}$ , defined in (4.1),  $\psi_{j,k}$  is multiplied with the user  $j$ 's stage 1 decision bit,  $\hat{b}_j^{(1)}$ . From (4.3), the number of multiplications per bit for MAI generation,  $NMB_{RG}$ , corresponding to *Block E* in Figure 4.2, is 1.
- The regenerated MAI is then subtracted from the  $k$ -th correlation values, giving  $y_{k,1}^{(1)}$  in (2.31). From (4.4), for each MAI cancellation, the number of cancellations per bit involved is 1. This corresponds to *Block F* in Figure 4.3. It is equivalent to regenerating user 1's signal and canceling it from the baseband received signal. The difference is, however, instead of signal regeneration and cancellation at chip level (i.e. time domain), the cross-correlation method performs the operation as a multiplication and subtraction of constants at bit level (i.e. correlation domain). After user 1 is cancelled, a total of  $(K - 1)$  MAI has been generated and cancelled.
- The composite correlation values are passed into  $SS^2$  and the maximum correlation is selected and defined as user 2. Again,  $SS^2$  informs the MS so that the corresponding correlation  $y_2$  is selected and passed on to the next stage. Here, the number of MAI regeneration is  $(K - 2)$ . The number of MAI cancellations is also  $(K - 2)$ .

- This process is repeated until all users are detected. Therefore, the total MAI regeneration in the first stage is:

$$(K - 1) + (K - 2) + \dots + 2 + 1 = \frac{K(K - 1)}{2}$$

The total number of MAI cancellations is the same as the above expression.

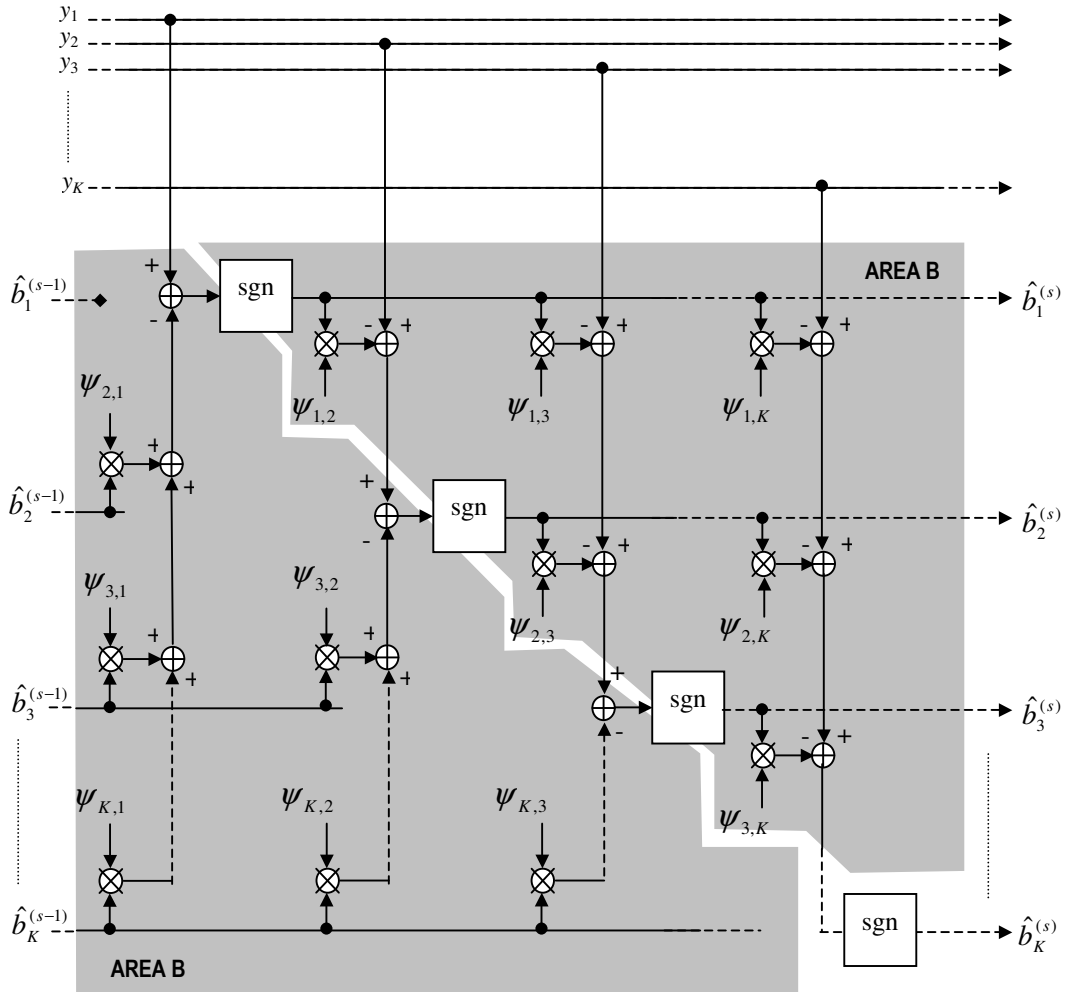


**Figure 4.6:**  $s$ -th stage of the SIC using CCI

For the remaining  $(S - 1)$  stages, the schematic is shown in Figure 4.6, which is the CCI derived from (2.22). Area A and Area B in the above figure is equivalent to the third term and second term in (2.22) respectively. For each of the remaining  $(S - 1)$  stages, each user generates and cancels  $(K - 1)$  MAI (corresponding to *Block E*

and *Block F*). This produces  $(S - 1) \times K(K - 1)$  MAI generations and  $(S - 1) \times K(K - 1)$  MAI cancellations.

We have also mentioned earlier that arithmetic operations are needed to calculate  $\psi_{j,k}$ . In the CCI-SICRM, we calculate all the possible combinations, which is  $\frac{1}{2}K(K - 1)$  pairs of  $\psi_{j,k}$  and  $\psi_{k,j}$ .

Therefore, the total number of multiplications per bit for the CCI-SICRM,  $NMB_{CCI}^{SICRM}$ , and the total number of additions per bit,  $NAB_{CCI}^{SICRM}$  are respectively given by:

$$\begin{aligned}
 NMB_{CCI}^{SICRM} &= K \cdot NMB_{MF} + \frac{K(K-1)}{2} \cdot NMB_{RG'} + (S-1)K(K-1) \cdot NMB_{RG'} \\
 &\quad + \frac{K(K-1)}{2} \cdot NMB_{\psi} \\
 &= K(2N+2) + \frac{K(K-1)}{2}(1) + (S-1)K(K-1)(1) + \frac{K(K-1)}{2}(N+6) \\
 &= K(2N+2) + K(K-1)\left(S + \frac{N}{2} + \frac{5}{2}\right)
 \end{aligned} \tag{4.10}$$

$$\begin{aligned}
 NAB_{CCI}^{SICRM} &= K \cdot NAB_{MF} + \frac{K(K-1)}{2} \cdot NAB_{CANC'} + (S-1)K(K-1) \cdot NAB_{CANC'} \\
 &\quad + \frac{K(K-1)}{2} \cdot NAB_{\psi} \\
 &= K(2N-1) + \frac{K(K-1)}{2}(1) + (S-1)K(K-1)(1) + \frac{K(K-1)}{2}(N+1) \\
 &= K(2N-1) + K(K-1)\left(S + \frac{N}{2}\right)
 \end{aligned} \tag{4.11}$$

For the single stage CCI-SICRM, where  $S = 1$ , we only need to calculate  $\psi_{j,k}$  for  $j > k$ . Therefore, (4.7) and (4.8) are respectively changed to:

$$NMB_{\psi, S=1} = N + 3 \tag{4.12}$$

$$NAB_{\psi, S=1} = N \tag{4.13}$$

Therefore, for the single stage CCI-SICRM:

$$\begin{aligned} NMB_{CCI}^{SICRM} \Big|_{S=1} &= K \cdot NMB_{MF} + \frac{K(K-1)}{2} \cdot NMB_{RG'} + \frac{K(K-1)}{2} \cdot NMB_{\psi, S=1} \\ &= K(2N+2) + K(K-1)\left(\frac{N}{2} + 2\right) \end{aligned} \quad (4.14)$$

$$\begin{aligned} NAB_{CCI}^{SICRM} \Big|_{S=1} &= K \cdot NAB_{MF} + \frac{K(K-1)}{2} \cdot NAB_{CANC'} + \frac{K(K-1)}{2} \cdot NAB_{\psi, S=1} \\ &= K(2N-1) + K(K-1)\left(\frac{N+1}{2}\right) \end{aligned} \quad (4.15)$$

From Figure 4.7, using the CCI in SICRM, there is a reduction of about 45% in terms of  $NMB$  and  $NAB$ . This makes the SICRM more acceptable to be implemented to achieve a better BER performance or capacity.

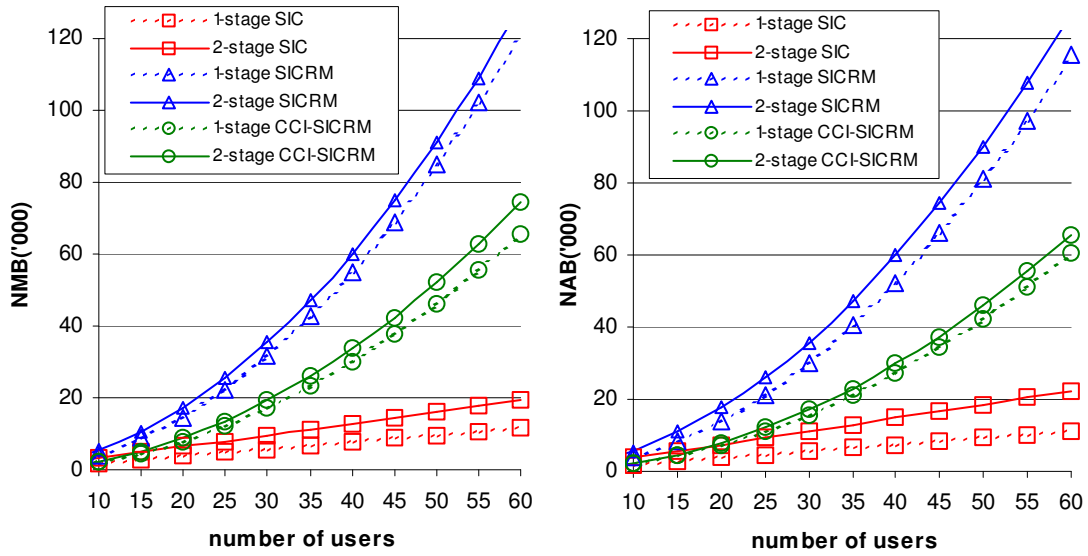


**Figure 4.7:**  $NMB$  and  $NAB$  comparison between the conventional SIC and SICRM against the CCI-SICRM, processing gain = 31

### 4.3 Asynchronous application of CCI

So far, we had considered only the synchronous CDMA system. In the asynchronous system, for the calculation of the cross-correlation, the total number of multiplications per bit and additions per bit for the calculation of both continuous-

time partial cross-correlation  $\Gamma_{jk}$  and  $\bar{\Gamma}_{jk}$  in (1.29) and (1.30) are respectively given by:

$$NMB_{\Gamma} = N, \quad (4.16)$$

$$NAB_{\Gamma} = N - 2. \quad (4.17)$$

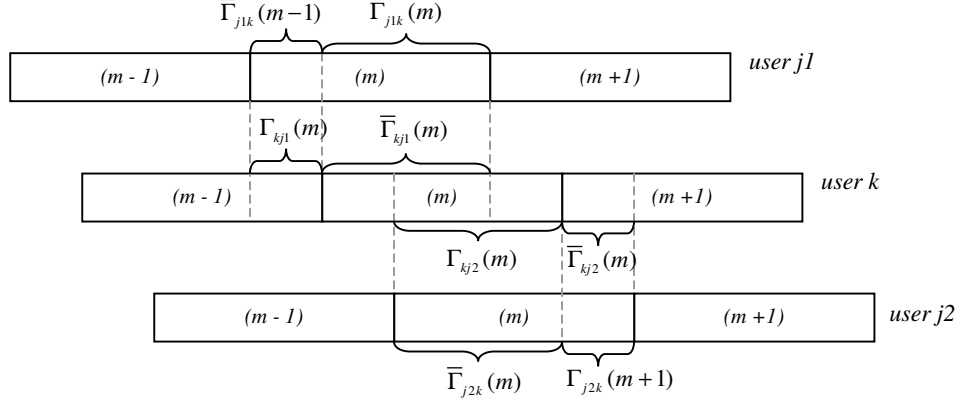


**Figure 4.8:** Partial cross-correlation between 3 users, with  $\tau_{j2} > \tau_k > \tau_{j1}$

From Figure 4.8, we observe that there is no need to calculate  $\Gamma_{kj}$  and  $\bar{\Gamma}_{kj}$  because:

$$\Gamma_{kj}(m) = \bar{\Gamma}_{jk}(m) \text{ and } \bar{\Gamma}_{kj}(m) = \Gamma_{jk}(m+1) \text{ for } \tau_j > \tau_k \quad (4.18)$$

$$\Gamma_{kj}(m) = \bar{\Gamma}_{jk}(m-1) \text{ and } \bar{\Gamma}_{kj}(m) = \Gamma_{jk}(m) \text{ for } \tau_j < \tau_k \quad (4.19)$$

From (2.26), in the asynchronous channel, we need to generate two MAI coefficients for the CCI instead of one as required in the synchronous case:

$$\psi_{j,k}^{asy}(m) = \begin{cases} \text{Re}\{\hat{\alpha}_j(m-1)e^{-j\theta_k(m)}\}\Gamma_{jk}(m) & \tau_j > \tau_k \\ \text{Re}\{\hat{\alpha}_j(m)e^{-j\theta_k(m)}\}\Gamma_{jk}(m) & \tau_k > \tau_j \end{cases} \quad (4.20)$$

$$\bar{\psi}_{j,k}^{asy}(m) = \begin{cases} \text{Re}\{\hat{\alpha}_j(m)e^{-j\theta_k(m)}\}\bar{\Gamma}_{jk}(m) & \tau_j > \tau_k \\ \text{Re}\{\hat{\alpha}_j(m+1)e^{-j\theta_k(m)}\}\bar{\Gamma}_{jk}(m) & \tau_k > \tau_j \end{cases} \quad (4.21)$$

Therefore, for asynchronous MAI cancellation, (2.43) can be rewritten as:

$$M\hat{A}I_{j,k}(m) = \begin{cases} \hat{b}_j(m-1)\psi_{j,k}(m) + \hat{b}_j(m)\bar{\psi}_{j,k}(m) & ; \tau_j > \tau_k \\ \hat{b}_j(m)\psi_{j,k}(m) + \hat{b}_j(m+1)\bar{\psi}_{j,k}(m) & ; \tau_j < \tau_k \end{cases} \quad (4.22)$$

This means that the  $NMB$  for MAI generation is 2 and  $NAB$  for cancellation is also 2:

$$NMB_{RG'}^{asy} = 2 \quad (4.23)$$

$$NAB_{CANC'}^{asy} = 2. \quad (4.24)$$

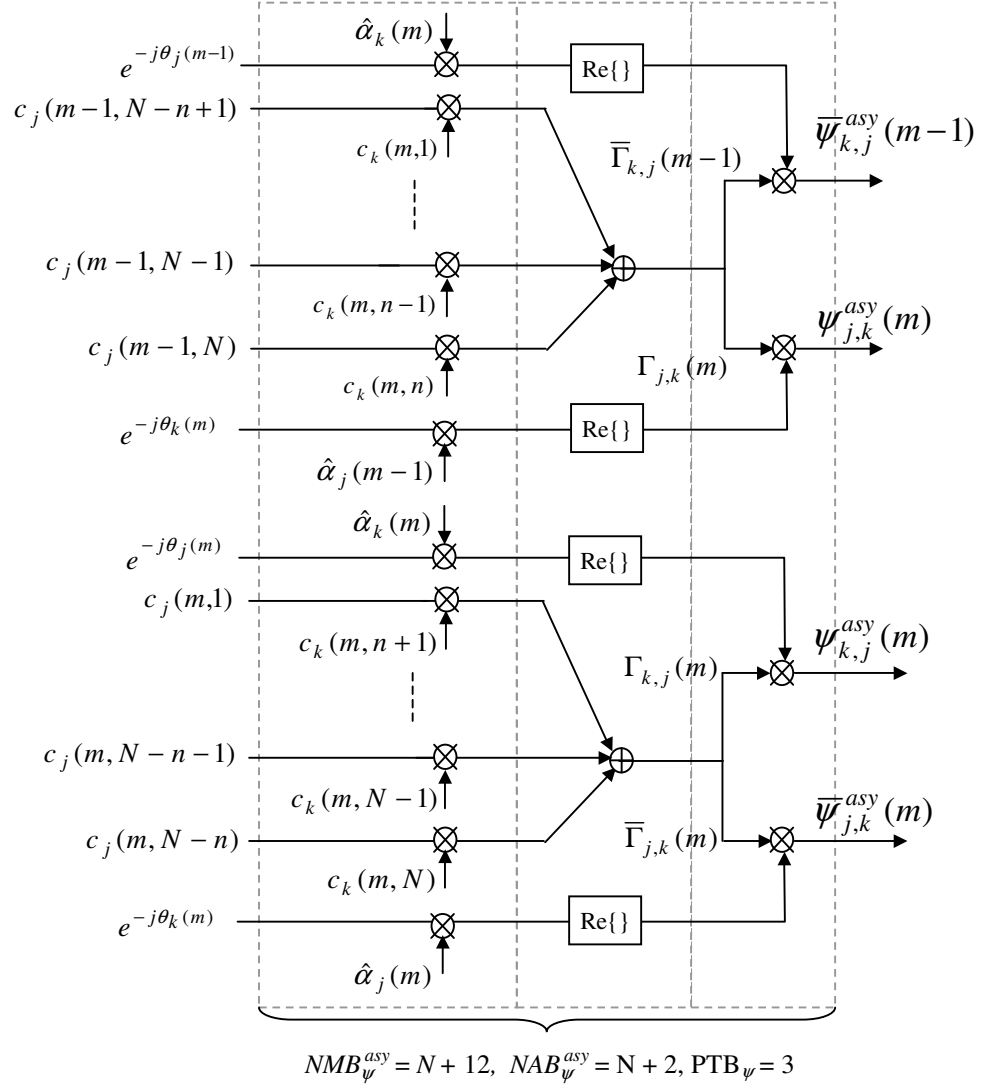


**Figure 4.9:** MAI co-efficient calculation for asynchronous channel ( $\tau_j > \tau_k$ ) in terms of  $NMB$ ,  $NAB$  and  $PTB$  where  $c_j(m,n)$  is the  $n$ -th chip of the  $m$ -th bit's signature waveform in a block of  $M$  bits

The  $\psi_{j,k}^{asy}(m)$  generation block for  $\tau_j > \tau_k$  is shown in the Figure 4.9. Similar to the case of a synchronous case, there are  $K(K-1)/2$  cross-correlation calculations to obtain  $\psi_{j,k}^{asy}$ ,  $\bar{\psi}_{j,k}^{asy}$ ,  $\psi_{k,j}^{asy}$ ,  $\bar{\psi}_{k,j}^{asy}$  values where each of these calculations requires:

$$NMB_{\psi}^{asy} = N + 12 \quad (4.25)$$

$$NAB_{\psi}^{asy} = N + 2 \quad (4.26)$$

$$PTB_{\psi} = 3 \quad (4.27)$$

Applying these equations into (4.10) and (4.11) produces:

$$NMB_{CCI}^{SICRM(asy)} = K(2N + 2) + K(K - 1)(2S + 5 + N/2) \quad (4.28)$$

$$NAB_{CCI}^{SICRM(asy)} = K(2N - 1) + K(K - 1)(2S + N/2)$$

For  $S = 1$ ,  $\psi_{k,j}^{asy}$  and  $\bar{\psi}_{k,j}^{asy}$  are not required. Therefore,

$$NMB_{\psi,S=1}^{asy} = N + 6 \quad (4.29)$$

$$NAB_{\psi,S=1}^{asy} = N \quad (4.30)$$

Thus,

$$NMB_{CCI}^{SICRM(asy)} \Big|_{S=1} = K(2N + 2) + K(K - 1)(4 + N/2) \quad (4.31)$$

$$NAB_{CCI}^{SICRM(asy)} \Big|_{S=1} = K(2N - 1) + K(K - 1)(1 + N/2) \quad (4.32)$$

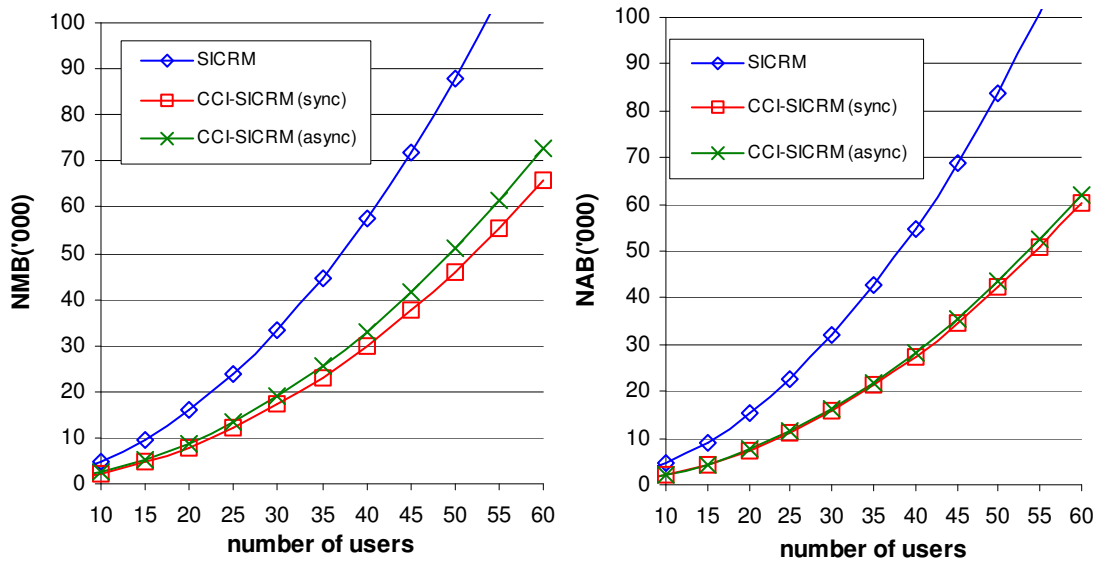


**Figure 4.10:**  $NMB$  and  $NAB$  comparison between synchronous SICRM, using conventional implementation and CCI, and asynchronous CCI-SICRM, processing gain = 31



Even though there is an increase in the number of operations, it is very small (Figure 4.10). This is because in the CCI, the bulk of the computation complexity is not on the signal regeneration and cancellation, but on the MAI coefficient calculation. Therefore, even though the number of cancellations and regenerations has doubled, the increase in the overall number of operations is very small.

#### 4.4 Processing time Reduction in CCI-SICRM

When the CCI is used, the calculation of  $K(K - 1)/2$  MAI coefficient pairs,  $\psi_{j,k}$  and  $\psi_{k,j}$ , can be performed in parallel. This is achieved within 3 PTB as shown in Figure 4.4. Cross-correlation calculation is performed after stage 0's bank of matched filters.

For the  $S$ -stage CCI-SICRM, there is 1 column of  $K$  matched filters in parallel (stage 0), 1 column of  $K(K-1)/2$  cross-correlation calculation in parallel,  $(K - 1)$  columns of MAI generations and cancellations in series for stage 1 (user  $K$ 's MAI is not required to be cancelled),  $(S - 1)K$  serial columns of parallel MAI generations and cancellations after stage 1. Each of these MAI generation and cancellation (combination of *Block E* and *Block F*) requires processing time of:

$$PTB_{MC} = 2. \quad (4.33)$$

Thus, the  $PTB$  for the CCI-SICRM is given by:

$$\begin{aligned} PTB_{SICRM}^{CCI} &= 1 \cdot PTB_{MF} + 1 \cdot PTB_{\psi} + [K - 1 + K(S - 1)]PTB_{MC} \\ &= 5 + 2KS \end{aligned} \quad (4.34)$$

An example to illustrate how  $PTB$  measures the different IC schemes is shown in *Appendix C*.

From Figure 4.11, the processing time of the 1-stage CCI- is below 40% of the processing time of the conventional 1-stage SICRM or SIC after 20 users. This figure

drops below 33% for  $S = 2$ ). Thus, by using the CCI, the processing time of the SIC can be reduced tremendously, making it a more attractive choice of interference cancellation scheme.

Also, the CCI allows more stages to be implemented given a processing time tolerance. For example, we can implement the 2-stage CCI-SICRM at about  $\frac{3}{4}$  the processing time of 1-stage SIC or SICRM.

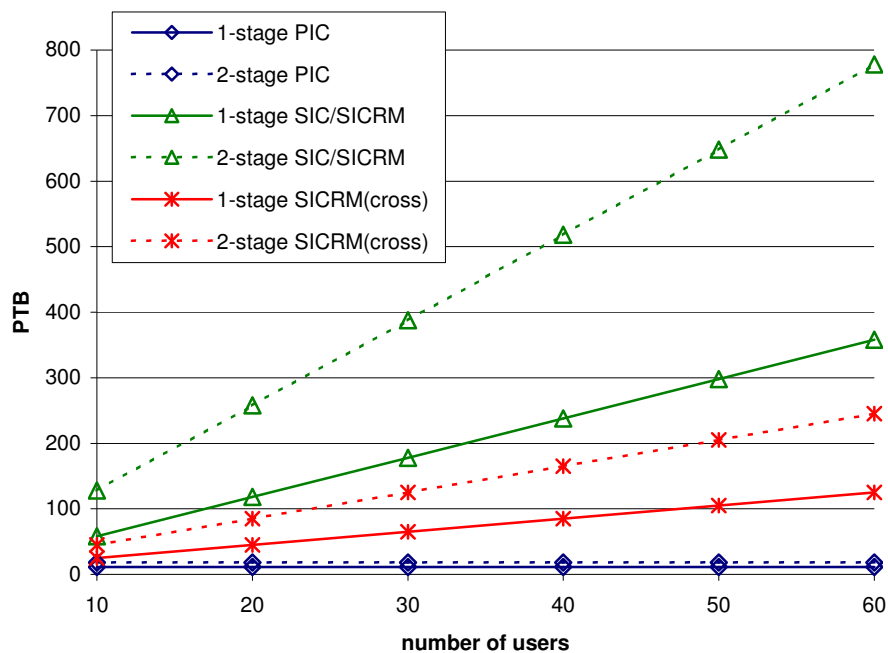


**Figure 4.11:** Processing time block comparison between SIC, conventional SICRM, PIC and cross correlation SICRM for  $S=1$  and  $S=2$

#### 4.5 Another Application: Pipelined SIC

The cross-correlation method reduces the computation complexity and processing time of interference cancellation schemes system that has a lot of matched filters, signal cancellations and signal regenerations. As mentioned earlier, the CCI proposed is an alternate IC building block and thus, applicable to any IC scheme. To demonstrate this, we apply it to another IC scheme – the pipelined SIC.

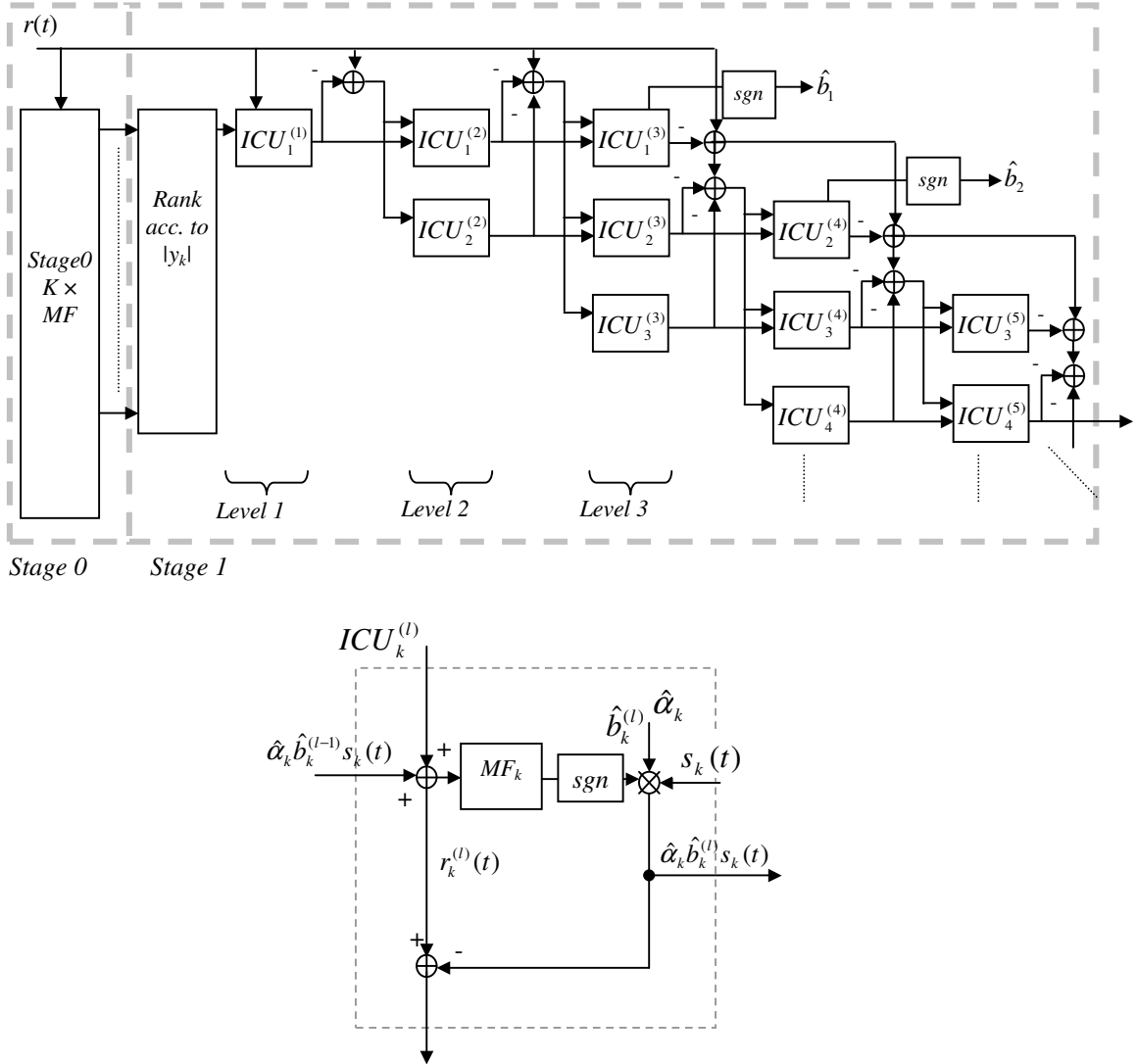


**Figure 4.12:** Pipelined Successive Interference Cancellation with 3 “pipelines”

Consider a 1-iteration pipeline successive interference cancellation (PSIC) scheme proposed in [17]. The structure of the PSIC is shown in Figure 4.12. The PSIC has  $P$  “pipelines” to perform additional interference cancellations to improve the BER performance. User  $k$ 's decision bits are updated  $(P-1)$  times. At the final update, user  $k$ 's signal is less the  $(k-1)$  signals of users higher ranked than user  $k$  and the  $(P-2)$  signals of users weaker than user  $k$ . For the  $l$ -th level of the  $k$ -th user's ICU unit in a PSIC scheme with  $P$  “pipelines”, the composite signal before  $k$ -th user's

matched filter,  $r_{k,PSIC}^{(l)}(t)$ , and its corresponding correlation value,  $y_{k,PSIC}^{(l)}$ , are respectively given by:

$$r_{k,PSIC}^{(l)}(t) = \begin{cases} r(t) - \sum_{j=1, j \neq k}^{l-1} \hat{\alpha}_j \hat{b}_j^{(l-1)} s_j(t) & \text{for } l \leq P \\ r(t) - \sum_{j=l-P+1, j \neq k}^{l-1} \hat{\alpha}_j \hat{b}_j^{(l-1)} s_j(t) \\ - \sum_{m=P}^{l-1} \hat{\alpha}_{m-P+1} \hat{b}_{m-P+1}^{(m)} s_{m-P+1}(t) & \text{for } P < l \leq K \\ r(t) - \sum_{j=l-P+1, j \neq k}^K \hat{\alpha}_j \hat{b}_j^{(l-1)} s_j(t) \\ - \sum_{m=P}^{l-1} \hat{\alpha}_{m-P+1} \hat{b}_{m-P+1}^{(m)} s_{m-P+1}(t) & \text{for } K < l \leq (K + P - 1) \end{cases} \quad (4.35)$$

$$y_{k,PSIC}^{(l)} = \begin{cases} y_k - \text{Re}\left\{ \sum_{j=1, j \neq k}^{l-1} \hat{\alpha}_j \hat{b}_j^{(l-1)} \rho_{j,k} \right\} & \text{for } l \leq P \\ y_k - \text{Re}\left\{ \sum_{j=l-P+1, j \neq k}^{l-1} \hat{\alpha}_j \hat{b}_j^{(l-1)} \rho_{j,k} \right\} \\ - \text{Re}\left\{ \sum_{m=P}^{l-1} \hat{\alpha}_{m-P+1} \hat{b}_{m-P+1}^{(m)} \rho_{m-P+1,k}(t) \right\} & \text{for } P < l \leq K \\ y_k - \text{Re}\left\{ \sum_{j=l-P+1, j \neq k}^K \hat{\alpha}_j \hat{b}_j^{(l-1)} \rho_{j,k} \right\} \\ - \text{Re}\left\{ \sum_{m=P}^{l-1} \hat{\alpha}_{m-P+1} \hat{b}_{m-P+1}^{(m)} \rho_{m-P+1,k} \right\} & \text{for } K < l \leq (K + P - 1) \end{cases} \quad (4.36)$$

In terms of BER performance, we refer to [17]. For a BER of 1% in an AWGN channel, the capacity of the PSIC with 4 “pipelines” is 85% higher than that of the conventional SIC (processing gain is 63). However, this comes at a cost of greatly increased complexity. A detailed study of the computation complexity and processing time is presented in [19]. Here, we present a simple arithmetic analysis of the PSIC.

From Figure 4.12, the number of additional additions (or cancellations) outside an ICU unit is  $(P - 1) \times K \times NAB_{CANC}$  where  $P$  is the number of “pipelines”. Also, there are additional  $(P - 1) \times K$  ICUs in the PSIC. Each of these ICUs contributes additional  $NMB$  of  $2N + 2$  (from matched filter) and  $2N + 2$  (from signal regeneration). Each

also contribute an additional  $NAB$  of  $2N - 1$  (from matched filter) and  $2N$  (from signal addition). Therefore,  $NMB_{PSIC}$  and  $NAB_{PSIC}$  for  $S = 1$  is given by:

$$\begin{aligned} NMB_{PSIC} &= NMB_{SIC}|_{S=1} + K(P-1)(NMB_{MF} + NMB_{RG}) \\ &= K(2(1)+1)(2N+2) + K(P-1)(2N+2+2N+2) \\ &= 2K(2P+1)(N+1) \end{aligned} \quad (4.37)$$

$$\begin{aligned} NAB_{PSIC} &= NAB_{SIC}|_{S=1} + (P-1) \cdot K \cdot NAB_{CANC} + K(P-1)(NAB_{MF} + NAB_{RG}) \\ &= K((1)+1)(2N-1) + 2NK(2(1)-1) + 2N(P-1)K + K(P-1)(2N-1+2N) \\ &= 2K(3N-1) + K(P-1)(6N-1) \end{aligned} \quad (4.38)$$

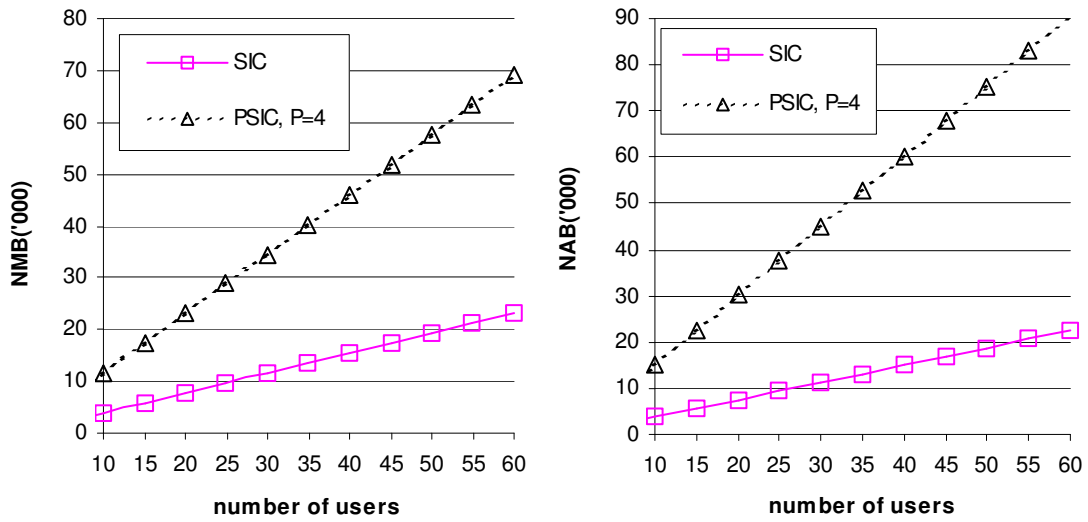


**Figure 4.13:**  $NMB$  and  $NAB$  comparison between SIC and SPIC, processing gain,  $N = 63$ ,  $S = 1$ ,  $P = 4$

From Figure 4.13, it is obvious that the PSIC requires a lot of additional operations to achieve the improvement in capacity. However, using the CCI, the number of operations is reduced. Consider Figure 4.14 and 4.15 as the design for the CCI-PSIC.

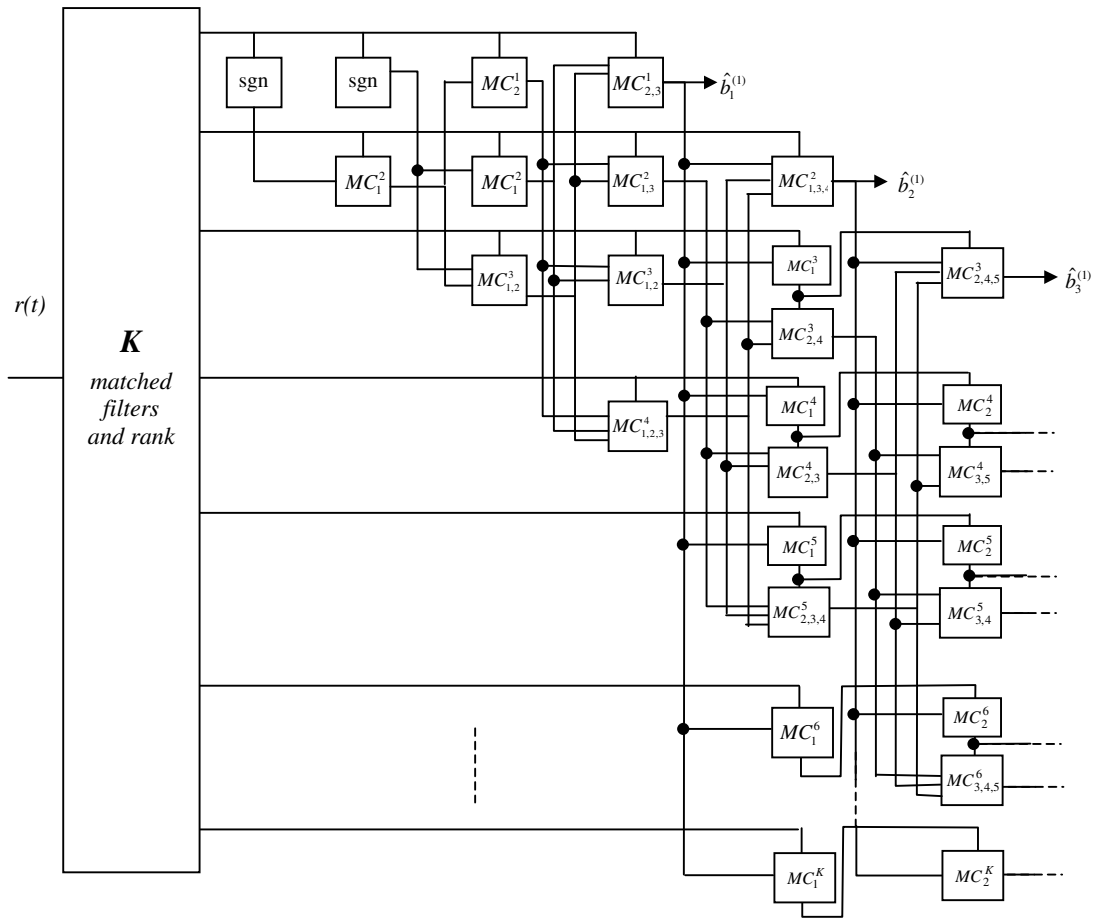


**Figure 4.14:** CCI-PSIC's equivalent scheme of the conventional PSIC for 4 “pipelines”

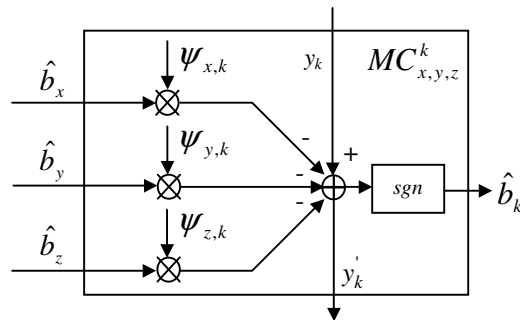


**Figure 4.15:** The MAI cancellation unit (MC) with input from decision bit of  $x^{\text{th}}$ ,  $y^{\text{th}}$  and  $z^{\text{th}}$  user, and  $k^{\text{th}}$  user's correlation value

In Figure 4.15, the MAI cancellation unit (MC) is a combination of a few Block  $F$ 's, Block  $E$ 's and one Block  $D$ . The number of MAI cancellations for the PSIC with  $K$  users and  $P$  “pipelines” is:

$$\begin{aligned}
\Pi(K, P) &= 2 \sum_{x=1}^{P-1} x^2 + \sum_{x=1}^{K-P-1} x + (K-P)(P^2 - P + 1) \\
&= \frac{1}{3} P(P-1)(2P-1) + \frac{1}{2} (K-P)(K-P-1) + (K-P)(P^2 - P + 1)
\end{aligned} \tag{4.39}$$

Other operations include the first bank of  $K$  matched filters and the calculation of the  $K(K-1)/2$  pairs of  $\psi_{j,k}$  and  $\psi_{k,j}$ . We have explained in Section 4.1 that  $\psi_{j,k}$  can be reused instead of being regenerated every time MAI cancellation is performed. The required number of  $\psi_{j,k}$  in a 1-iteration PSIC is:

$$\Omega(K, P) = K(P-2) + K(K-1)/2. \tag{4.40}$$

From the above expression, there are  $K(P-2)$  number of  $\psi_{j,k}, \psi_{k,j}$  pairs and  $[K(K-1)/2 - K(P-2)]$  number of  $\psi_{j,k}$  where  $j > k$ . Therefore, the number of multiplications per bit and the number of additions per bit for the CCI-PSIC with  $K$  users and  $P$  “pipelines” are respectively given by:

$$\begin{aligned}
NMB_{CCI}^{PSIC} \Big|_{S=1} &= K \cdot NMB_{MF} + \Pi(K, P) NMB_{RG} + K(P-2) NMB_{\psi} \\
&\quad + \left[ \frac{K(K-1)}{2} - K(P-2) \right] NMB_{\psi, S=1} \\
&= K(2N+2) + \Pi(K, P) + 3K(P-2) + \frac{1}{2} K(K-1)(N+3)
\end{aligned} \tag{4.41}$$

$$\begin{aligned}
NAB_{CCI}^{PSIC} \Big|_{S=1} &= K \cdot NAB_{MF} + \Pi(K, P) NAB_{CANC} + K(P-2) NAB_{\psi} \\
&\quad + \left[ \frac{K(K-1)}{2} - K(P-2) \right] NAB_{\psi, S=1} \\
&= K(2N-1) + \Pi(K, P) + K(P-2) + \frac{1}{2} NK(K-2)
\end{aligned} \tag{4.42}$$

From [11], when the number of “pipelines” is increased to 12 from 4, there is an improvement of 8.5dB for BER of 0.01% in AWGN channel and an improvement of 13dB for a BER of 1% in a fading channel for 20 users. However, from Figure 4.16, the computation complexity when  $P = 4$  for the conventional implementation is more than two and half times when  $P = 12$ . For the CCI-PSIC, the increase in computation complexity is less than 10%, which is very small. For example, when  $K = 30$ , for a

slightly higher computation complexity of a conventional PSIC with 4 “pipelines”, we can implement a 12 “pipelines” CCI-PSIC to achieve a better BER performance.

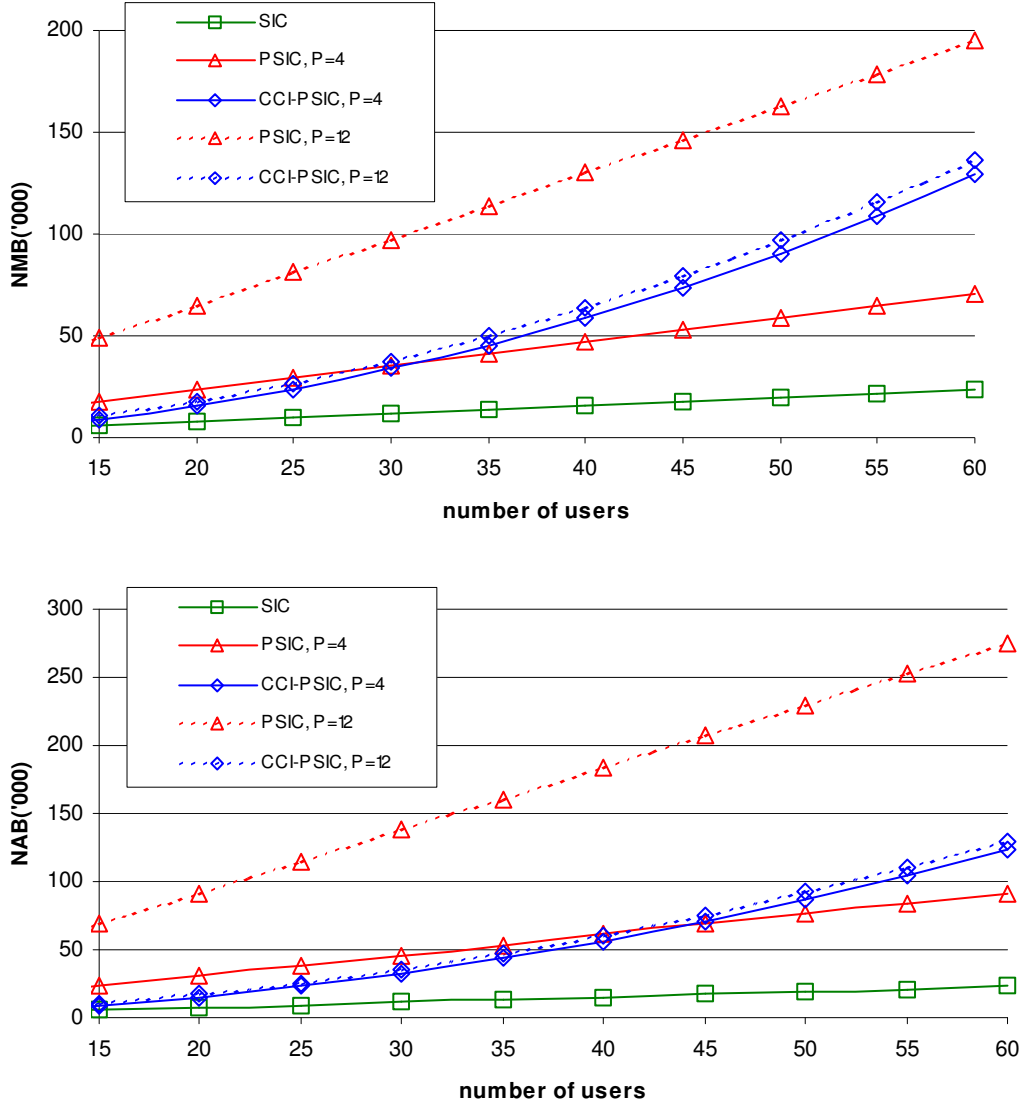


**Figure 4.16:** NMB and NAB comparison between conventional PSIC and CCI-PSIC with  $P = 4$  and  $P = 12$ , processing gain  $N = 64$

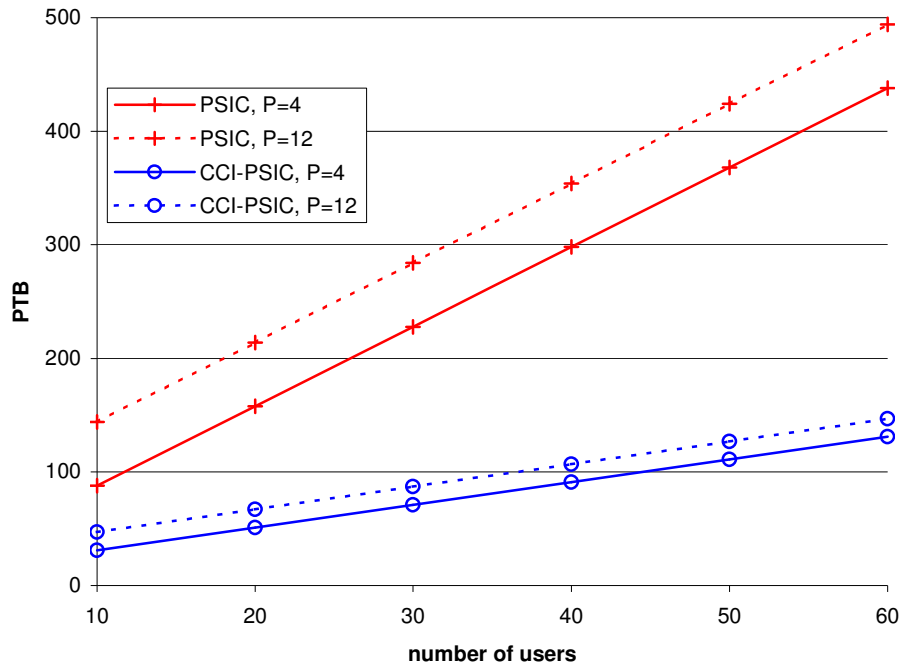
In terms of the processing time delay, for the conventional PSIC, there are effectively 1 column of stage 0’s  $K$  matched filters in parallel,  $(K + P - 2)$  columns of signal regeneration,  $(K + P - 2)$  columns of signal cancellation,  $(K + P - 2)$  columns of signal addition and  $(K + P - 2)$  columns of matched filters. Therefore, the processing time of the conventional PSIC is:



$$\begin{aligned}
 PTB_{PSIC} &= 1 \cdot PTB_{MF} + (K + P - 2)(PTB_{RG} + PTB_{CANC} + PTB_{CANC} + PTB_{MF}) \\
 &= 4 + (K + P - 2)(1 + 1 + 1 + 4) \\
 &= 7(K + P) - 10
 \end{aligned} \tag{4.43}$$

From Figure 4.14, it is observed that for the CCI-PSIC, the processing time is equivalent to the CCI-SICRM plus an additional  $(P - 1)$  MAI Cancellation Units. From Figure 4.15, one MC requires  $PTB_{MC} = 2$ . Therefore, the effective processing time for the CCI-PSIC is:

$$\begin{aligned}
 PTB_{PSIC}^{cross} &= PTB_{SIC}^{cross} |_{S=1} + (P - 1)(1 \cdot PTB_{MC}) \\
 &= 5 + 2(1)K + (P - 1)(2) \\
 &= 2(K + P) + 3
 \end{aligned} \tag{4.44}$$



In Figure 4.17, we compare the processing time blocks of the CCI-PSIC with the conventional PSIC for 4 “pipelines” and 12 “pipelines”. In both cases, the PTB of the cross-correlation method is about 1/3 of the conventional method. Again, we have demonstrated the efficiency of the cross-correlation method in reducing the processing time of advanced IC schemes.

## 4.6 Conclusion

The cross-correlation implementation or CCI, which can be implemented in any interference cancellation schemes, has many benefits (very evident in successive cancellation scheme) to allow more practical implementation of these schemes.

The CCI reduces the computation complexity of interference schemes that employ a lot of matched filters (or ICUs) to improve the BER performance or capacity. The higher the number of additional matched filters or ICUs (compared to the conventional SIC and PIC) used, the more significant the reduction in the computation complexity through the usage of the cross-correlation method. Reduction in computation complexity leads to lower resources required to process the received signal both at the base station and the mobile station.

Through the CCI, the processing time of ICs is reduced. The reduction is very obvious for the SIC and hybrid ICs that uses successive cancellations. The cross-correlation method performs the operations of a conventional SIC or SICRM in less than half the processing time. In the case of the SIC, this requires a trade-off in terms of additional computation complexity. However, for the SICRM, the CCI is very beneficial because not only it reduces the processing time by more than half, it also reduces the computation complexity. In another advanced SIC scheme, the PSIC, it reduced the processing time to a third. This is very important as processing time has always been a problem with SIC schemes.

We have also demonstrated the flexibility of the CCI. Application is very simple. To apply to any interference cancellation scheme, all that is required is to identify the correlation equations, which are the matched filter output equations. Then, the alternate implementation is constructed from them using the alternative building block shown in Figure 4.1.

The concept behind the CCI is simple. In fact, various papers and research work have indirectly used this method. However, there has not been any extensive study that standardizes this implementation into an alternative building block shown in Figure 4.1. With components of the basic building block equations (shown in Section 2.4.1) and the alternate building block equations (Section 4.1), it is now simpler to analyze various IC schemes with respect to their computation complexity and processing time.

## **CHAPTER 5**

### **IMPROVED SUCCESSIVE INTERFERENCE CANCELLATION**

In Chapter 3, we have concluded that the SIC is a better IC scheme as compared to the PIC in terms of the overall BER performance. In the same chapter, we have discussed two of the issues faced by the SIC – computation complexity and processing time. To enhance the BER performance of the SIC, SICRM is used and the additional computation complexity is very large as shown in Section 3.2. In Chapter 4, we have introduced the cross-correlation implementation that reduced the computation complexity of the SICRM while retaining its BER performance.

In this chapter, we introduce the improved successive interference cancellation (ISIC) scheme with an adaptive bit-select cancellation (ABC) function. This scheme improves the BER performance of the SIC with minimal computation complexity and processing time increase.

Section 5.1 discusses the issues encountered when using IC schemes such as decision devices, block cancellations, varying channel conditions and inaccurate ranking. In Section 5.2, we introduce the adaptive bit-select cancellation (ABC) device and discuss its functions. In Section 5.3, we consider the improved successive interference cancellation scheme with the ABC device and investigate its performance in comparison to other interference schemes. In Section 5.4, we discuss the implementation of the cross-correlation method in the ISIC. Section 5.5 concludes this chapter.

## 5.1 Issues of Successive Interference Cancellation Schemes

### 5.1.1 Mapping functions for Decision Bit

In Section 2.4.1, we mentioned that although interference cancellations are meant to lower the multiple access interference (MAI), they may add to the interference if erroneous bit decisions are used. Also, since the users' amplitude, phase and delay are estimated, erroneous estimation degrades the performance of IC schemes.

To control the contribution of erroneous regenerated signals, mapping functions are used. Figure 5.1 shows some of the various mapping functions that have been proposed [30-32]. These devices are applied to the correlation values of the matched filters to obtain the data estimates. Then, these data estimates are used to regenerate the users' received signals. So far, all our simulations and analysis are based on the hard decision device shown in (b) of Figure 5.1.

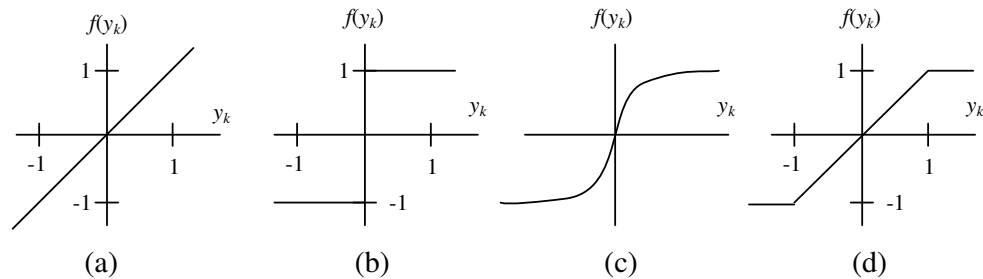


**Figure 5.1:** Decision devices. (a) Linear (b) Hard-limited  
(c) Hyperbolic tangent (d) Clipped soft decision

Small correlation values lead to unreliable decisions, and this produces unreliable signal regenerations. These unreliable regenerated signals can degrade the performance of the IC scheme. Therefore, the contribution of these unreliable signals should be as small as possible, if not none at all. The hard limiter does not account for this and only maps the correlation value to either +1 or -1. The linear, hyperbolic

tangent and clipped soft decision accounts for this and therefore, has better performance than the hard limiter.

Large correlation values usually signify more reliable data estimates. Therefore, full cancellations should be carried out for these correlation values. However, the linear decision, which does not limit large correlation value outputs, would feedback these values into the detector, causing occasional large cancellations (or ‘over-cancellation’).

The clipped soft decision and the hyperbolic tangent (modified from clipped soft decision) retains the advantages of hard limiter (full cancellation when correlation value is large) and linear detection (small cancellation when correlation value is small) while avoiding their shortcomings. The clipped soft decision is shown to be better performing than hard decision and linear decision [30]. Reliable data estimate is very important in multiple stages in order to avoid error propagations.

### 5.1.2 Block cancellations

Another issue in interference cancellation is performing cancellations in a block of bits or symbols. This is called block cancellation. In an asynchronous channel, signals are processed in blocks of  $M$  bits. In a fading channel, assuming that channel conditions do not vary too much within one block (slow fading), block processing allows better estimation of the amplitude, delay and phase. Typically,  $M$  should be as large as possible for more accurate channel estimates. At the same time, it cannot be too large because if channel conditions vary too much within one block, it could lead to inaccurate estimations.

Although block processing allows improvement in performance through better channel estimates, it can also degrade the performance of some IC schemes. The

length of bits in a block affects an IC scheme that uses successive cancellations. SIC scheme ranks its users before cancellations. With block processing, SIC has to rank the users according to the averaged ranking value across the block. Therefore, as the detection continues, the whole block of regenerated signals is cancelled from the composite received signal. Although a user's regenerated block seems reliable enough for cancellation (based on its averaged parameter), it does not necessary means that all the regenerated signals (at bit-level) within that block are reliable enough. One bit might be having low MAI but the next bit might be suffering from high MAI. Therefore, for SIC, block cancellation is not as efficient as bit cancellation.

Schemes adopting parallel cancellation cancels out every interfering regenerated signal blocks. As discussed earlier, this can lead to performance degradation because not every regenerated signal is reliable. This is clearly shown in a fading channel where the PIC becomes inferior to the SIC. Therefore, there is a need for selectivity on which bit's regenerated signal is reliable enough for interference cancellation.

### **5.1.3 Varying channel conditions**

In a practical mobile environment, the channel conditions are not necessarily fixed. For example, a channel could switch from Ricean fading to Rayleigh fading within a few blocks of bits.

Most of the mapping functions researched so far is based on trial and error methods to obtain certain parameters that give the optimum performance. These sets of parameters might be different for different channel conditions. In a practical environment, one cannot easily tell whether he or she is in a fading channel or an AWGN channel and, consequently, cannot instruct the detector to choose the correct set of parameters. Therefore, there is a need for an adaptive function or device that

varies these parameters automatically for optimum performance, whatever channel conditions it is operating in. This function has to have a simple algorithm to minimize any additional computation complexity.

#### 5.1.4 Ranking System

The SIC depends heavily on its ranking system to perform optimally. Power ranking ranks the users according to the received power. Since the received envelope of a user is proportional to the user's received power, ranking the users according to the estimated received envelope  $|\hat{\alpha}_k| = A_k$  achieves the same performance as power ranking. The other ranking mentioned in this thesis is correlation ranking. A performance comparison between these two ranking methods is shown in [18].

We have shown in Section 3.1 that power ranking is ineffective in a perfect power control environment where users are selected randomly for cancellation. However, power ranking is superior to correlation ranking in a fading channel. Therefore, we have to select different ranking system for different channel conditions. As mentioned in the previous section, this is not practical because the channel conditions can change within blocks of data.

Another problem faced by the SIC due to the ranking system is that users who are cancelled first suffer from MAI due to the rest of the users. This causes their decision bits to be less reliable. For example, if power ranking was used, a user with high received signal power is selected first to be cancelled. If that user suffers from very severe MAI, there is a chance of error in the decision bit although power ranking considered the signal to be reliable. Therefore, it is desirable to 'clean' the initial users before any cancellation to improve their decision bits' reliability, and consequently, improve the performance of the system.



## 5.2 Adaptive Bit-Select Cancellation (ABC) Device

To resolve the varying channel conditions and block cancellation problems mentioned earlier, an adaptive decision bit device that filters out unreliable data estimates before they are used for signal regenerations and cancellations is proposed.

The function has two inputs - the  $m$ -th correlation value of user  $k$ ,  $y_k(m)$ , and the adaptive control parameter,  $p(m)$ :

$$f(y_k(m)) = f_k(m) = \text{nsgn}(y_k(m)) = \begin{cases} 1, & y_k(m) > p(m) \\ 0, & -p(m) \leq y_k(m) \leq p(m) \\ -1 & y_k(m) < -p(m) \end{cases} \quad (5.1)$$

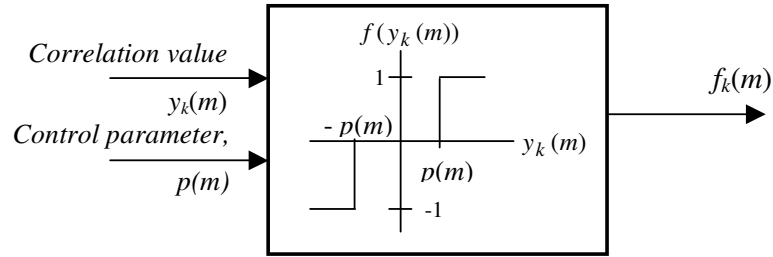


**Figure 5.2:** Adaptive Bit-wise Cancellation Function

From Figure 5.2, the adaptive control parameter,  $p(m)$ , is a parameter that decides which user's decision bit is reliable enough for cancellation and which one is not. Notice that the parameter is a function of  $m$ , which means that the control parameter is varying within one block of bits. This allows flexibility and accuracy in the selection process. A similar device is proposed in [29] but it lacks an adaptive part.

The adaptive control parameter has to be a channel-variant parameter to adapt to channel variations. Therefore, the control parameter used is given by:

$$p(m) = p' \times \bar{y}(m) \quad (5.2)$$

where

$$\bar{y}(m) = \frac{1}{K} \sum_{k=1}^K y_k(m) \quad (5.3)$$

is the  $m$ -th bit's averaged correlation value and  $p'$  is a scaling factor. Notice that not only  $\bar{y}(m)$  varies from block to block, but it also varies from bit to bit.

The scaling factor  $p'$  is very important in controlling the number of signal regenerations and cancellations. For optimum performance, the scaling factor is different for different channel conditions. Therefore, it is crucial to look into methods of linking the optimum scaling factor (the scaling factor for optimum BER performance) with the channel conditions. From the simulations, it is observed that different channel conditions have different variances of the user's averaged correlation value

$$\bar{y}_k = \frac{1}{M} \sum_{m=1}^M y_k(m) \quad (5.4)$$

where  $M$  is the number of bits in one block. This variance is a function of the SNR, number of users  $K$ , processing gain  $N$  and channel conditions (AWGN, fading, etc.).

Using this observation, we formulate the procedures to calibrate the ABC device for the IC of which it is used in:

Step A: Using simulations or measurements, for the IC scheme considered, the optimum scaling factors in different channel conditions is obtained with respect to the number of users  $K$ .

Step B: Using simulations or measurements, the empirical variances of  $\bar{y}_k$  in the considered channel conditions are obtained with respect to the number of users  $K$ .

Step C: Using the values from Step A and Step B, and  $K$  as a common factor, a graph that relates both sets of values is plotted out.

Step D: Using this graph, a function for  $p'$  is obtained with respect to the empirical variance. However, to apply this function into the ABC, we need a real-time

parameter which relates to the empirical variances and can be obtained while the signals are being processed. Therefore, the simplest method (although not necessarily the most accurate) is using the instantaneous variance of  $\bar{y}_k$ .

Therefore, the optimum scaling factor function, given by:

$$p' = g(\sigma^2) \tag{5.5}$$

is a function of the instantaneous variance of  $\bar{y}_k$ ,  $\sigma^2$ , calculated using the correlation values using the following relationship:

$$\sigma^2 = \frac{1}{K} \sum_{k=1}^K (\bar{y}_k - \bar{y})^2 \tag{5.6}$$

where the overall averaged correlation value,  $\bar{y}$ , is given by:

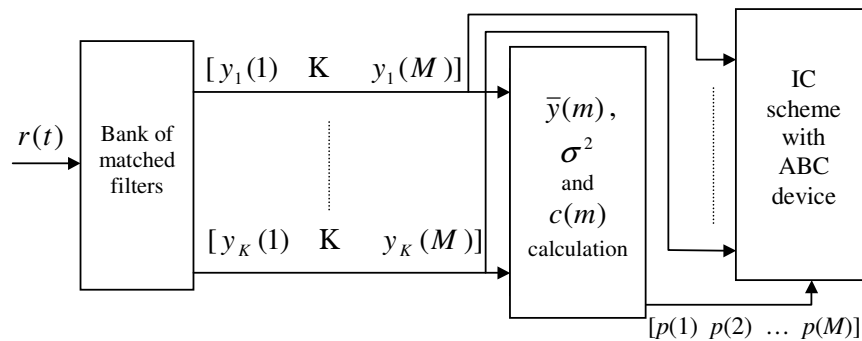
$$\bar{y} = \frac{1}{K} \sum_{k=1}^K \bar{y}_k . \tag{5.7}$$

Notice that  $\sigma^2$  is obtained using the  $M \times K$  correlation values from the zeroth bank of matched filters.

Using (5.5), (5.2) is rewritten as:

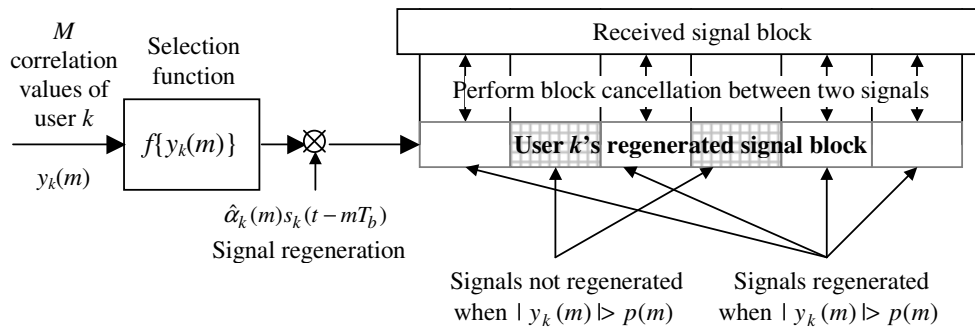
$$p(m) = g(\sigma^2) \bar{y}(m) . \tag{5.8}$$

Figure 5.3 shows how the control parameter is calculated from the correlation values. In the next section, after the ISIC is introduced, we show the implementation of the ABC (using Step A to Step D) in the ISIC.



**Figure 5.3:** Calculation of the control parameter using correlation values

The ABC device is applied on bit-level instead of block level. Thus, it enables bit-wise cancellation even though block processing is used (Figure 5.3). After the calibration procedure mentioned earlier, the ABC can recognize the channel condition within one block of data and selects the appropriate control parameters for optimum performance.



**Figure 5.4:** Bit-wise Cancellation Within a Block Processing System

In the following section, we introduce the improved successive interference canceller (ISIC) and the application of the ABC device in the ISIC is discussed.

### 5.3 Improved Successive Interference Cancellation Scheme (ISIC)

In a SIC scheme, the first users suffers MAI from user 2 to user  $K$ , user 2 suffers MAI from user 3 to user  $K$  and so on. This reduces the reliability of the users that are cancelled first. Therefore, to improve their reliability, we ‘clean’ the signal by introducing a conditional or selective parallel interference canceller into a SIC scheme. We use a conditional PIC instead of the conventional PIC because the conventional PIC is unstable in a fading channel. The conditional PIC allows us to select which user is reliable and which user is not for ‘cleaning’ the signal.

### 5.3.1 ISIC Structure

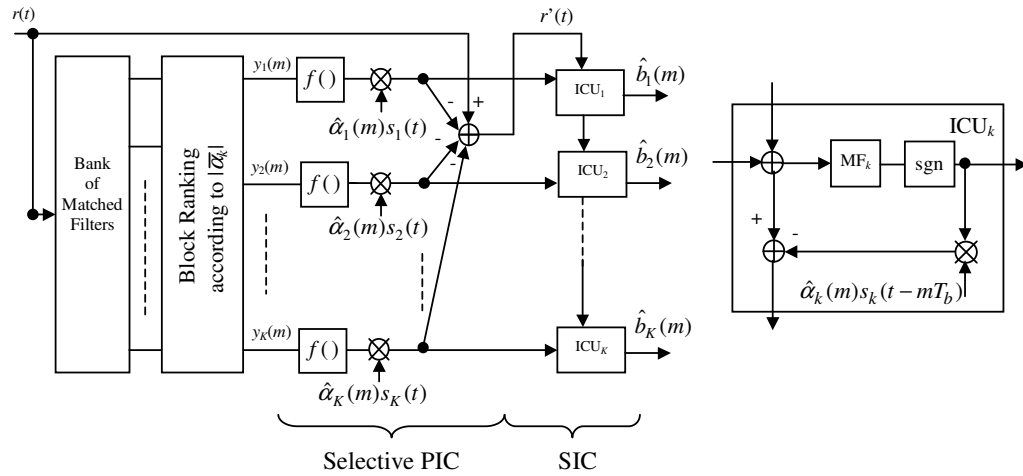


**Figure 5.5:** Improved Successive Interference Cancellation (ISIC)

Figure 5.5 shows the improved successive (or serial) interference cancellation (ISIC). The received signal  $r(t)$  is passed through a bank of  $K$  matched filters to obtain a block of correlation value values  $y_k(m)$ . The users' block of correlation values is then ranked according to the averaged value of the amplitude,  $\bar{\alpha}_k$  (equivalent to power ranking). The correlation value  $y_k(m)$  is passed through a filtering device that determines whether the correlation value is large enough to be used in the 'cleaning' process. We use the adaptive bit-select cancellation (ABC) device introduced in Section 5.2 as the filtering device.

Using the ABC device, the decision bit  $b_k(m)$  in (2.24) for the conventional is replaced by the ABC function  $f_k(m)$  in (5.1). Therefore, the 'cleaned' signal before the successive interference cancellation part (asynchronous channel) is:

$$r'(t) = r(t) - \sum_{k=1}^K \sum_{m=1}^M \hat{\alpha}_k(m) f_k(m) s_k(t - mT_b - \tau_k) \quad (5.9)$$

After the parallel interference cancellation, the successive interference cancellation takes over. In  $ICU_k$  (Figure 5.5), the  $k$ -th user's regenerated signal is

added back to the composite received signal before matched filtering. In a synchronous channel with  $M$  bits per block, the input signal of the  $k$ -th ICU's matched filter,  $r_k(t)$ , corresponding correlation value of the  $m$ -th bit in user  $k$ 's block of bits,  $y_k^{(1)}(m)$ , and the decision bit,  $\hat{b}_k^{(1)}(m)$  are respectively given by:

$$r_k(t) = r(t) - \sum_{j=k+1}^K \sum_{m=1}^M \hat{\alpha}_j(m) f_j(m) s_j(t - mT_b) - \sum_{j=1}^{k-1} \sum_{m=1}^M \hat{\alpha}_j(m) \hat{b}_j^{(1)}(m) s_j(t - mT_b) \quad (5.10)$$

$$y_k^{(1)}(m) = y_k(m) - \sum_{j=k+1}^K \operatorname{Re}\{\hat{\alpha}_j(m) e^{-j\theta_k(m)}\} f_j(m) \rho_{j,k}(m) - \sum_{j=1}^{k-1} \{\hat{\alpha}_j(m) e^{-j\theta_k(m)}\} \hat{b}_j^{(1)}(m) \rho_{j,k}(m) \quad (5.11)$$

$$\hat{b}_k^{(1)}(m) = \operatorname{sgn}\{y_k(m)\}. \quad (5.12)$$

For an asynchronous channel model, (5.10) and (5.11) are rewritten as:

$$r_k(t) = r(t) - \sum_{j=k+1}^K \sum_{m=1}^M \hat{\alpha}_j(m) f_j(m) s_j(t - mT_b - \tau_j) - \sum_{j=1}^{k-1} \sum_{m=1}^M \hat{\alpha}_j(m) \hat{b}_j^{(1)}(m) s_j(t - mT_b - \tau_j) \quad (5.13)$$

$$y_k^{(1)}(m) = y_k(m) - \left[ \sum_{j=k+1}^K \operatorname{Re}\{\alpha_j(n) e^{-j\theta_k(m)}\} f_j(n) \Gamma_{j,k}(m) + \operatorname{Re}\{\alpha_j(n+1) e^{-j\theta_k(m)}\} f_j(n+1) \bar{\Gamma}_{j,k}(m) \right] - \left[ \sum_{j=1}^{k-1} \operatorname{Re}\{\alpha_j(n) e^{-j\theta_k(m)}\} \hat{b}_j^{(1)}(n) \Gamma_{j,k}(m) + \operatorname{Re}\{\alpha_j(n+1) e^{-j\theta_k(m)}\} \hat{b}_j^{(1)}(n+1) \bar{\Gamma}_{j,k}(m) \right] \quad (5.14)$$

where  $n = m - 1$  for  $\tau_j \geq \tau_k$  and  $n = m$  for  $\tau_j < \tau_k$ .

The ABC device serves two purposes in the ISIC scheme. The first one is to select which users signals are reliable for 'cleaning' the received signal. This is very important especially for the first few users that are detected first in the successive interference cancellation part. An early erroneous detection has severe impact on those users that are detected later.

Second, it is used to perform bit-wise cancellation. As discussed in Section 5.2, although the ISIC performs interference cancellation in blocks of  $M$  bits, the ABC device is applied bit-wise to the correlation values  $y_k(m)$ . Therefore, not every decision bit (within one block) is used for interference cancellation in the PIC section.

Now, we show the calibration process of the ABC device in the ISIC. In this thesis, we considered two channel conditions - AWGN channel in perfect power control environment with  $E_b/N_0 = 10\text{dB}$  and Rayleigh fading channel with  $E_b/N_0 = 40\text{dB}$ . Now, we use the guidelines established earlier in Section 5.2:

- *Step A:* Obtaining the optimum scaling values for the channel conditions

Simulations are performed for the two conditions mentioned above (described in Section 3.1) for the ISIC. For a fixed number of users, we swept the values of the scaling factor  $p'$  in (5.2) from 0 to 1.0 and plotted the BER versus  $p'$  graph. We considered the fixed numbers of users  $K$  as 20, 30, 40, 50 and 60 users.

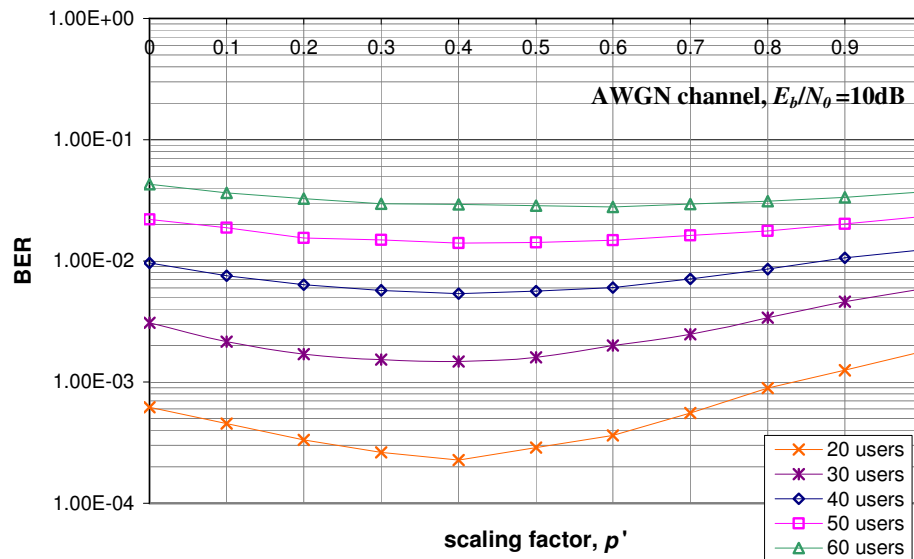


**Figure 5.6:** Performance of ISIC with various scaling factors  $p'$  in AWGN channel

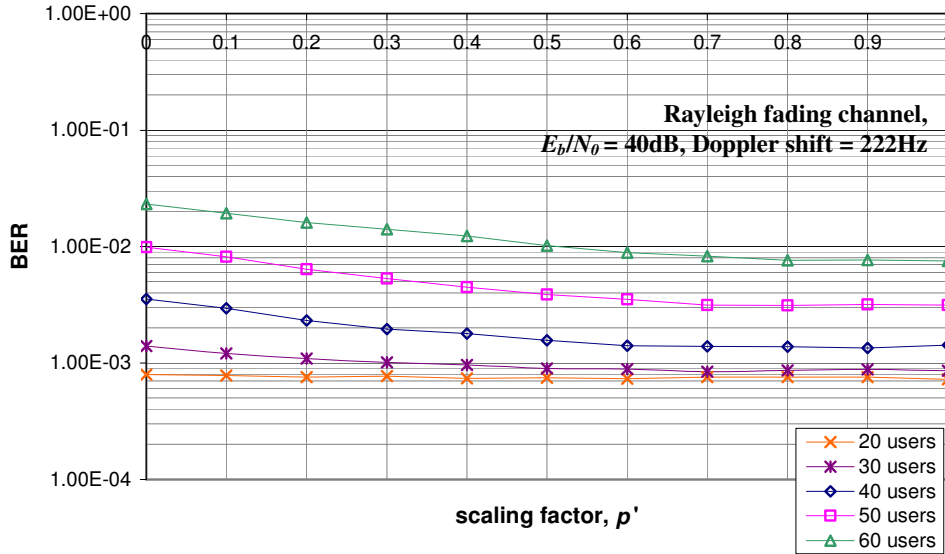


**Figure 5.7:** Performance of ISIC with various scaling factors  $p'$  in Rayleigh fading channel

From Figure 5.6 and Figure 5.7, we take a range of scaling factors that gives the lowest BER for the ISIC and tabulate the range against the corresponding number of users:

Users		20	30	40	50	60
Range of optimum $p'$	AWGN 10dB	0.3 - 0.5	0.3 - 0.5	0.3 - 0.5	0.3 - 0.6	0.4 - 0.6
	Rayleigh 40dB	0.5 - 1.0	0.5 - 1.0	0.6 - 1.0	0.7 - 1.0	0.8 - 1.0

**Table 5.1:** Range of  $c'$  for optimum performance in ISIC

- *Step B:* Obtaining the variance of  $\bar{y}_k$  for the channel conditions considered

Again, we fixed the number of users  $K$  to 20, 30, 40, 50 and 60 users. Using simulations of the matched filter, we collected the statistics of  $\bar{y}_k$  for both channel conditions considered and plotted out the various pdf's. From these pdf's, the empirical variance of  $\bar{y}_k$  is calculated and tabulated against the corresponding number of users and channel condition:



Users		20	30	40	50	60
Variance of $\bar{y}_k$	AWGN 10dB	0.023	0.031	0.038	0.043	0.049
	Rayleigh 40dB	0.182	0.175	0.169	0.161	0.159

**Table 5.2:** Variance of  $\bar{y}_k$  in an AWGN channel and fading channel

Notice that there is a big gap between two channel conditions. The variance in the AWGN channel is less than 0.05 while the variance in the fading channel is more than 0.15.

- *Step C:* Plotting the scaling factor versus empirical variance graph

Using  $K$  as the common factor of the optimum scaling factor and empirical variance, a graph showing the upper limit and lower limit of optimum  $p'$  value is plotted against the corresponding empirical variance:

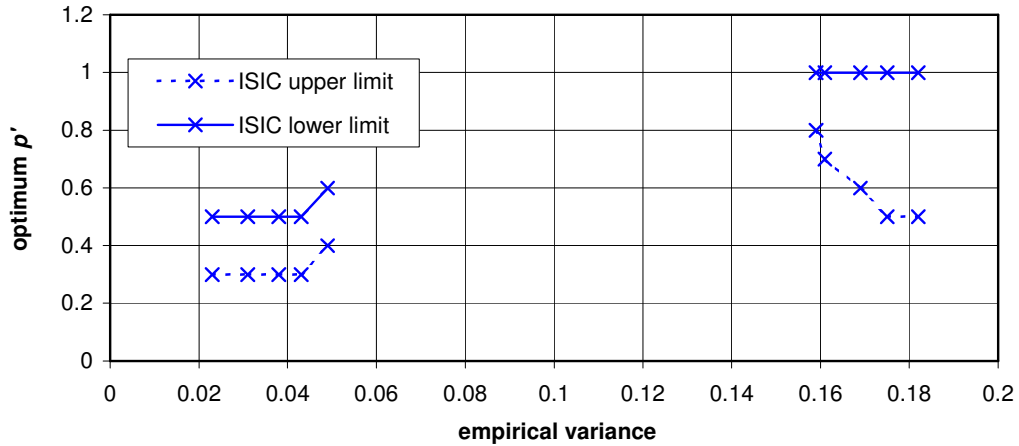


**Figure 5.8:** Scaling factor  $p'$  versus empirical variance of  $\bar{y}_k$  graph

- *Step D:* Obtaining the  $p'$  function with respect to instantaneous variance  $\sigma^2$

From simulations, we observed that for Rayleigh fading, the instantaneous variance value is always above 0.07. Therefore, we set the border value to differentiate the AWGN channel from the fading channel to  $\sigma^2 = 0.07$ . Using Figure 5.8 and the border value, we obtain the simplest function that lies between the upper limit and the lower limit:

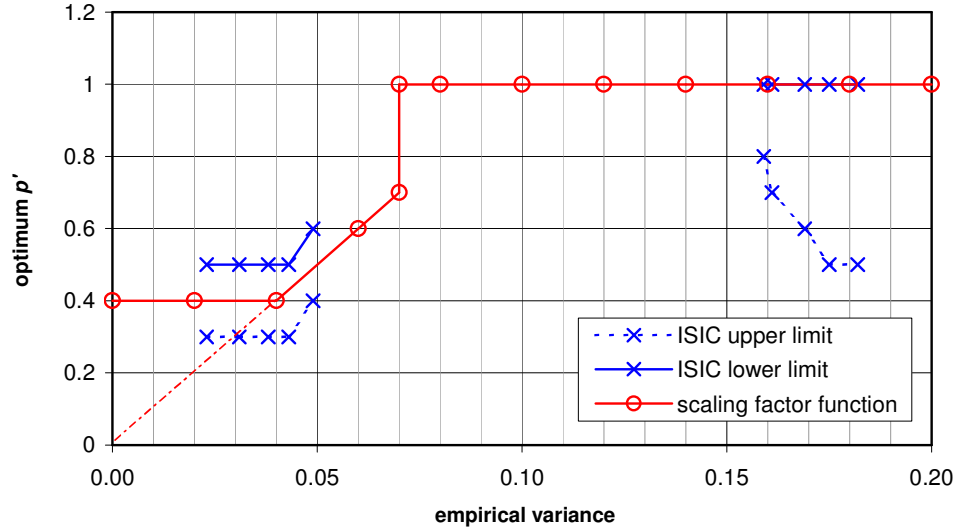


**Figure 5.9:** Obtaining the scaling factor function

From Figure 5.9, the scaling factor function, or  $p'$  function, is:

$$p' = g(\sigma^2) = \begin{cases} 0.4 & \sigma^2 < 0.04 \\ 10\sigma^2 & 0.04 \leq \sigma^2 \leq 0.07 \\ 1.0 & \sigma^2 > 0.07 \end{cases} \quad (5.15)$$

The  $p'$  function in (5.15) is not unique. It is one of the many functions that we can form from Figure 5.8. Through the adaptive feature of the ABC device, the ISIC can now operate optimally in both channel conditions. In the next sub-section, we discuss and compare the performance of the ISIC with other interference cancellation schemes.

### 5.3.2 BER Performance of the ISIC

In this section, we investigate how the ISIC fare against the other interference cancellation schemes. Using the channel conditions in Section 3.1, we simulate the performance of the ISIC with the ABC device and compared it to other interference cancellation schemes.

From Figure 5.10, it is obvious that the ISIC is far superior as compared to the PIC. For a BER of 1% in AWGN channel with perfect power control, the ISIC has a capacity that is 40% higher than the PIC. Furthermore, the ISIC improves the SIC (with power ranking) capacity by more than 100%. Also, from Figure 5.11, the ISIC with 30 users has a 4 dB gain as compared to the SIC (power ranking) with 30 users for a BER of 1%.

In a Rayleigh fading channel, from Figure 5.12 at 1% BER, the ISIC improves the performance of the SIC (with power ranking) with an increase of 26% in capacity. Also, the ISIC has about 3 times the capacity of the PIC. Note that the ISIC even outperforms the SICRM.

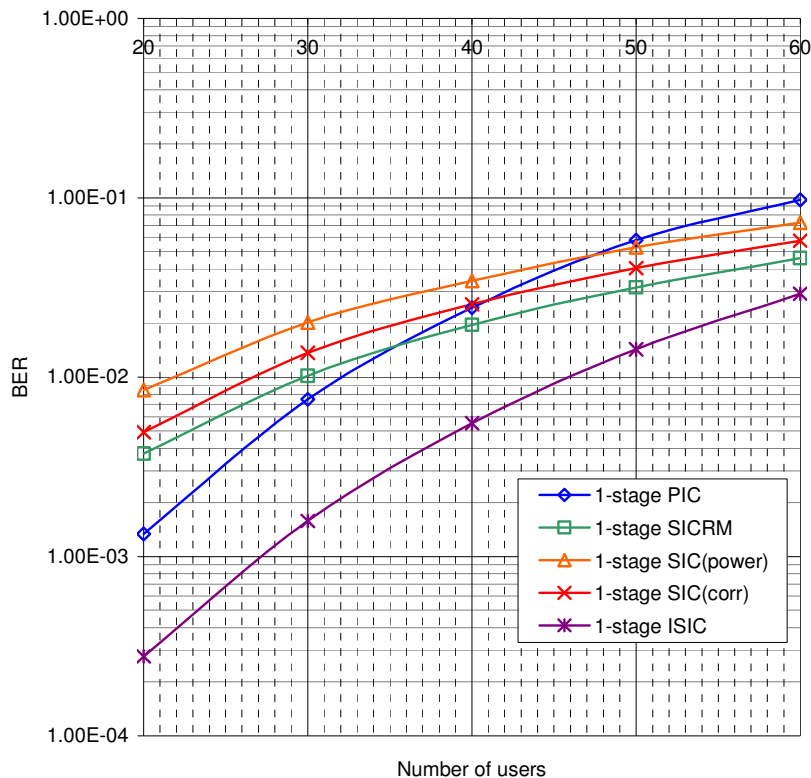


**Figure 5.10:** Capacity of SIC, PIC and ISIC in an AWGN channel with  $E_b/N_0 = 10\text{dB}$ ,  $N = 31$

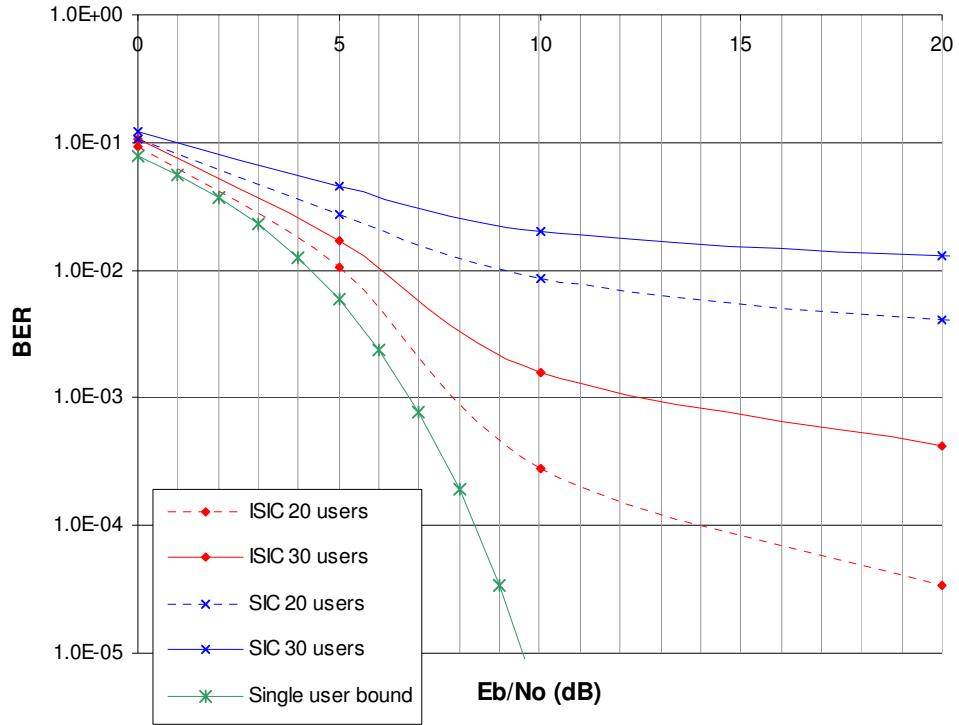


Figure 5.11: Performance of SIC and ISIC in a AWGN channel with  $N = 31$

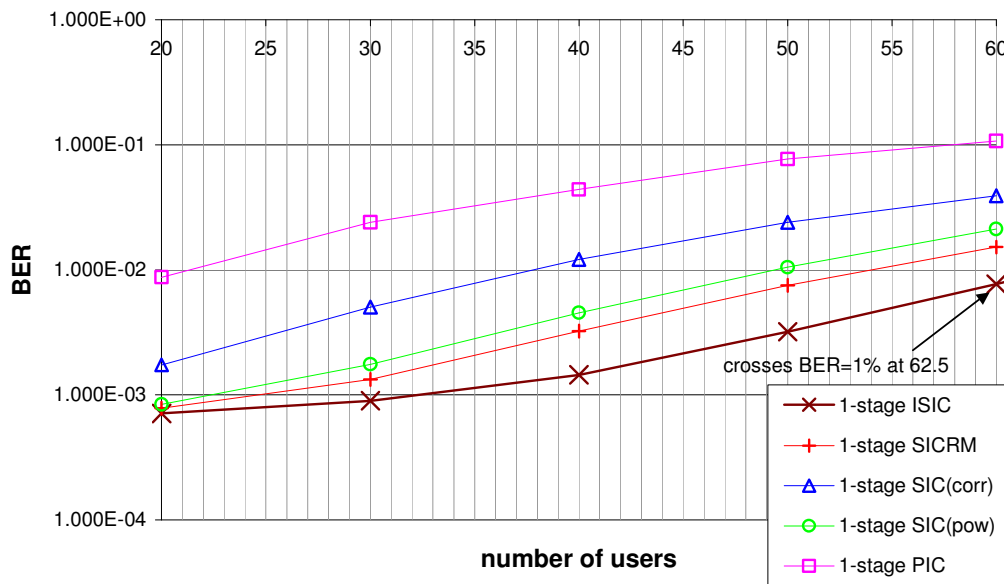


Figure 5.12: Capacity of SIC, PIC and ISIC in a Rayleigh fading channel with  $E_b/N_0 = 40\text{dB}$ ,  $N = 31$ , Doppler shift = 222Hz

In the above simulations we have used perfect channel estimation to perform ‘perfect’ cancellations where the performance of the cancellers depended mainly on reliability of the decision bits used for interference cancellations. But to see how well the ISIC performs under erroneous channel estimation, we perform the following simulations. We introduce a zero-mean Gaussian distributed error with variance  $\sigma_n^2$  to the estimated amplitude,  $|\hat{\alpha}_k|$ . Therefore, the new complex amplitude used for signal regeneration is:

$$\hat{\alpha}_k' = abs\{|\hat{\alpha}_k| + \eta(0, \sigma_n^2)\}e^{j\theta_k} \quad (5.16)$$

where  $\eta$  is a Gaussian distributed random variable with zero mean and variance  $\sigma_n^2$ . This error not only affects the effectiveness of the interference cancellation but also the ranking effectiveness of the SIC using power ranking and the ISIC.

The performance of the SIC, the PIC and the ISIC is compared in an AWGN channel with perfect power control and a Rayleigh channel in Figure 5.13 and 5.14 respectively. It is shown that in both channel conditions, the ISIC maintain superiority over the SIC (including the SICRM) and the PIC even when there is erroneous amplitude estimation. This is especially obvious in the fading channel where most of the SIC scheme have converged to the same capacity at  $\sigma^2 = 0.4$ . At this variance, ISIC still has a capacity that is 85% above the other SIC schemes. This shows that the ISIC is very resistant to amplitude estimation errors as compared to other SIC schemes.

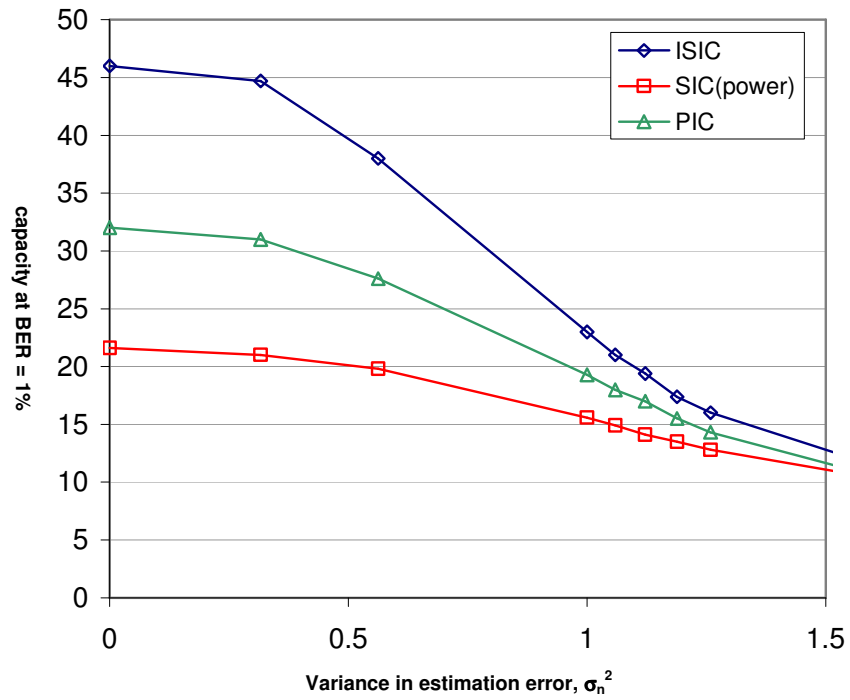


Figure 5.13: Capacity of SIC, PIC and ISIC in an AWGN with  $E_b/N_0 = 10\text{dB}$ ,  $N = 31$  with erroneous amplitude estimation

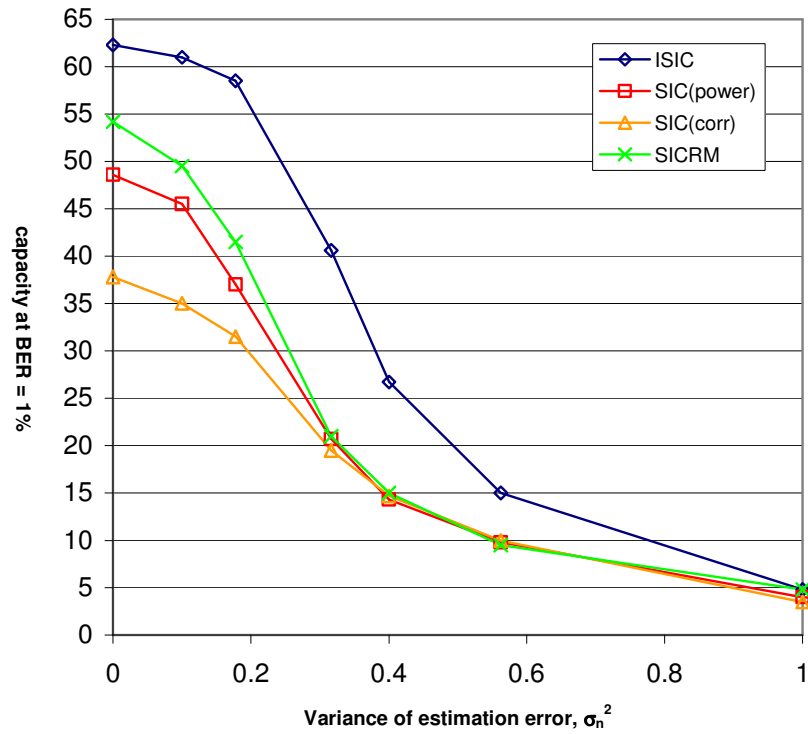


Figure 5.14: Capacity of SIC schemes and ISIC in a Rayleigh fading channel with  $E_b/N_0 = 40\text{dB}$ ,  $N = 31$ , Doppler shift = 222Hz with erroneous amplitude estimation

### 5.3.3 Computation Complexity and Processing Time of ISIC

The ISIC has shown tremendous performance improvement over the basic and conventional IC schemes. It is even better performing than the SICRM. In this section we analyse the computation complexity and processing time of ISIC.

Let us start by recapping the basic operation constants from Section 3.2. Recall that:

$$NMB_{MF} = 2N + 2,$$

$$NAB_{MF} = 2N - 1,$$

$$NMB_{RG} = 2 + 2N,$$

$$NAB_{CANC} = 2N.$$

The number of parallel cancellations of ISIC per bit,  $\gamma$ , varies from bit to bit.

Therefore, we use the averaged value obtained from simulations:

$E_b/N_0$	AWGN with perfect power control				
	Number of parallel cancellations, $\gamma$				
	20 users	30 users	40 users	50 users	60 users
0	14	21	27	33	37
10	16	24	31	37	43
20	17	24	31	38	44

$E_b/N_0$	Rayleigh Fading				
	Number of parallel cancellations, $\gamma$				
	20 users	30 users	40 users	50 users	60 users
0	9	13	17	22	26
20	9	13	18	22	26
40	9	14	18	22	26

**Table 5.3:** Average number of parallel cancellations in the ISIC for different channel conditions,  $E_b/N_0$  and number of users for processing gain of 31

The ISIC is a modified version of the SIC. Therefore, the average number of operations per bit for ISIC (referring to Figure 5.5) includes the number of operations per bit for SIC and the number of additional operations per bit required for the selective parallel interference cancellations (contributed by  $\gamma$  signal regenerations,  $\gamma$

signal cancellations and  $\gamma$  signal additions). In a synchronous channel, the number of operations per bit equations for the ISIC are:

$$\begin{aligned}
 NMB_{ISIC} &= NMB_{SIC} |_{S=1} + \gamma \cdot NMB_{RG} \\
 &= 3K(2N + 2) + \gamma(2 + 2N) \\
 &= (3K + \gamma)(2 + 2N) \\
 NAB_{ISIC} &= NAB_{SIC} |_{S=1} + 2\gamma \cdot NAB_{RG} \\
 &= 2K(3N - 1) + 2\gamma(2N) \\
 &= 2K(3N - 1) + 4\gamma N.
 \end{aligned} \tag{5.17}$$

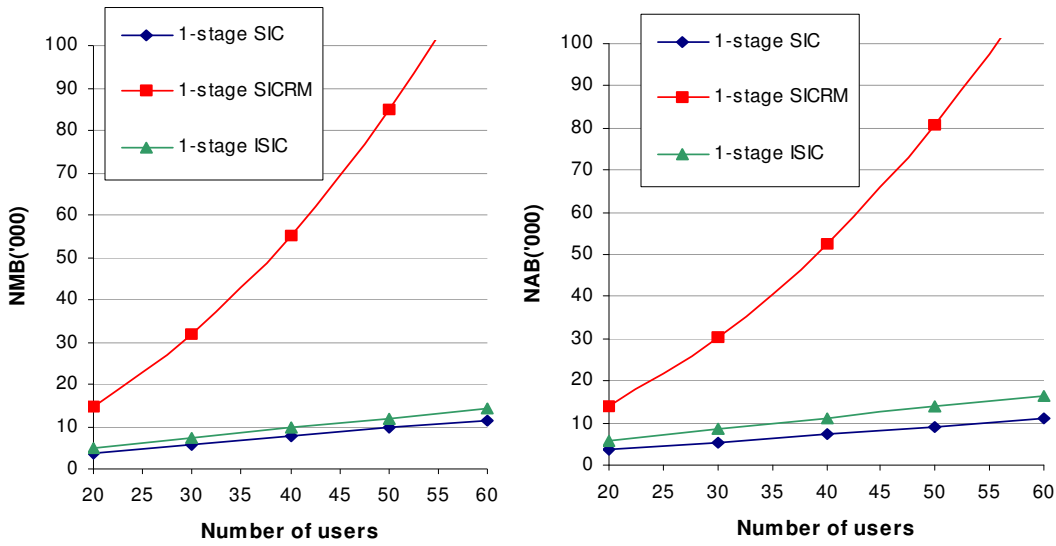


**Figure 5.15:**  $NMB$  and  $NAB$  comparison between conventional SIC, SICRM and ISIC with  $N = 31$ ,  $E_b/N_0 = 10\text{dB}$  in AWGN channel with perfect power control

We compare the number of operations per bit for 1-stage ISIC with other 1-stage SIC schemes in Figure 5.15. The computation complexity increase for the ISIC is about 54% for  $NAB$  and less than 30% for  $NMB$ . This is a very small amount when compared to the SICRM which increases the computation complexity by at least three times. Since there are less parallel cancellations in a Rayleigh fading channel (Table 5.3), the computation complexity of the ISIC in a Rayleigh fading channel is even lower than its computation complexity in an AWGN channel.



In terms of processing time blocks, the ISIC requires the  $PTB$  of a 1-stage SIC in addition to one column of  $\gamma$  signal regenerations in parallel, one column of  $\gamma$  signal cancellations in parallel and another column of  $\gamma$  signal additions in serial. Using (3.8) and (3.9), the average required  $PTB$  for the 1-stage ISIC is:

$$\begin{aligned}
 PTB_{ISIC} &= PTB_{SIC} |_{S=1} + 1 \cdot PTB_{RG} + 1 \cdot PTB_{CANC} + \gamma \cdot PTB_{CANC} \\
 &= (6K - 2) + 1 + 1 + \gamma \\
 &= 6K + \gamma
 \end{aligned} \tag{5.18}$$

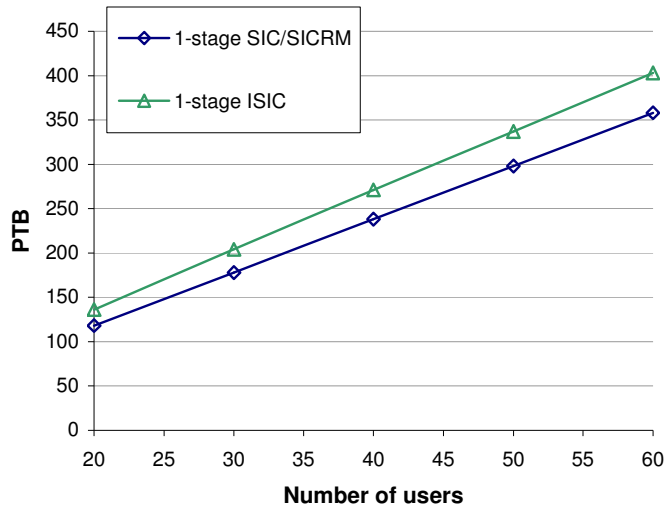


**Figure 5.16:** PTB comparison between conventional SIC, SICRM and ISIC with  $N = 31$

From Figure 5.16, the ISIC introduces additional processing time of about 15% to achieve the BER improvement. If processing time is to be lowered without degrading the BER performance, we use the CCI.

## 5.4 ISIC using the Cross-correlation Implementation

It is possible to reduce the processing time of ISIC by using the CCI described in Chapter 4. However, this increases the computation complexity of the ISIC. The cross-correlation implementation of the ISIC is shown in Figure 5.17.

The two shaded areas represent the two different parts of the ISIC described earlier – the selective PIC part and the SIC part. Calculation of the computation complexity of CCI-ISIC is fairly simple. Notice that the SIC part is almost similar to that of the SICRM in Figure 4.5 without the sub-selectors (SS). In fact, the only other difference is that there are additional MAI generations and cancellations performed in the selective PIC part.

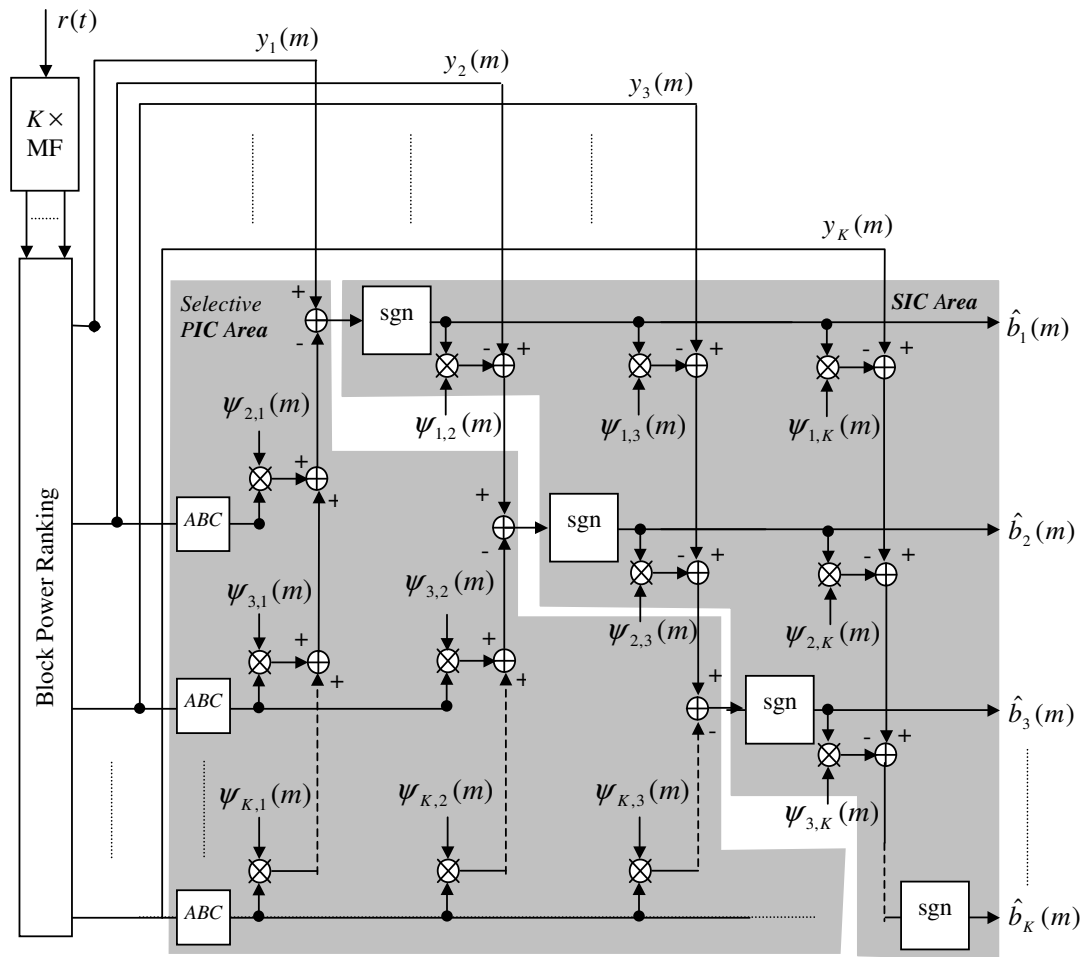


**Figure 5.17** CCI-ISIC with adaptive bit-select cancellation (ABC) device in a synchronous channel

The ABC device, which filters out unreliable bit decisions before MAI generation, is dependent on the users' correlation values. Therefore, we need simulations to

obtain the averaged additional MAI generation and cancellation.

We define these additional averaged number of MAI generations as  $\zeta$ . From simulations, we obtain their values with respect to channel conditions,  $E_b/N_0$  and number of users,  $K$  (Table 5.4). It is assumed that all  $\psi_{j,k}(m)$  and  $\psi_{k,j}(m)$  pairs (where  $k > j$ ) are calculated (Note: Only  $\psi_{j,k}(m)$  is required in the SICRM's case).

$E_b/N_0$	AWGN with perfect power control				
	Average number of additional MAI generation and cancellation per bit, $\xi$				
	20 users	30 users	40 users	50 users	60 users
0	137	304	529	799	1108
10	161	350	606	924	1300
20	165	357	615	936	1316

$E_b/N_0$	Rayleigh Fading				
	Average number of additional MAI generation and cancellation per bit, $\xi$				
	20 users	30 users	40 users	50 users	60 users
0	70	157	287	450	652
20	57	136	252	412	606
40	57	137	254	412	606

**Table 5.4:** Number of additional MAI generation and cancellations required in the selective PIC part of ISIC for different channels,  $E_b/N_0$  and number of users ( $N = 31$ )

Recall that the  $NMB$  required for MAI generation is 1 and  $NAB$  required for MAI cancellation is also 1. Therefore, the  $NMB$  and  $NAB$  for ISIC using cross-correlation method (in a synchronous channel) are respectively given by:

$$\begin{aligned}
NMB_{CCI}^{ISIC} \Big|_{S=1} &= K \cdot NMB_{MF} + \frac{K(K-1)}{2} NMB_{RG'} + \frac{K(K-1)}{2} NMB_{\psi} + \zeta \cdot NMB_{RG'} \\
&= K(2N+2) + K(K-1) \left( \frac{N+7}{2} \right) + \zeta \\
NAB_{CCI}^{ISIC} \Big|_{S=1} &= K \cdot NAB_{MF} + \frac{K(K-1)}{2} NAB_{CANC'} + \frac{K(K-1)}{2} NAB_{\psi} + \zeta \cdot NAB_{CANC'} \\
&= K(2N-1) + K(K-1) \left( \frac{N+2}{2} \right) + \zeta
\end{aligned} \tag{5.19}$$

In terms of processing time, the ISIC using CCI has the PTB of the CCI-SICRM plus one column of  $\zeta$  MAI cancellation units (MC) in parallel (from the selective PIC part) and this yields:

$$\begin{aligned}
 PTB_{CCI}^{ISIC} &= PTB_{cross}^{SICRM} |_{S=1} + 1 \cdot PTB_{MC} \\
 &= 6 + 2K
 \end{aligned}
 \tag{5.20}$$

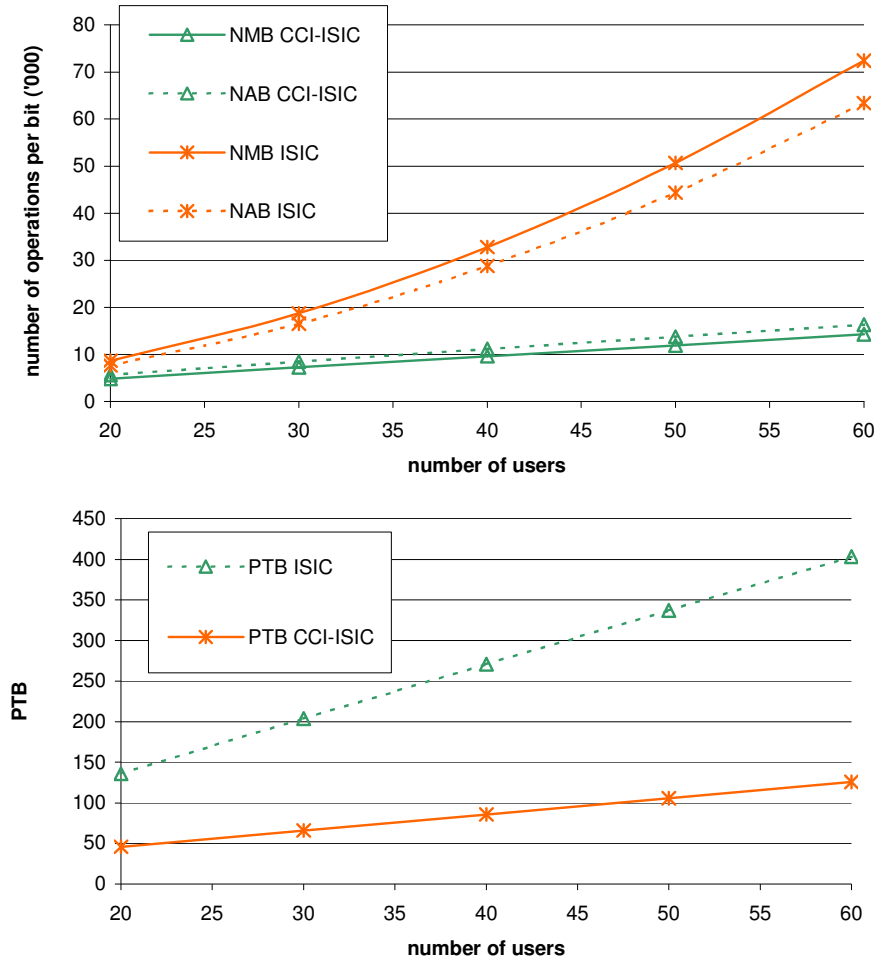


**Figure 5.18:** Comparison of computation complexity and processing time between conventional ISIC and CCI-ISIC

From Figure 5.18, the computation complexity of the cross-correlation based ISIC is much greater than the conventional ISIC. However, the processing time is greatly reduced by the CCI. Therefore, if computation complexity can be sacrificed for

processing, the CCI-ISIC (with the ABC device) is an ideal choice of IC scheme – superior BER performance, adaptive to channel conditions, moderate processing time and resistant to estimation errors.

## 5.4 Chapter Summary

The ISIC introduced in this chapter, with the ABC device, has shown several benefits. There is tremendous improvement in the BER performance over the basic SIC in an AWGN channel and a fading channel without introducing too much computation complexity or processing time.

By using the ABC device in the selection of the regenerated signals for ‘cleaning’ the received signal, we improve the reliability of decision bits of the higher ranked users. It allowed the ISIC to outperform the PIC, which is superior in an AWGN channel, and the SICRM, which is superior in the Rayleigh fading channel.

The adaptive feature of the ABC device also achieves the optimum performance of the ISIC both in a perfect power control environment and a fading channel without any external control. Since the adaptive algorithm is applied and updated after every block of bits, the detector is very flexible and performance is optimized even if it moves rapidly between different channel conditions.

Also, the parameters used in the adaptive algorithm are obtained easily. This is because they are various means of the users’ correlation values, which are obtained from the outputs of the zeroth stage bank of matched filters.

## CHAPTER 6

### CONCLUSION AND SUGGESTION FOR FUTURE WORKS

#### 6.1 Conclusion

In this thesis we have investigated thoroughly the performance of various interference cancellation schemes. Not only have we looked into their BER performance, we have introduced two sets of parameters - number of operations per bit, (further divided into number of additions per bit, *NAB*, and number of multiplications per bit, *NMB*) to measure computation complexity and the processing time block (*PTB*) to measure processing time. Using these three parameters, we have formulated basic operation equations that quantify the processing time and computation complexity required in matched filtering, signal regeneration and signal cancellations. These basic operation equations can be applied easily in any IC schemes to evaluate their processing time or computation complexity.

We have also introduced the cross-correlation implementation (CCI). This implementation is used to reduce the processing time of any IC scheme. For SIC schemes, the CCI reduces the processing time up to a third of the conventional method's value. When applied to advanced IC schemes (those that uses high amount of matched filters to enhance their performances), the CCI reduces the complexity by about 45%. The CCI is applicable to any IC schemes and implementation is simple.

Looking into various issues that are specific to SIC schemes, we have proposed the improved successive interference cancellation (ISIC) scheme together with the adaptive bit-select cancellation (ABC) device. In the AWGN channel, the ISIC's

capacity is 40% higher than the PIC's and two times the capacity of the SIC. In the fading channel, it is superior to the SIC and SICRM (capacity that is 26% higher than SIC, 14% higher than SICRM). These BER improvements are achieved at very low computation complexity and processing time increase.

Therefore, from our works in this thesis, we have improved SIC schemes in terms of BER performance, processing time and computation complexity.

## 6.2 Suggestions for Future Works

Our analysis of the computation complexity has been divided into *NMB* and *NAB* because of the various differences in digital signal processing (DSP) units. A multiplication might require the same amount of clock cycles for one addition in one DSP but requires an additional half a clock cycle in another DSP. Therefore, our analysis has been separated into multiplications and additions/subtractions. Future works can look into the relationship between additions and multiplications in terms of clock cycle level to make the analysis of IC schemes more accurate.

The bulk of the cross-correlation implementation depends very heavily on the calculation of the MAI coefficients. Thus, future works can look into designing the DSP or an algorithm that calculates these coefficients at a much lower computation complexity. In fact, one major area of application is downlink transmission. It is possible for the mobile to request these coefficient values (through some control channel) from the base station. The mobile would only need to send the various delays (due to multipath) of the received signal to the base station, and the base station would calculate these MAI coefficients (can be pre-calculated) and sends them to the mobile unit to perform interference cancellation. This can reduce the bulk of the computation from the mobile unit and even reduce the processing time.

Another area worth looking into is the ISIC scheme. In this thesis, we have used only a 1-stage ISIC. And like SIC, ISIC can have re-matched filtering to improve its bit estimates. Various methods can be used for re-matched filtering depending on the level of computation complexity allowed. Not only that, one can also look into the multi-stage implementation of the ISIC.

In multistage ISIC, the control coefficient would vary from stage to stage, and the ABC device can be calibrated to achieve optimum performance. Also, for further improvement of the ISIC, the mapping functions suggested earlier can be implemented in addition to the ABC function. This will turn the selective PIC into a soft decision selective PIC as those in [32-34]. In conclusion, the ISIC has many open ends for research to improve its performance.



## REFERENCES

- [1] Parkvall S., Dahlman E., Frenger P., Beming P., Persson M., “The evolution of WCDMA towards higher speed downlink packet data access,” *Vehicular Technology Conference 2001*, Vol. 3, pg. 2287 –2291.
- [2] Dahlman E., Gudmundson B., Nilsson M., Skold, A., “UMTS/IMT-2000 based on wideband CDMA,” *IEEE Communications Magazine*, Sep 1998, Vol. 36 No. 9, pg. 70- 80.
- [3] Lee W.C.Y., “Overview of Cellular CDMA,” *IEEE Transactions On Vehicular Technology*, May 1991, Vol. 40, No. 2, pg. 291-302.
- [4] Verdu S., *Multiuser Detection*, Cambridge University Press, 1998.
- [5] Proakis J.G., *Digital Communications*, McGrawHill Inc., Third Edition 1995.
- [6] Verdu S., “Minimum Probability of Error for Asynchronous Gaussian Multiple-Access Channels,” *IEEE Transactions On Information Theory*, Jan 1986, Vol. IT-32, pg. 85-96.
- [7] Schneider K.S., “Optimum detection of code division multiplexed signals,” *IEEE Transactions On Aerospace Electronic Systems*, Jan 1979, Vol. AES-15, No. 1, pg. 181-185.
- [8] Kohno R., Hatori M., Imai H., “Cancellation techniques of co-channel interference in asynchronous spread spectrum multiple access systems,” *Electronis and Comm. in Japan*, 1983, Vol. 66-A, No. 5, pg. 20-29.
- [9] Lupas R., Verdu S., “Near-far resistance of multiuser detectors in asynchronous channels,” *IEEE Transactions On Comm.*, April 1990, Vol. 38, No. 4, pg. 496-508.

- [10] Lupas R., Verdu S., "Linear multiuser detectors for synchronous code division multiple-access channels," *IEEE Transactions On Information Theory*, Jan 1989, Vol. 35, No. 1, pg. 123-136.
- [11] Honig M., Madhow U., Verdu S., "Blind adaptive multiuser detection," *IEEE Transactions On Information Theory*, July 1995, Vol. 41, No. 4, pg. 944-960.
- [12] Hui A.L.C., Letaief K.B., "Successive interference cancellation for multiuser asynchronous DS/CDMA detectors in multipath fading links," *IEEE Transactions on Comm.*, March 1998, Vol. 46, No. 3, pg. 384-391.
- [13] Kohno R., Imai H., Hatori M., Pasupathy S., "Combination of an adaptive array antenna and a canceller of interference canceller of interference for direct-sequence spread-spectrum multiple-access system," *IEEE Journal on Selected Areas of Comm.*, May 1990, Vol. 8, No. 4, pg. 675-682.
- [14] Kohno R., Imai H., Hatori M., Pasupathy S., "An adaptive canceller of cochannel interference for spread-spectrum multiple-access communication networks in power line," *IEEE Journal on Selected Areas of Comm.*, May 1990, Vol. 8, No. 4, pg. 691-699.
- [15] Nahler A., "Reduced and Differential Parallel Interference Cancellation for CDMA System," *IEEE Journals on Selected Areas in Comm.*, Feb. 2002, Vol. 20, No. 2, pg 239.
- [16] Patel P., Holtzmann J., "Analysis of a simple successive interference cancellation scheme in a DS-CDMA system," *IEEE Journals on Selected Areas in Comm.*, June 1994, vol.12 no.5, pg 796-807.
- [17] Taeyoon K., Daeki H., Changeon K., Daesik H., "Adaptive pipelined successive interference cancellation for a DS/CDMA system," *IEEE International Conference on Comm. 2000*, Vol. 2, pg 740-743.

- [18] Patel P. and Holtzman J., "Performance comparison of a DS/CDMA system using a successive interference cancellation (IC) scheme and parallel IC scheme under fading," *Proc. IEEE Int. Conf. On Comms.*, May 1994, pg. 510-514.
- [19] Dae-ki H., Ha-Young Y., Young-Hwan Y., Chang-Eon K., "Analysis of a Pipelined Successive Interference Cancellation Scheme for a DS/CDMA system," *IEEE Communications Letters*, Vol. 4, No.1, Jan.2000, pg 1-3.
- [20] Kim J.H., Jeong J.Y., Yeom S.J., Choi B.G., Park Y.W., "Performance Analysis of the Hybrid Interference Canceller for Multiple Access Interference Cancellation," *IEEE TENCON 1999*, pg. 1236-1239.
- [21] Sun S., Rasmussen L.K., Sugimoto H. and Lim T.J., "A hybrid interference canceller in CDMA," *Proc. IEEE Int. Symp. On Spread Spectrum Techniques and Applications*, Sept. 1998, pg. 150-154.
- [22] Ang K.W., Witold A.K., "A Method of Limiting the Processing time of the Improved Multi-stage Variable Group Hybrid Interference Cancellation Scheme for CDMA System," *Vehicular Technology Conference 1999*, 1999, Vol. 3, pg. 1648 –1652
- [23] Malik R.; Dubey V.K.; McGuffin B., "A hybrid interference canceller for CDMA systems in Rayleigh fading channels," *Vehicular Technology Conference 2001*, 2001, Vol. 2, pg. 1523 –1527.
- [24] Varansi M.K., Aazhang B., "Multistage detection in asynchronous code-division multiple access communications," *IEEE Transactions on Comm.*, April 1990, Vol. 38, pg. 509-519.
- [25] Viterbi A.J., "Very low rate convolutional codes for maximum theoretical performance of spread-spectrum multiple-access channels," *IEEE Transactions on Comm.*, April 1990, Vol. 38, pg. 509-519.

- [26] Jakes W. C., *Microwave Mobile Communications*, IEEE Press, 1994.
- [27] Patel P.R., Holtzman J.M., "Analysis of a DS/CDMA successive interference cancellation scheme using correlation values," *IEEE Global Telecommunications Conference*, 1993, Vol. 1, pg 76 –80.
- [28] Kim Y. W., Kim S. R., Choi I.K., Cho S.H., "Implementation issues on the interference cancellation over asynchronous multipath channels," *Vehicular Technology Conference 2001*, May 2001, Vol. 3, pg.1589 –1592.
- [29] Han S.H., Lee J.H., "Performance of multi-rate DS-CDMA system with multi-stage partial parallel interference cancellation," *Vehicular Technology Conference Proceeding 2000*, Vol. 2 pg. 765-769.
- [30] Sugimoto H., Rasmussen L.K., Lim T.J.; Oyama T., "Mapping Functions For Successive Interference Cancellation in CDMA," *Vehicular Technology Conference 1998*, Vol. 3 , pg. 2301 –2305.
- [31] Divsalar D., Simon M.K., Raphaeli D., "Improved Parallel Interference Cancellation for CDMA," *IEEE Transactions on Comm.*, Feb 1998, Vol. 46 No. 2, pg. 258-268.
- [32] Wei Z., Blostein S.D., "Soft-decision successive interference cancellation CDMA receiver with amplitude averaging and robust to timing errors," *IEEE Global Telecommunications Conference 2001*, Nov. 2001, Vol. 2, pg. 743 –747.
- [33] Wei Z., Blostein S.D., "Soft-decision Multistage Multiuser Interference Cancellation," *IEEE Transactions on Vehicular Technology*, March 2003, Vol. 52, No. 2, pg 380-389.
- [34] Sequeira R.E., Stewart K.A., "Improved performance of pilot-assisted DS-CDMA receivers through partial interference cancellation," *Vehicular Technology Conference 2002*, May 2002, Vol. 4, pg. 2047 –2051.

- [35] *Technical Specifications of 3GPP*, “Spreading and Modulation (FDD),”  
TS25.213, V5.30, 2003.

## **LIST OF SUBMITTED INVENTION DISCLOSURES**

- 1) Ho K.S.D., Ang K.W., Chew Y.H., Yen K., “Computation Complexity and Processing Time Reduction for Serial Type Interference Cancellation Algorithm,” ID No. D2002-13, April 2003.
- 2) Ho K.S.D., Ang K.W., Chew Y.H., Yen K., “Improved Successive Interference Cancellation,” ID No. P2003046, July 2003.
- 3) Ho K.S.D., Ang K.W., Chew Y.H., Yen K., “Adaptive Bit-Select Cancellation,”  
(In preparation for reviewing)

## **LIST OF PUBLICATION**

- 1) Yen Kai, Ho K.S.D., “An Improved BER Calculation for Nonlinear Successive Interference Cancellation,” To appear in the Proceedings of the Vehicular Technology Conference (VTC)'03 Fall, Orlando, Florida

## APPENDIX A

### Minimizing The Likelihood Function in Decorrelating Detector

For the decorrelating detector discussed in Section 2.2, recall that the likelihood function (2.5):

$$\begin{aligned}\Lambda(\hat{\mathbf{b}}) &= (\mathbf{y} - \mathbf{R}\mathbf{A}\hat{\mathbf{b}})^T \mathbf{R}^{-1} (\mathbf{y} - \mathbf{R}\mathbf{A}\hat{\mathbf{b}}) \\ &= \mathbf{y}^T \mathbf{R}^{-1} \mathbf{y} - \mathbf{y}^T \mathbf{A}\hat{\mathbf{b}} - \hat{\mathbf{b}}^T \mathbf{A}^T \mathbf{y} + \hat{\mathbf{b}}^T \mathbf{A}^T \mathbf{R}\mathbf{A}\hat{\mathbf{b}}\end{aligned}\quad (\text{A-1})$$

We obtain the gradient of  $\Lambda(\hat{\mathbf{b}})$  with respect to  $\hat{\mathbf{b}}$ :

$$\begin{aligned}\frac{\partial \Lambda(\hat{\mathbf{b}})}{\partial \hat{\mathbf{b}}} &= \frac{\partial}{\partial \hat{\mathbf{b}}} (\mathbf{y}^T \mathbf{R}^{-1} \mathbf{y} - \mathbf{y}^T \mathbf{A}\hat{\mathbf{b}} - \hat{\mathbf{b}}^T \mathbf{A}^T \mathbf{y} + \hat{\mathbf{b}}^T \mathbf{A}^T \mathbf{R}\mathbf{A}\hat{\mathbf{b}}) \\ &\equiv -\mathbf{A}^T \mathbf{y} - \mathbf{A}^T \mathbf{y} + 2\mathbf{A}^T \mathbf{R}\mathbf{A}\hat{\mathbf{b}} \\ &= 2\mathbf{A}^T \mathbf{R}\mathbf{A}\hat{\mathbf{b}} - 2\mathbf{A}^T \mathbf{y}\end{aligned}\quad (\text{A-2})$$

To minimize (A-1), we equate (A-2) to a zero:

$$2\mathbf{A}^T \mathbf{R}\mathbf{A}\hat{\mathbf{b}} - 2\mathbf{A}^T \mathbf{y} = \mathbf{0}\quad (\text{A-3})$$

Simplifying (A-3), we obtain

$$\mathbf{A}\hat{\mathbf{b}} = \mathbf{R}^{-1} \mathbf{y}\quad (\text{A-4})$$

Recall from (1.17) that  $\mathbf{A}$  is a diagonal matrix. Thus, it only scales the data estimate vector  $\hat{\mathbf{b}}$ :

$$\mathbf{A}\hat{\mathbf{b}} = \begin{bmatrix} \alpha_1 \hat{b}_1 \\ \mathbf{M} \\ \alpha_K \hat{b}_K \end{bmatrix}\quad (\text{A-5})$$

Therefore, the data estimate vector  $\mathbf{b}^0$  for the decorrelating detector is:

$$\mathbf{b}^0 = \mathbf{A}\hat{\mathbf{b}} = \mathbf{R}^{-1} \mathbf{y}\quad (\text{A-6})$$

## APPENDIX B

### Minimizing The Mean Square Error Function in MMSE Detector

For the MMSE detector discussed in Section 2.3, recall that the likelihood function (2.9):

$$\begin{aligned}
 J(\mathbf{b}) &= E[(\mathbf{A}\mathbf{b} - \mathbf{b}^0)^T (\mathbf{A}\mathbf{b} - \mathbf{b}^0)] \\
 &= E[(\mathbf{A}\mathbf{b} - \mathbf{M}\mathbf{y})^T (\mathbf{A}\mathbf{b} - \mathbf{M}\mathbf{y})] \\
 &= E[\mathbf{b}^T \mathbf{A}^T \mathbf{A} \mathbf{b} - \mathbf{y}^T \mathbf{M}^T \mathbf{A} \mathbf{b} - \mathbf{b}^T \mathbf{A}^T \mathbf{M} \mathbf{y} + \mathbf{y}^T \mathbf{M}^T \mathbf{M} \mathbf{y}]
 \end{aligned} \tag{B-1}$$

To minimize (B-1), we obtain the gradient of  $J(\mathbf{b})$  with respect to  $\mathbf{M}$ :

$$\begin{aligned}
 \frac{\partial J(\mathbf{b})}{\partial \mathbf{M}} &= \frac{\partial}{\partial \mathbf{M}} E[\mathbf{b}^T \mathbf{A}^T \mathbf{A} \mathbf{b} - \mathbf{y}^T \mathbf{M}^T \mathbf{A} \mathbf{b} - \mathbf{b}^T \mathbf{A}^T \mathbf{M} \mathbf{y} + \mathbf{y}^T \mathbf{M}^T \mathbf{M} \mathbf{y}] \\
 &\equiv E\left[\frac{\partial}{\partial \mathbf{M}} (\mathbf{b}^T \mathbf{A}^T \mathbf{A} \mathbf{b} - \mathbf{y}^T \mathbf{M}^T \mathbf{A} \mathbf{b} - \mathbf{b}^T \mathbf{A}^T \mathbf{M} \mathbf{y} + \mathbf{y}^T \mathbf{M}^T \mathbf{M} \mathbf{y})\right] \\
 &= E[-\mathbf{A}\mathbf{b}\mathbf{y}^T - \mathbf{A}\mathbf{b}\mathbf{y}^T + 2\mathbf{M}\mathbf{y}\mathbf{y}^T] \\
 &= 2E[(\mathbf{M}\mathbf{y} - \mathbf{A}\mathbf{b})\mathbf{y}^T]
 \end{aligned} \tag{B-2}$$

The steps in calculating the gradient in (B-2) is shown below:

$$\begin{aligned}
 \mathbf{y}^T \mathbf{M}^T \mathbf{A} \mathbf{b} &= \begin{bmatrix} y_1 \\ \mathbf{M} \\ y_K \end{bmatrix}^T \begin{bmatrix} M_{1,1} & \Lambda & M_{1,K} \\ \mathbf{M} & \mathbf{O} & \mathbf{M} \\ M_{K,1} & \Lambda & M_{K,K} \end{bmatrix}^T \begin{bmatrix} \alpha_1 & \Lambda & 0 \\ \mathbf{M} & \mathbf{O} & \mathbf{M} \\ 0 & \Lambda & \alpha_K \end{bmatrix} \begin{bmatrix} b_1 \\ \mathbf{M} \\ b_K \end{bmatrix} \\
 &= \begin{bmatrix} \left( \begin{array}{c} y_1 M_{1,1} \\ + y_2 M_{1,2} \\ \mathbf{M} \\ + y_K M_{1,K} \end{array} \right) & \Lambda & \left( \begin{array}{c} y_1 M_{K,1} \\ + y_2 M_{K,2} \\ \mathbf{M} \\ + y_K M_{K,K} \end{array} \right) \end{bmatrix} \begin{bmatrix} \alpha_1 b_1 \\ \alpha_2 b_2 \\ \mathbf{M} \\ \alpha_K b_K \end{bmatrix} \\
 &= \alpha_1 b_1 \begin{bmatrix} y_1 M_{1,1} \\ + y_2 M_{1,2} \\ \mathbf{M} \\ + y_K M_{1,K} \end{bmatrix} + \Lambda + \alpha_K b_K \begin{bmatrix} y_1 M_{K,1} \\ + y_2 M_{K,2} \\ \mathbf{M} \\ + y_K M_{K,K} \end{bmatrix} \\
 \therefore \frac{\partial}{\partial \mathbf{M}} (\mathbf{y}^T \mathbf{M}^T \mathbf{A} \mathbf{b}) &= \begin{bmatrix} \alpha_1 b_1 y_1 & \alpha_1 b_1 y_2 & \Lambda & \alpha_1 b_1 y_K \\ \alpha_2 b_2 y_1 & \alpha_2 b_2 y_2 & \Lambda & \alpha_2 b_2 y_K \\ \mathbf{M} & \mathbf{M} & \mathbf{O} & \mathbf{M} \\ \alpha_K b_K y_1 & \alpha_K b_K y_2 & \Lambda & \alpha_K b_K y_K \end{bmatrix} = \mathbf{A}\mathbf{b}\mathbf{y}^T
 \end{aligned}$$



$$\begin{aligned}
\mathbf{b}^T \mathbf{A}^T \mathbf{M} \mathbf{y} &= \begin{bmatrix} \alpha_1 & \Lambda & 0 \\ \mathbf{M} & \mathbf{O} & \mathbf{M} \\ 0 & \Lambda & \alpha_K \end{bmatrix}^T \begin{bmatrix} b_1 \\ \mathbf{M} \\ b_K \end{bmatrix}^T \begin{bmatrix} M_{1,1} & \Lambda & M_{1,K} \\ \mathbf{M} & \mathbf{O} & \mathbf{M} \\ M_{K,1} & \Lambda & M_{K,K} \end{bmatrix} \begin{bmatrix} y_1 \\ \mathbf{M} \\ y_K \end{bmatrix} \\
&= [\alpha_1 b_1 \quad \alpha_2 b_2 \quad \Lambda \quad \alpha_K b_K] \begin{bmatrix} (M_{1,1} y_1 + M_{1,2} y_2 + \Lambda + M_{1,K} y_K) \\ (M_{2,1} y_1 + M_{2,2} y_2 + \Lambda + M_{2,K} y_K) \\ \mathbf{M} \\ (M_{K,1} y_1 + M_{K,2} y_2 + \Lambda + M_{K,K} y_K) \end{bmatrix} \\
&= \alpha_1 b_1 \begin{pmatrix} y_1 M_{1,1} \\ + y_2 M_{1,2} \\ \mathbf{M} \\ + y_K M_{1,K} \end{pmatrix} + \Lambda + \alpha_K b_K \begin{pmatrix} y_1 M_{K,1} \\ + y_2 M_{K,2} \\ \mathbf{M} \\ + y_K M_{K,K} \end{pmatrix} \\
&= \mathbf{y}^T \mathbf{M}^T \mathbf{A} \mathbf{b}
\end{aligned}$$

$$\therefore \frac{\partial}{\partial \mathbf{M}} (\mathbf{b}^T \mathbf{A}^T \mathbf{M} \mathbf{y}) = \frac{\partial}{\partial \mathbf{M}} (\mathbf{y}^T \mathbf{M}^T \mathbf{A} \mathbf{b}) = \mathbf{A} \mathbf{b} \mathbf{y}^T$$

$$\begin{aligned}
\mathbf{y}^T \mathbf{M}^T \mathbf{M} \mathbf{y} &= \begin{bmatrix} y_1 \\ \mathbf{M} \\ y_K \end{bmatrix}^T \begin{bmatrix} M_{1,1} & \Lambda & M_{1,K} \\ \mathbf{M} & \mathbf{O} & \mathbf{M} \\ M_{K,1} & \Lambda & M_{K,K} \end{bmatrix}^T \begin{bmatrix} M_{1,1} & \Lambda & M_{1,K} \\ \mathbf{M} & \mathbf{O} & \mathbf{M} \\ M_{K,1} & \Lambda & M_{K,K} \end{bmatrix} \begin{bmatrix} y_1 \\ \mathbf{M} \\ y_K \end{bmatrix} \\
&= \begin{pmatrix} y_1 M_{1,1} \\ + y_2 M_{1,2} \\ \mathbf{M} \\ + y_K M_{1,K} \end{pmatrix}^2 + \Lambda + \begin{pmatrix} y_1 M_{K,1} \\ + y_2 M_{K,2} \\ \mathbf{M} \\ + y_K M_{K,K} \end{pmatrix}^2
\end{aligned}$$

$$\therefore \frac{\partial}{\partial \mathbf{M}} (\mathbf{y}^T \mathbf{M}^T \mathbf{M} \mathbf{y}) = \begin{bmatrix} 2 \begin{pmatrix} y_1 M_{1,1} \\ + y_2 M_{1,2} \\ \mathbf{M} \\ + y_K M_{1,K} \end{pmatrix} y_1 & \Lambda & 2 \begin{pmatrix} y_1 M_{1,1} \\ + y_2 M_{1,2} \\ \mathbf{M} \\ + y_K M_{1,K} \end{pmatrix} y_1 \\ \mathbf{M} & \mathbf{O} & \mathbf{M} \\ 2 \begin{pmatrix} y_1 M_{K,1} \\ + y_2 M_{K,2} \\ \mathbf{M} \\ + y_K M_{K,K} \end{pmatrix} y_K & \Lambda & 2 \begin{pmatrix} y_1 M_{K,1} \\ + y_2 M_{K,2} \\ \mathbf{M} \\ + y_K M_{K,K} \end{pmatrix} y_K \end{bmatrix} = 2 \mathbf{M} \mathbf{y} \mathbf{y}^T$$

To obtain the minimum for  $J(\mathbf{b})$ , we equate (B-2) to zero, which is equivalent to forcing the error  $(\mathbf{M}\mathbf{y} - \mathbf{A}\mathbf{b})$  to be orthogonal to the correlation value vector  $\mathbf{y}$  [5].

Thus,

$$\begin{aligned} E[(\mathbf{M}\mathbf{y} - \mathbf{A}\mathbf{b})\mathbf{y}^T] &= \mathbf{0} \\ \mathbf{M}E[\mathbf{y}\mathbf{y}^T] - E[\mathbf{A}\mathbf{b}\mathbf{y}^T] &= \mathbf{0} \end{aligned} \quad (\text{B-3})$$

Consider the case of synchronous transmission. From (1.23) and (B-3) we have

$$\begin{aligned} E[\mathbf{A}\mathbf{b}\mathbf{y}^T] &= E[\mathbf{A}\mathbf{b}(\mathbf{R}\mathbf{A}\mathbf{b} + \mathbf{n}')^T] \\ &= E[\mathbf{A}\mathbf{b}\mathbf{b}^T \mathbf{A}^T \mathbf{R}^T] + E[\mathbf{A}\mathbf{b}\mathbf{n}'^T] \\ &= \mathbf{B}\mathbf{R}^T \end{aligned} \quad (\text{B-4})$$

and

$$\begin{aligned} E[\mathbf{y}\mathbf{y}^T] &= E[(\mathbf{R}\mathbf{A}\mathbf{b} + \mathbf{n}')(\mathbf{R}\mathbf{A}\mathbf{b} + \mathbf{n}')^T] \\ &= E[\mathbf{R}\mathbf{A}\mathbf{b}\mathbf{b}^T \mathbf{A}^T \mathbf{R}^T] + E[\mathbf{R}\mathbf{A}\mathbf{b}\mathbf{n}'^T] + E[(\mathbf{R}\mathbf{A}\mathbf{b})^T \mathbf{n}'] + E[\mathbf{n}'\mathbf{n}'^T] \\ &= \mathbf{R}\mathbf{B}\mathbf{R}^T + \frac{N_0}{2} \mathbf{R} \end{aligned} \quad (\text{B-5})$$

where  $\mathbf{B}$  is a diagonal matrix with diagonal elements  $\{\alpha_k^2, 1 \leq k \leq K\}$ . By substituting (B-3) and (B-4) into (B-2),

$$\mathbf{M}(\mathbf{R}\mathbf{B}\mathbf{R}^T + \frac{N_0}{2} \mathbf{R}) - \mathbf{B}\mathbf{R}^T = \mathbf{0} \quad (\text{B-6})$$

Solving (B-6), we obtain  $\mathbf{M}$  that minimizes (B-1):

$$\mathbf{M} = [\mathbf{R} + \frac{N_0}{2} \mathbf{B}^{-1}]^{-1}. \quad (\text{B-7})$$

## APPENDIX C: PROCESSING TIME BLOCK COMPARISON BETWEEN THE SIC, PIC, CONVENTIONAL AND CCI-SICRM

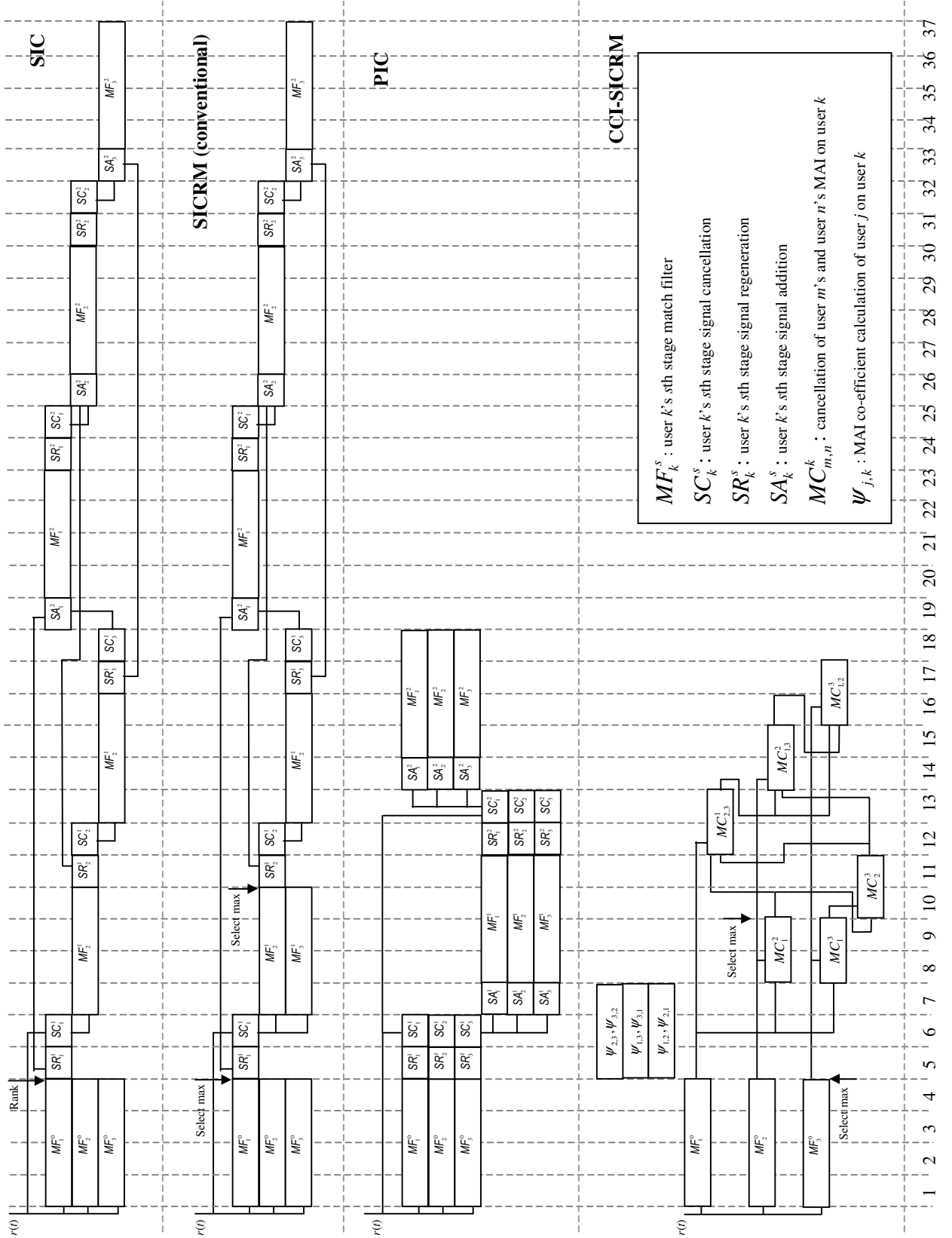


**Figure C: Processing Time Chart of the SIC, conventional SICRM, PIC and cross-correlation SICRM for  $K=3, S=2$**